Intelligent Tire Based Tire Force Characterization and its Application in Vehicle Stability and Performance

Anup Cherukuri

Thesis submitted to the faculty of the Virginia Polytechnic Institute and State University in partial fulfillment of the requirements for the degree of

Master of Science

In

Mechanical Engineering

Saied Taheri, Chair

John B. Ferris, Member

Ronald H. Kennedy, Member

June 28th, 2017

Blacksburg, VA

Keywords: Intelligent Tire, Signal Processing, Tire Force, CarSim

Intelligent Tire Based Tire Force Characterization and its Application in Vehicle Stability and Performance

Anup Cherukuri

ABSTRACT

In any automotive system, the tires play a very crucial role in defining both the safety and performance of the vehicle. The interaction between the tire and the road surface determines the vehicle's ability to accelerate, decelerate and steer. Having information about this interaction in real-time can be very valuable for the onboard advanced active safety systems to mitigate the risks ahead of time and keep the vehicle stable. The crucial information which can be obtained from the tire includes but are not limited to tire-road friction, tire forces (longitudinal, lateral), normal load, road surface characteristics and tire pressure. This information can be acquired through indirect vehicle dynamics based estimation algorithms or through direct measurements using sensors inside the tire. However, the indirect estimations fail to give an accurate measure of the vehicle state in certain conditions (e.g. side winds, road banking, surface change) and require ABS or VSC activation before the estimation begins. Therefore, to improve the performance of these active stability systems, direct measurement based approaches must be explored.

This research expands the applications of Intelligent tire and focusses on using the sensor based measurement approach to develop estimation algorithms relating to tire force measurement. A tri-axial accelerometer is attached to the inner liner of the tire (Intelligent Tire) and two of such tires are placed on an instrumented (MSW, VBox, IMU, Encoders) VW Jetta. Different controlled tests are carried out on the instrumented vehicle and the Intelligent tire signal is analyzed to extract features related to the tire forces and pressure. Due to unavailability of direct force measurements at the wheel, a VW Jetta simulation model is developed in CarSim and the extracted features are validated with a good correlation.

Intelligent Tire Based Tire Force Characterization and its Application in Vehicle Stability and Performance

Anup Cherukuri

GENERAL AUDIENCE ABSTRACT

The automotive industry is heading towards autonomous vehicles driven at various levels of autonomy. Autonomous vehicles require a thorough understanding of the vehicle characteristics such as load, current state of the vehicle (speed, heading). It also requires a good grasp of the tire-road interaction to be able to estimate the future state of the vehicle.

This research focuses on exploring the tire-road interaction using sensor based approach. The tires are instrumented using a tri- axial accelerometer and different algorithms have been developed using signal processing techniques to estimate parameters such as Tire forces, tire pressure and load of the vehicle. The experiments are conducted on an instrumented VW Jetta vehicle which also has other sensors such as Inertial Measurement Unit, GPS based speed estimation sensor and steering angle measurement sensor. The results obtained from the sensor signal are processed using a code developed in MatLab software and validated using a simulation model in CarSim. Knowing the Tire Characteristics such as Tire force, pressure is essential for accurate estimation of the vehicle state which in turn will refine the autonomous capability of the vehicle.

ACKNOWLEDGMENT

I would like to take this opportunity to thank my graduate advisor Dr. Saied Taheri, who has always shown immense faith in me and guided me throughout my research. He has always supported me with my ideas and gave me freedom to explore new possibilities in research.

I would also like to thank Dr. John Ferris and Dr. Ron Kennedy for serving as my committee members and giving valuable feedback in my research.

I thoroughly enjoyed working at CenTiRe and would like to extend a note of thank you for Dr. Meysam Khaleghian for supporting me throughout my research. A big thank you for all those who directly or indirectly helped me with my research.

Last but not the least, I would like to thank my parents for all their love for believing in me, without their support I would not have been here. I would also like to thank all my friends and well-wishers for constantly keeping me motivated throughout my stay at Virginia Tech.

Table of Contents

List of Figures

List of Tables

1 Introduction

The global automotive industry is fast changing triggered by technological advancements and increased focus in the areas of active safety and autonomous driving. The new technologies being developed require the vehicle to sense its surroundings and its own state, which requires advanced sensing techniques. One of the information which is crucial for the vehicle to know is the surface which it is running on and the limits which it can go to without losing control. Tires serve an important role in knowing these characteristics through the sensing of tire-road contact parameters. It thus becomes essential to progress towards Intelligent Tires with the ability to estimate conditions such as friction[1], forces, pressure, load. The knowledge of knowing the measured tire forces is valuable for all the stability and performance systems onboard. Controlling the vertical tire forces can improve the ride comfort, lateral tire forces the stability/handling and longitudinal force improve the traction/braking ability. An accurate estimation of these contact characteristics is required for a good feedback based stability system. Currently, the forces are estimated through indirect vehicle dynamics based model which are accurate in general driving conditions but are susceptible to inaccuracies in certain conditions such as sudden surface change, banking in road, side wind. Therefore, the need arises for measuring the contact parameters using Intelligent tires. The first studies in this field were conducted as a part of the APOLLO[2] program, the objectives being to improve the safety by providing the information from the tire to Advanced Driver Assist systems(ADAS) and to enable the introduction of innovative services of tire road conditions to groups outside the vehicle. This technology of Intelligent Tire has seen a lot of advancements since then and is heading towards commercialization in the automotive market.

1.1 Background

The information of tire forces is critical for the vehicle stability systems and can be acquired in two ways.

- Estimation using Vehicle Dynamics Models
- Direct measurement using sensors

1.1.1 Estimation using Vehicle Dynamics Models

The information about vehicle stability state is critical for the active safety systems such as ABS, ESC. A lot of study has been conducted to estimate the states of the vehicle such as side slip, slip angle. The most common approach used to estimate the vehicle state is to use a bicycle model as shown below.

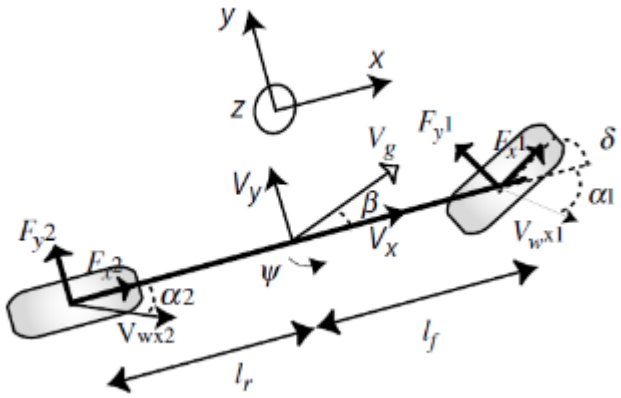

Figure 1-Bicycle model[58]

$$\ddot{\psi} = \frac{1}{I_z}\left[l_f \left[F_{x1}\sin\delta + F_{y1}\cos\delta \right] - l_r F_{y2} \right]$$

$$\dot{\beta} = \frac{1}{m_v V_g}\begin{bmatrix} -F_{x1}\sin(\beta-\delta) + F_{y1}\sin(\beta-\delta) \\ +F_{y2}\cos\beta - F_{x2}\sin\beta \end{bmatrix} - \dot{\psi}$$

$$\dot{V}_g = \frac{1}{m_v}\begin{bmatrix} F_{x1}\cos(\delta-\beta) - F_{y1}\sin(\delta-\beta) \\ +F_{x2}\cos\beta + F_{y2}\sin\beta \end{bmatrix}$$

The study conducted in [3] estimates the slip angle, based on vehicle dynamics and tire model. This study also proposes an idea of using a combination of measurement and model based approach for estimation of vehicle states. The study conducted by [4] measures the yaw rate, longitudinal ,lateral acceleration , steering angle along with the wheel and vehicle velocity to estimate the lateral tire forces and side slip angle using a bicycle model/ Burckhardt tire model and Kalman Filtering.

In the research conducted by [5] only yaw rate is used as an input to estimate the side slip angle, a nonlinear observer is used and stability was obtained from analysis of energy to peak

performance of estimation error system. In some studies GPS based system is used to improve the estimation of the state of the vehicle[6][7].

Some studies use a planar model to estimate the vehicle state[8], however using planar model requires makes the estimation more computationally intensive and also it requires more states to be measured. The study conducted in [9] claims to estimate the side slip angle without the information of tire/vehicle model and uses a vehicle observer along with Kalman Filter. Lateral Velocity estimation is an important parameter to get accurate side slip angle, the study conducted by[10] estimates the tire lateral velocity which is not sensitive to changes in tire parameters and vehicle mass.

1.1.2 Contact Deformation Sensors

This section studies the different sensor based approaches available to measure the tire deformation, this measurement can be then used to estimate the forces, friction. A detailed study has been conducted by [11] reviewing the different types of sensing and signal processing techniques used to extract features using intelligent tires. The different sensing approaches used are described in detail below.

- **Magnetic sensors**: The study conducted in [12] uses a magnet embedded in the tire along with a hall cross to monitor the change in voltage caused due to deformation in the tire.
- **Ultrasonic sensors:** Ultrasonic sensors are used a lot these days for sensing distance, for e.g. to detect objects during reversing the vehicle. This method has been used by[13] in his study to measure tire deformation. An ultrasonic sensor is placed on the rim pointing towards the contact patch and it measures the deformation in the vertical direction based on the distance of the sensor from the inner wall.
- **SAW sensors:** Surface Acoustic Wave consists of a piezoelectric substrate with metallic structure as a sensor element for measuring the deformations. In the study conducted by[14] deformation of tread was measured by inserting a pin into the tread, this pin acts like a lever and the deformation caused in the tire induces a change in the sound acoustic wave.
- **Optical sensors:** Optical sensors can be used to measure the global deflection of the

tires. Optical sensor have been used by[15] to measure the carcass deflection and correlate that to the force on the tire. In optical based systems, a small Light Emitting Diode(LED) is attached to the inner liner and its light is focused onto the position detector on the rim, a lens is generally used to converge the light onto the detector. The APOLLO project stated the optical based system to be of good application since it can estimate the forces with good accuracies. However, a calibration is required from time to time since there is a misalignment between detector and the LED with time and usage of tire.

- **Strain Sensors:** Most of the strain sensors used are Piezo electric based with Polyvinylidene Fluoride as the substrate. In the studies conducted in[16][17][18] a strain based sensor is used for identifying different aspects such as friction, tire forces.

  The strain sensors have their own merits and demerits. Strain sensors measure the deflection in the tire which has a direct relation with the force acting in the tire, they have less noise in the signal compared to accelerometers. However, strain sensors are susceptible to detachment from the tire under high deformation and can cause a change to the stiffness in the local area of the attachment of sensor.
- **Accelerometer Sensors:** Accelerometers have been used in a lot of studies conducted to estimate tire contact parameters[19]–[27]. The advantage using accelerometers is that they have good signal linearity and stability over time and are insensitive to temperature changes. They have a compact size and are relatively inexpensive. Also, the accelerometers can be used in a variety of applications like surface characterization, force and friction measurement. However, a disadvantage of accelerometer measurement is that it is very sensitive to noise generated from the road surface and contains rotational vibrational and gravitational accelerations.

1.2 Motivation

The vehicle state estimation using vehicle dynamics/tire models and Kalman filter has a good accuracy in estimating tire forces, sideslip in the linear region. However, in the nonlinear range and in conditions of road banking and side wind, the estimation algorithms are not that accurate.

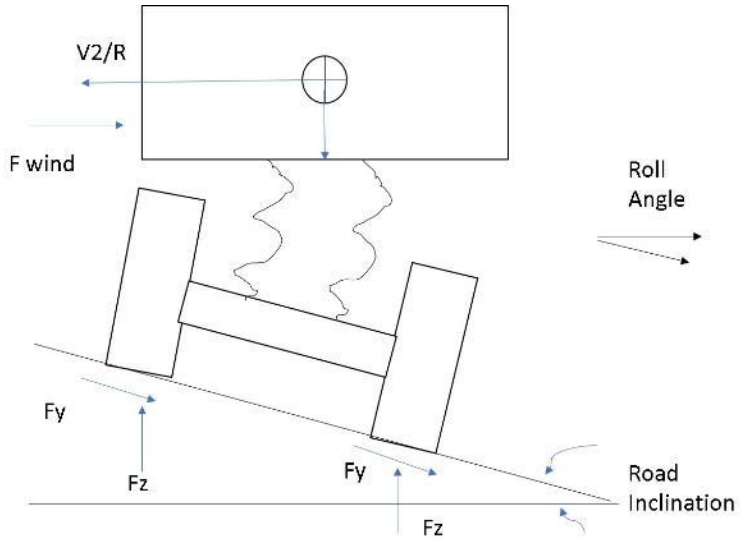

Figure 2-Combined effect of Road Banking and Side Wind

As can be seen from figure above the lateral acceleration and the force acting on the tire are not parallel to each other, this causes an error in estimation when using the lateral acceleration as an input state. There are ways to rotate the lateral acceleration based on the roll angle estimate however estimation of banking angle is difficult and direct measurement of tire forces is very helpful in this situation. Also, the effect of side wind is not captured by any of the estimation algorithm's. Even when the vehicle is running straight with side wind, there is a significant amount of side force generated by the tires.

The study conducted in [28] uses measured tire forces to eliminate the lateral acceleration as an input state to improve the accuracy of the estimation. A similar study conducted[29] explores the benefits of having a measured tire force input in the estimations. The study states that when the friction is constant on the surface, the vehicle dynamic based observers give a good estimation however, during mu jumps having a measurement of tire forces improves the accuracy of the estimations.

Studies using intelligent tire have been done to estimate friction[24], surface characterization[30], hydroplaning[22] and host of other parameters. The paper published by Pirelli[31] summarizes the different applications of Intelligent tire technology. This study extends the applications of Intelligent tires for lateral/longitudinal force estimation and to estimate the load transfer. The main applications of knowing the tire contact forces are:

- Use in stability systems to improve the accuracy of estimations as described above.
- Use in benchmarking of tires during tire development.
- The tire forces can be used as an input to the tire wear model, to estimate the tire wear.

The study also does a preliminary analysis of the Intelligent tire signal to extract features related to tire pressure change.

1.3 Objectives of Thesis

The main objectives of this thesis are:

- Instrument a VW Jetta with sensors (Inertial Measurement Unit, VBox, Steering Sensor, wheel encoders) and Intelligent Tires.
- Setup a data acquisition system using a NI DAQ and LabView interface.
- Check the robustness of Load estimation algorithm to estimate lateral/longitudinal load transfer.
- Analysis of Intelligent Tire signal for regressors related to Lateral/Longitudinal force.
- Develop a simulation model in CarSim to validate the regressors extracted.
- Preliminary study for regressors related to Tire pressure in frequency domain.

1.4 Organization of Chapters

The methodologies used and the results have been summarized into five chapters.

Chapter1 gives a brief introduction of the existing Vehicle dynamics model based state estimation algorithms and states the advantage of measuring the real-time interaction between the road and the tire. It then discusses about the different sensing techniques used to measure the tire road characteristics along with the literature review for the same. It then lists the motivations for using an accelerometer based sensing technique and the contributions to this study.

Chapter2 discusses the test setup developed for this study which is an instrumented VW Jetta. The chapter discusses the different sensors and the used to instrument along with their specifications. It also discusses about the modification done to the wheel to instrument an

accelerometer inside the tire. Finally, it explains the data acquisition and collecting setup.

Chapter3 explores the different techniques used for extracting features from the Intelligent tire signal. It analyses the signal in time and frequency domain for different vehicle maneuvers. A comprehensive analysis is done to check the robustness of the load transfer estimation algorithm and features are extracted from the signal relating to lateral and longitudinal force. A preliminary analysis in the frequency domain is conducted to develop an algorithm for tire pressure monitoring system.

Chapter4 utilizes a simulation model developed in CarSim to validate the regressors relating to the force extracted in the previous chapter. The CarSim model developed is first validated using the actual test results obtained. This model is then used with the same steering and speed input as the actual test to get a measure of the tire force which are then compared to the regressors from Intelligent tire. The chapter also shows the results of a simple Neural Network based algorithm developed for tire pressure estimation.

Chapter5 summarizes the study and lists out the tasks to be conducted to expand the scope of this study. It critically analyzes each part of the study and the improvements which need to be conducted to make the algorithms more robust.

2 Experimental Setup

In this chapter, the experimental test setup which was used in the study is discussed. The primary test setup which was used was an Instrumented VW Jetta 2002. The Jetta was procured and instrumented as a part of this study.

2.1 Instrumented VW Jetta

The setup which was used for this project was a VW Jetta 2002. The reason behind choosing this model was the availability of vehicle parameters (K&C, mass, spring stiffness etc.). The vehicle was instrumented with various sensors as shown in Figure 3. The sensors are described in detail below

Figure 3-Schematic Jetta Instrumentation

2.1.1 Corsys Datron MSW

A Corsys Datron MSW (Measuring Steering Wheel) as show in Figure 4 was used to measure the steering wheel angle and torque. The specifications for the MSW are shown in Table 1.

Figure 4-Corsys Datron MSW

The encoder resolution	Up to 7200 pulses per revolution
Powers supply	10-36 V- DC
Mass moment of inertia	60 $kgcm^2$
Angle resolution	0.1 Degree
Max steering torque measurement range	± 50 Nm
Max steering speed	1000 degree /sec

Table 1-MSW Specs

2.1.2 Inertial Measurement Unit

To measure the dynamics of the vehicle (accelerations in X, Y, Z & Roll, Pitch, Yaw) a six DOF IMU from TEXYS(IB6-XY3-Z5-GX100-GY100-GZ100 IMU) instruments was used. Since the vehicle parameters were available, the IMU was placed at the CG (Center of Gravity) of the Vehicle. The specifications for the IMU are shown in Table 2

Range of XY Acceleration	± 3g
XY sensitivity	≈ 660 mV/g
Range of Z Acceleration	± 5g
Z sensitivity	≈ 385 mV/g
Range of Gyro XYZ	± 50°
Gyroscope sensitivity	≈ 20 mV/°/s
Gyroscope offset drift	± 25 mV

Gyroscope gain drift	± 1 %

Table 2-IMU Specs

The orientation of the IMU is shown below along with the directions of lateral and longitudinal accelerations acting on it.

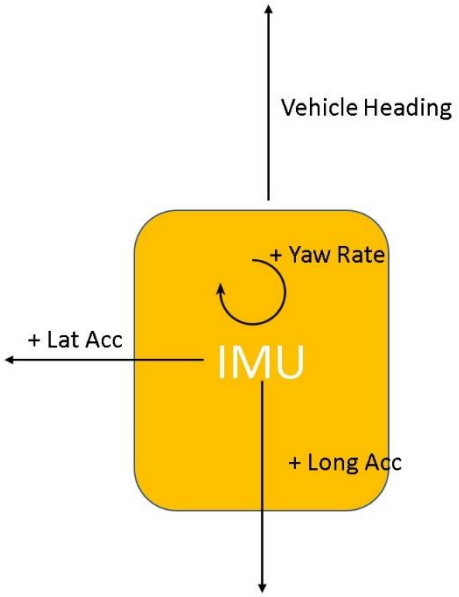

Figure 5-IMU Orientation

2.1.3 VBox

To measure the speed of the vehicle accurately, a GPS based speed measuring system was used as can be seen in Figure 6 . The specifications for the VBox are shown in Table 3.

Figure 6- VBox

Accuracy	0.1 km/h
Update Rate	100 Hz
Maximum Velocity	160 km/h
Minimum Velocity	0.1 km/h
Resolution	0.01 km/h

Latency	8.5±1.5 mS

Table 3-VBox Specs

2.1.4 Encoder/Slip Ring

To measure the angular speed of the wheel and to transmit the accelerometer signal from inside the rotating tire a waterproof slip ring with built in encoder from Michigan Scientific (SR10AW/PE512) was used. The adapter to mount the slip ring onto the wheel as can be seen in Figure 7 was designed and machined in house. The specifications of the encoder are shown in Table 4

Figure 7-Slip Ring and Adaptor

Number of circuits	10
Current capacity	500 mA
RPM rating	10000
Maximum peak noise	0.1 ohm
Temperature range	-40°C to 100°C

Table 4- Encoder Specs

2.1.5 Intelligent Tire

The intelligent tire was instrumented using a tri axial accelerometer as shown Figure 8. The accelerometer was attached to the tire using an epoxy which was strong enough to keep the accelerometer in its position without altering the stiffness in the local area. The specifications of the accelerometer are shown in Table 5 A hole was made in the rim and a connector was fixed inside it. This connector connected the sensor inside to the slip ring as seen in Figure 9. The

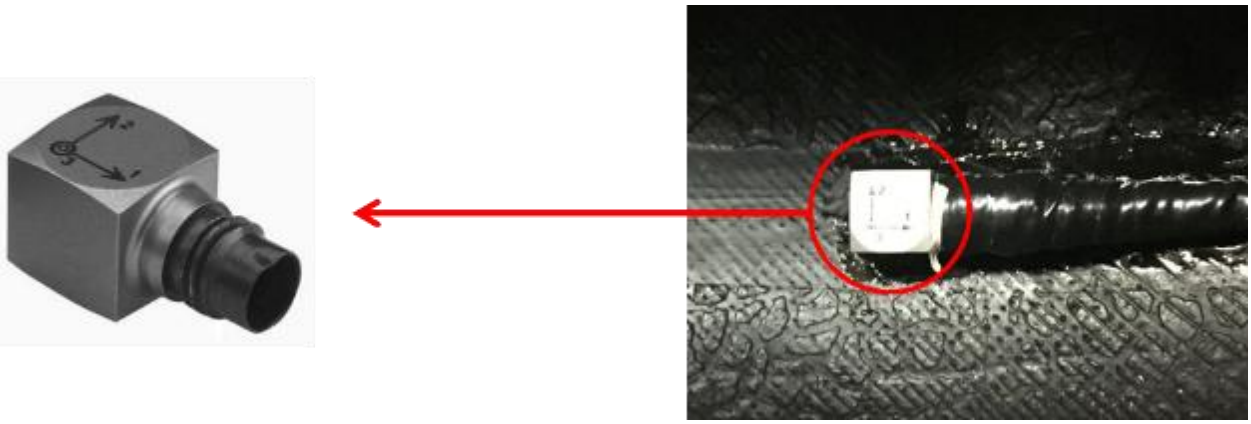

Figure 8-Accelerometer for Intelligent Tire

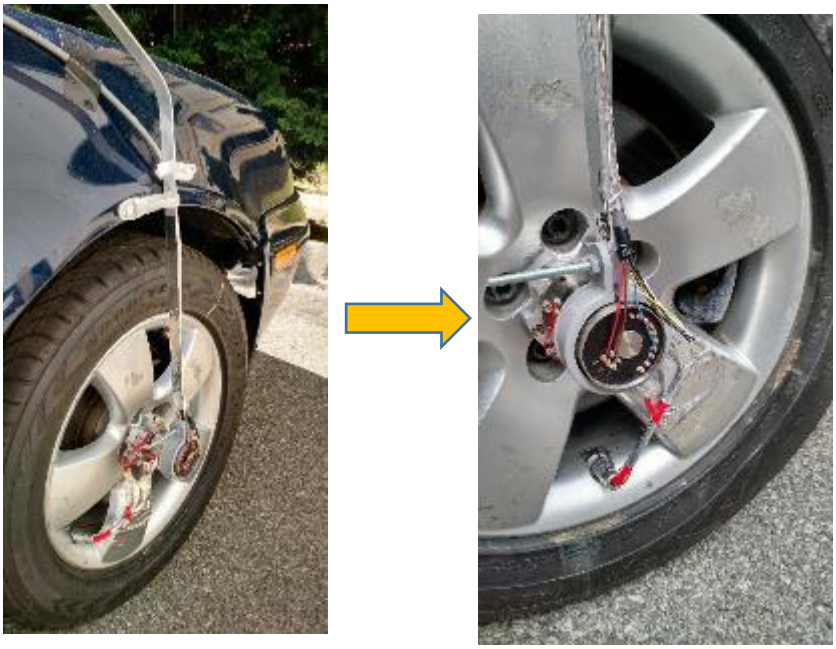

Figure 9-Slip Ring fixture

Sensitivity, $\pm 5\%$	$10\,mV/g$
Range for $\pm 5 volts$ output	$\pm 5000 g$
Supply current range	$2 to 20 mA$
Compliance Voltage Range	$18-30 volts$

Table 5-Tire Accelerometer Specs

2.1.6 Data Acquisition and analysis

The data acquisition was done using a National Instruments DAQ(NI-USB-6363), the DAQ supports up to thirty-two analog 16 bit channels, four 32 bit counters and can be used for a maximum sampling rate of 1MHz. The DAQ and signal conditioner showed in Figure 11 required AC power to operate which was provided by using a DC-AC converter and car battery shown in Figure 10. A stand was designed to hold the DAQ and signal conditioner in place when the vehicle is in motion as seen in Figure 11.

Figure 11-DAQ-Signal Conditioner

Figure 10-DC-AC Converter

A data collection routine was developed in LabVIEW, to avoid the time sync issues a common clock was used for all the sensors to acquire the data at the same sampling rate. The LabVIEW interface is shown in Figure 12.

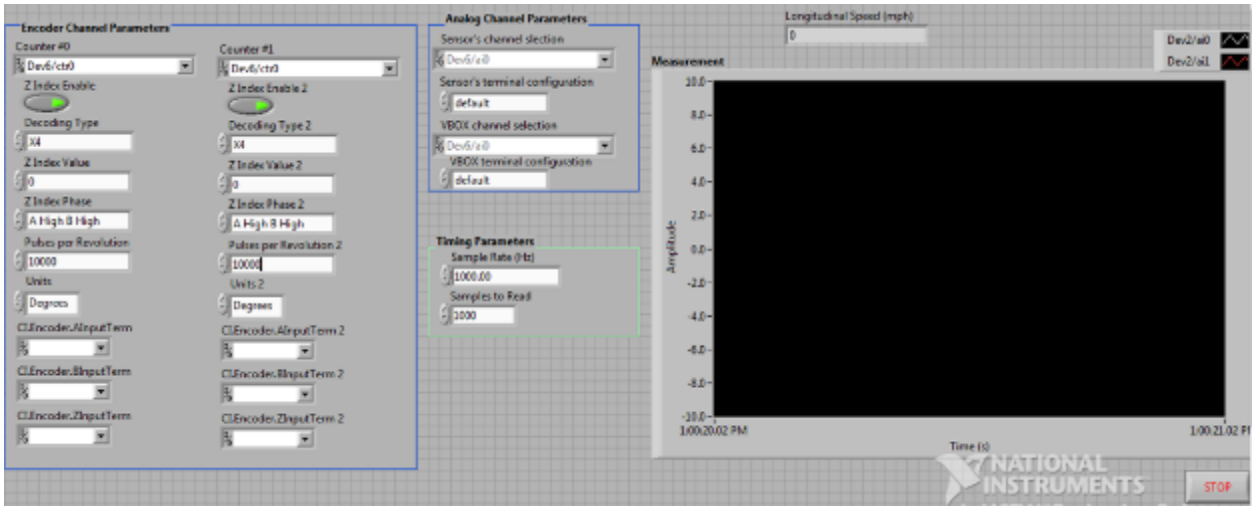

Figure 12-LabVIEW Interface

3 Signal Analysis and Feature extraction of Intelligent Tire Signal

This chapter primarily describes the different techniques used for processing the intelligent tire signal and the analysis carried out to extract different regressors which correlate with the tire forces. The main contents of this chapter are

- Frequency & Time domain analysis techniques
- Tire contact patch dynamics
- Frequency domain analysis of intelligent tire signal with change in vehicle speed, steering.
- Analysis of regressors relating to Tire force and Tire pressure.

3.1 Frequency, Time domain analysis techniques

Signals carry have a lot of information in them both in the frequency domain and the time domain. The frequency domain gives good indications of the distribution of energies across various frequencies and knowing the frequency range of interest, one can extract a lot of meaningful data such as resonance modes. On the other hand, time domain analysis of the signal can be used to extract features which are more dynamic in nature such as jerks, zero crossings etc. Hence it becomes essential to analyze the signal using both these techniques to develop a more robust algorithm.

3.1.1 Frequency Domain Analysis

Tires are made of rubber which is elastic in nature and can be considered as an equivalent of spring. Hence it is worth it to look in to the frequency domain of the accelerometer signal to extract some meaningful information. Studies have been conducted on characterizing tire vibrations in frequency domain [32] and also on extracting some indicator for tire friction analyzing the tire wheel speed vibration in frequency domain[33]. The sections below describe the different techniques of frequency, frequency-time domain analysis.

3.1.1.1 Fast Fourier Transform

The fast Fourier transform or the Discrete Fourier transform is the most commonly used Fourier transform. This transform is used primarily for discrete time and frequency signals. The underlying principle of a Fourier transform is that the time domain signal is reconstructed using sine & cosine waves of different frequencies /amplitudes and is then plotted on the magnitude vs frequency plot. The FFT/DFT can only be applied to stationary signals (long term statistics do not change with time). Hence it is not a good tool to be used on real time signals, however for analyzing the effects of different parameters (tire pressure, load, speed) on the intelligent tire signal Fast Fourier transform can be used. Also, FFT does not preserve the time data of the signal which is another disadvantage of using it on real time non-stationary signals. Mathematically the DFT can be described using the formula below.

$$f[N] = \frac{1}{N}\sum_{m=0}^{N-1}[\sum_{k=0}^{N-1} f[k]\exp(\frac{-i2\pi mk}{N})]\exp(\frac{i2\pi mn}{N}) \quad n = 0,1,2 \dots \dots N-1$$

Equation 1[34]

The term within the square bracket in Equation 1is the DFT. MATLAB has an inbuilt function to calculate the FFT, however the disadvantage of using this function is that the frequency plot data is noisy and difficult to comprehend. The solution to this problem is to use another function called PWelch. Welch's periodogram method divides the data into small bins averages it out and uses a window function on the data to prevent spectral leakage. The result is a much smoother frequency plot. The comparison of FFT and PWelch is shown in Figure 13.

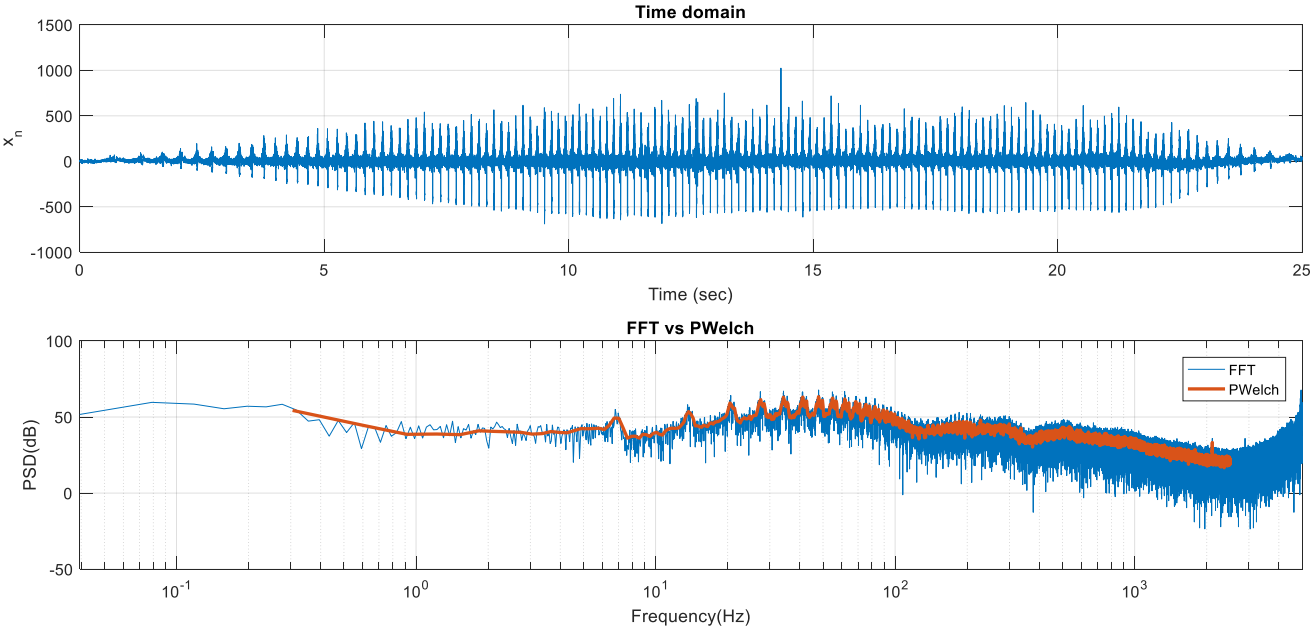

Figure 13-FFT vs PWelch

3.1.1.2 Short time Fourier Transform

The main difference between Short Time Fourier Transform(STFT) and FFT is that STFT gives frequency content of the signal w.r.t to time which is an advantage for continuously varying signals[35]. The STFT analysis is carried out with certain window limit which is moved slowly along with the signal. STFT can be used on nonlinear and non- stationary signals unlike FFT. The STFT can be mathematically represented by the following formula.

$$F(v;u) = \int_{-\infty}^{\infty} \frac{1}{a} rect\left(\frac{t-u}{a}\right) u(t) \exp(i2\pi bt) \exp(-i2\pi vt)\, dt$$

Equation 2[36]

A rectangular window of width a and height 1/a is used centered around t=u in Equation 2

In MATLAB STFT can be calculated using the function SPECTROGRAM which takes in the window type/size and the overlap as its inputs and has the STFT complex number, normalized frequency and time as outputs.

[s w t] = spectrogram (x, window, noverlap, nfft)

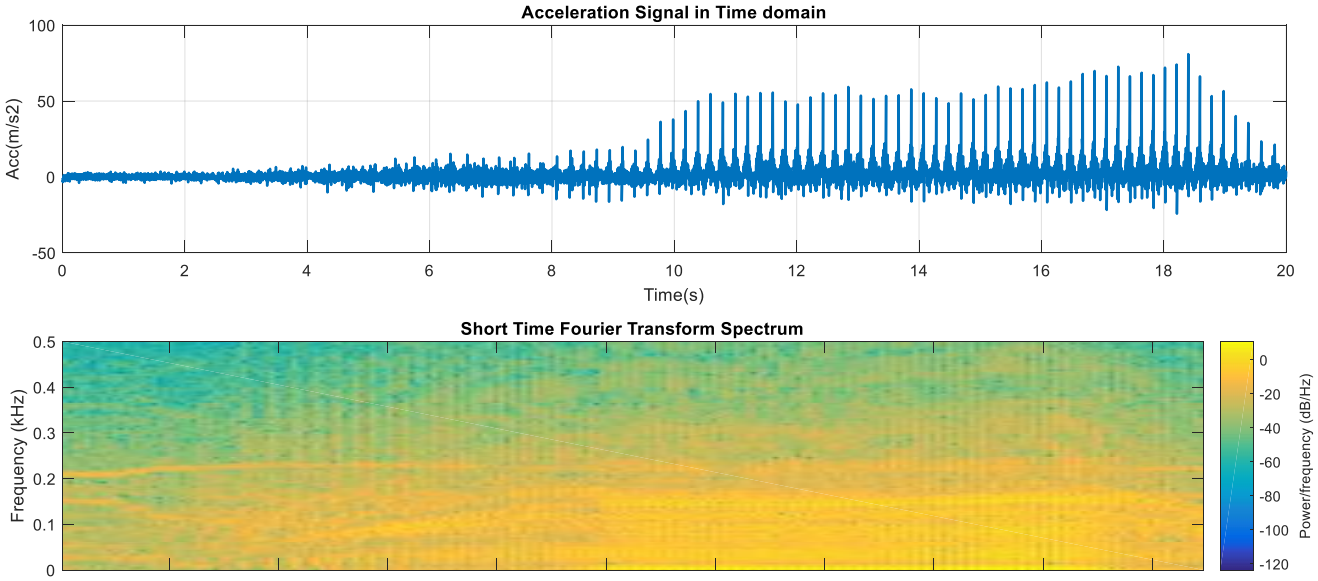

Figure 14-STFT

The STFT of the accelerometer signal is shown in Figure 14 . It can be seen from the spectrogram that the areas of higher energy in the spectrogram correspond to the high acceleration signal in time domain. Hence STFT is an excellent tool which can be utilized to do frequency – time domain analysis.

3.1.2 Time Domain Analysis

Time domain analysis of the signal explores the signal in statistical terms, the signal can also be analyzed in terms of some features such as peaks, slopes etc. Some of the time domain analysis used are shown in Table 6.

No.	Time Domain Technique	Remark
1.	Autocorrelation	Comparison of signal with itself at different lag. Used to check the periodicity of signal.

2.	Cross Correlation	Comparison of signal with another signal to get trends similar in nature. Can be used for fault analysis.
3.	Mean	$Mean = \frac{1}{n}\sum_{i=1}^{n} x_i$
4.	RMS	$RMS = \sqrt{\frac{1}{n}\sum_{i=1}^{n} x_i^2}$
5.	Zero Crossing Rate	Used to detect the random noise. If the rate is too high it can be an indication of noise.
6.	Maxima Minima Peaks	Peaks can give indication of high energy of the signal at that instant.

Table 6-Time Domain Techniques

Another important analysis which needs to be done on signals is to check if the signal is having a normal distribution or not. Different techniques can be used to check the normal distribution, Histogram being one of them.

3.2 Tire Contact Patch Dynamics

The tire contact patch dynamics plays an important role in vehicle safety and performance. To better understand the intelligent tire signal, it is first important to study the tire – road surface interaction as it can give further clues in feature extraction for intelligent tire signal. The tire contact patch dynamics can be divided into four broad categories based on the forces acting on it.

- Lateral Dynamics
- Vertical Dynamics
- Longitudinal Dynamics
- Combined Lateral Longitudinal Dynamics

In this research, combined longitudinal – lateral dynamics interaction has not been considered and will not be discussed in detail further.

3.2.1 Tire Contact Patch: Lateral Dynamics

When a rolling tire is under a vertical force F_z and a lateral force F_y at the tire axis, its path of motion on the road makes an angle α with respect to the tire-plane. The angle is called sideslip angle and is proportional to the lateral force.

$$Fy = -C_\alpha \alpha$$

Equation 3[37]

Where C_α is the cornering stiffness and can be defined by Equation 4

$$C_\alpha = \left| \lim_{\alpha \to 0} \frac{\partial F_y}{\partial \alpha} \right|$$

Equation 4[37]

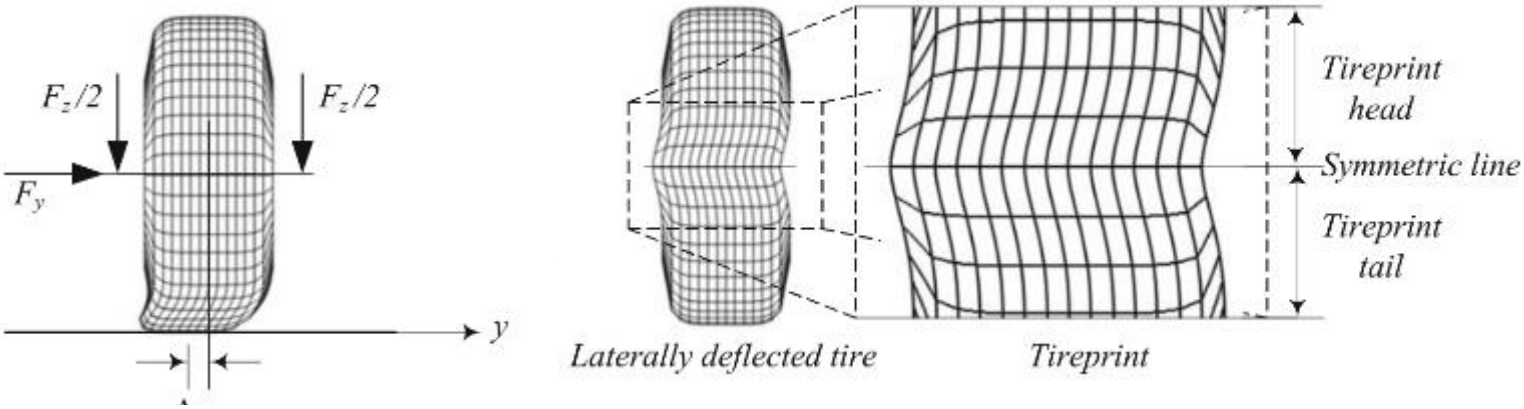

Figure 15-Tire Lateral Deflection[37]

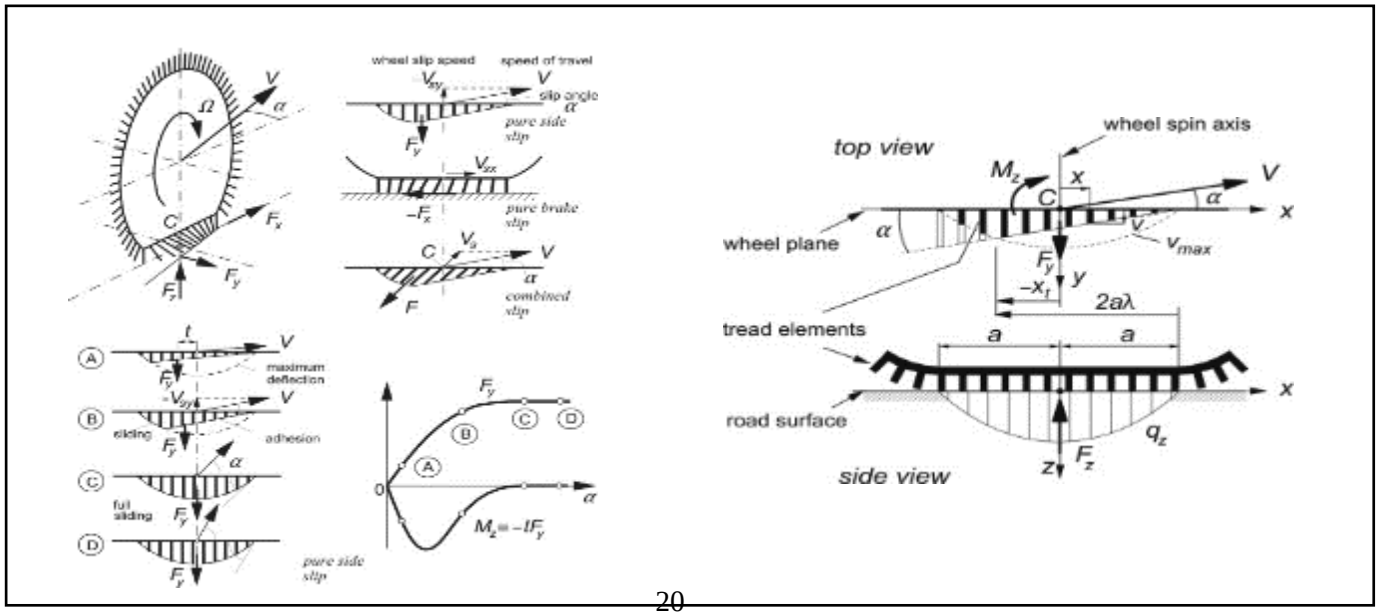

Figure 16-Tire Brush Model[38]

The tire brush model consists of a belt which is rigid in horizontal direction and a “brush” which represents the tread element of the tire. The deflection of the brush elements corresponds to the force/moment generation in the tire.

It is also worthwhile to look at parameters which affect the generation of the cornering force from the tire. These indicators have been used later while developing intelligent tire based estimation algorithms. The parameters affecting the force generation are:

- Slip angle
- Tire vertical load
- Tire rolling speed
- Tire pressure

The effect of these parameters on lateral force generation have been shown below

3.2.1.1 Slip angle vs Lateral Force

For a given vertical load and tire pressure. The tire cornering force increases linearly with slip angle till some limit and then starts saturating, this is the general trend observed for the Lateral Force vs slip angle curve. This is illustrated in Figure 17.

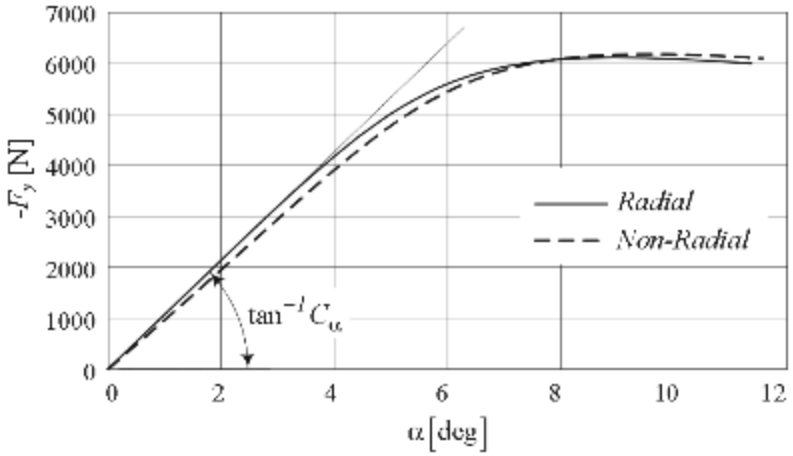

Figure 17-Effect of Slip angle for Constant vertical load[37]

3.2.1.2 Effect of load on Lateral Force vs Slip angle

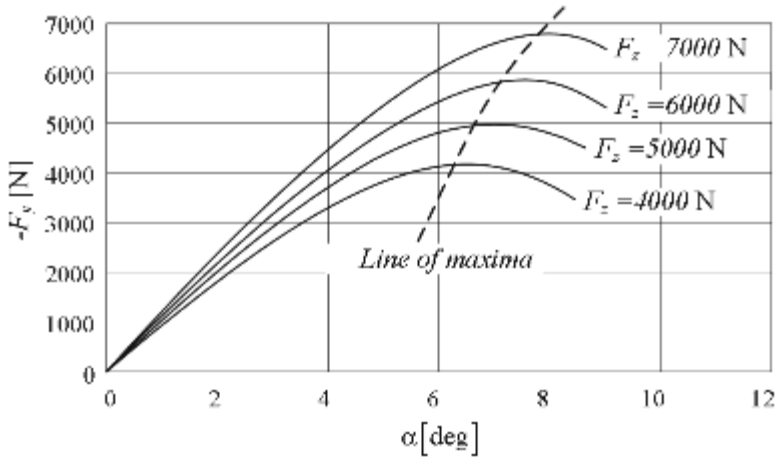

Figure 18-Effect of Load on Fy vs slip angle[37]

As can be seen from Figure 18 the Lateral force increases for a given slip angle with increase in load. Also, the peak slip angle value increases with increase in load.

3.2.1.3 Effect of Velocity on Force vs Slip angle

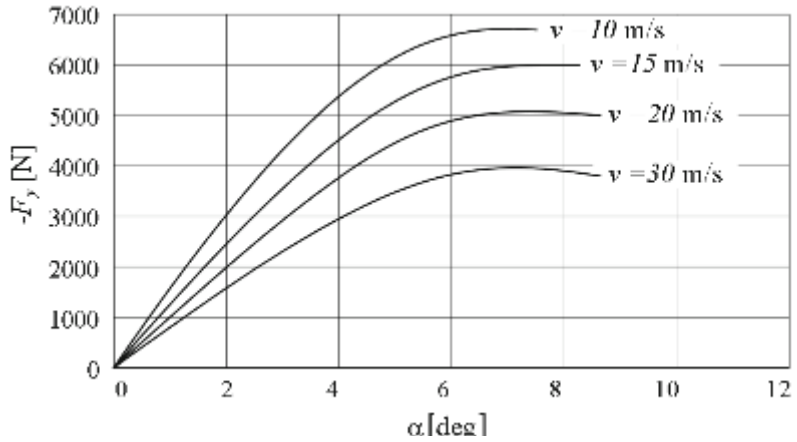

Figure 19-Effect of Velocity on Fy vs Slip angle[37]

As can be seen from Figure 19 the curve of the lateral force vs slip angle decreases as velocity increases. Hence the sideslip angle needs to be increased at higher velocities to generate same lateral force.

3.2.1.4 Effect of Tire pressure on Force vs Slip angle

Increasing the inflation pressure increases the carcass stiffness but reduces contact length, hence the net influence of tire pressure on cornering stiffness cannot be generalized. However, its generally accepted that increasing the inflation pressure increases the cornering stiffness for passenger car tires[38].

3.2.2 Tire Contact Patch: Longitudinal Dynamics

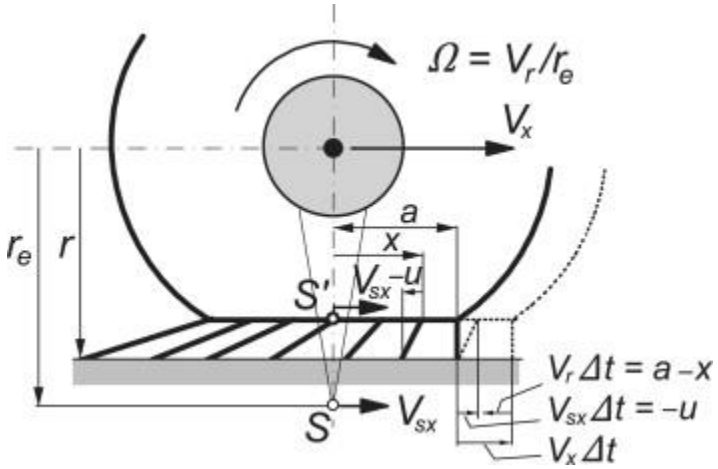

Figure 20-Brush Model Braking[38]

The tire contact patch dynamics for longitudinal deformation can also be explained using the Tire brush model. In case of the longitudinal deformation as can be seen in Figure 20 the bristles are deflected backwards for braking and forward in case of acceleration.

The Longitudinal force has a correlation with the slip ratio, the slip ratio depends on the vehicle translational velocity and the wheel rotational velocity as shown in Equation 5

$$s = \frac{R\omega_w}{V_x} - 1$$

Equation 5[37]

$$R: Radius\ of\ tire$$

$$\omega_w: Angular\ velocity\ of\ \ wheel$$

$$V_x: Translational\ Velocity\ of\ Vehicle$$

Figure 21 shows the nature of the Friction vs Slip Ratio Curve

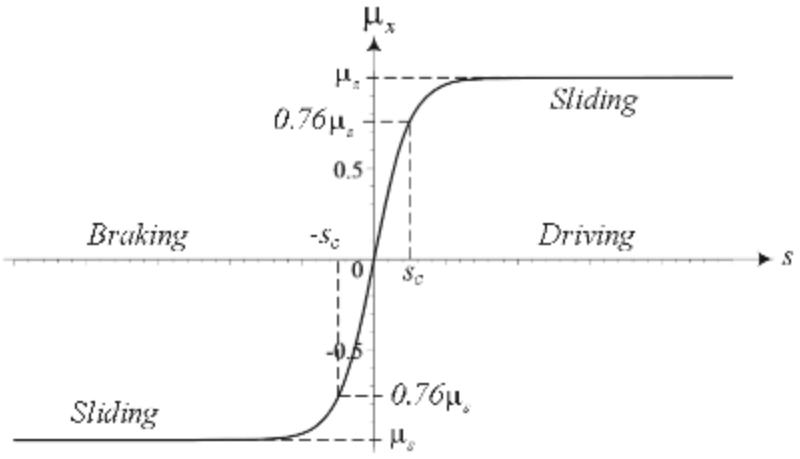

Figure 21-Friction vs Slip Ratio[37]

3.2.3 Tire Contact Patch: Vertical Force

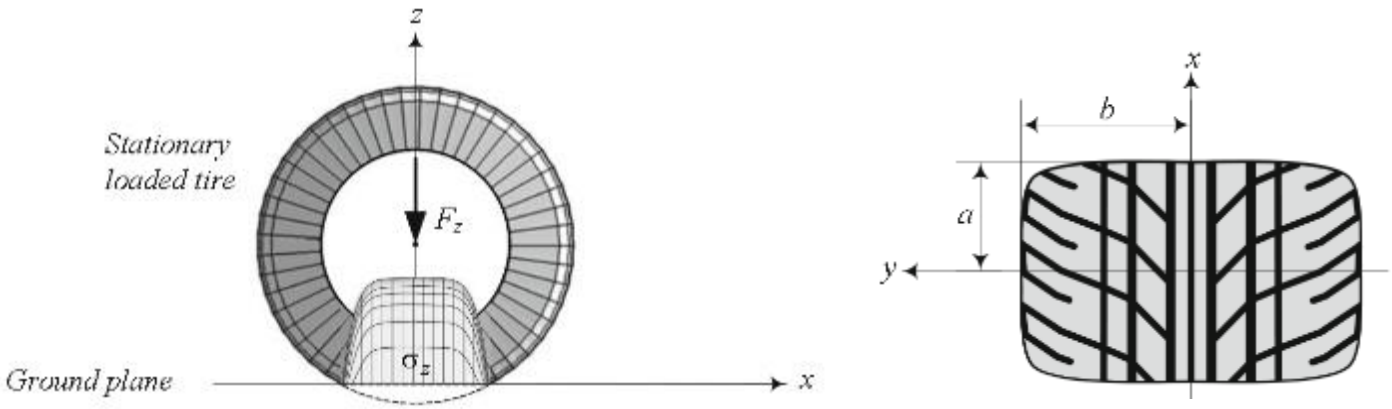

Figure 22-(Left)Loaded Tire (Right) Tire Footprint[37]

The force per unit area applied on a tire in the tire print area can be decomposed into a component normal to the ground and a tangential component on the ground. The normal component is the contact pressure while the tangential component can be further divided into x and y directions (longitudinal and lateral shear stress)

The normal stress and tire footprint shape (radial tire) can be approximated using the function

shown in Equation 6 & Equation 7 respectively.

$$\sigma_z(x,y) = \sigma_{zM}(1 - \frac{x^6}{a^6} - \frac{y^6}{b^6})$$

Equation 6

$$\frac{x^6}{a^6} + \frac{y^6}{b^6}$$

Equation 7

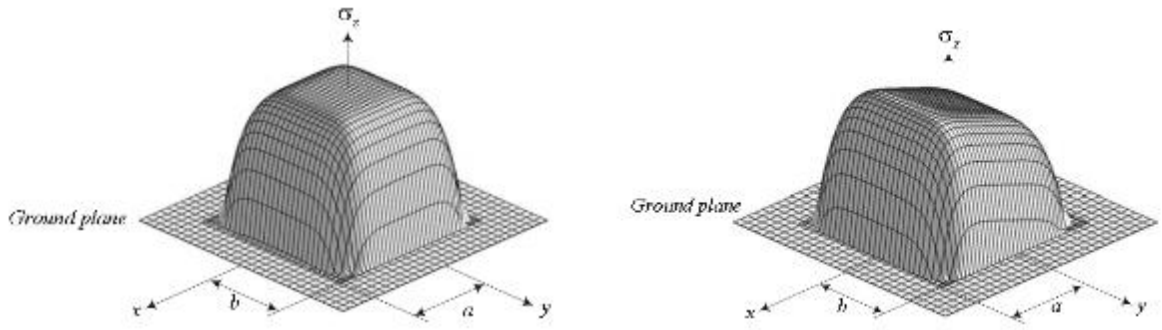

Figure 23-(Left)Normal Stress Distribution for a static tire (Right) Normal stress distribution for a rolling tire[37]

As can be seen from Figure 23 the normal stress distribution changes when the tire is rolling, this change can be accounted because of the rolling resistance or the longitudinal force acting on the tire.

3.3 Intelligent tire signal characteristics and sensitivity analysis

This section describes the characteristics of the Radial, Lateral, Circumferential signal obtained using the intelligent tire accelerometer. The signals have been analyzed for noise characteristics and sensitivity to speed and steering input. This analysis is essential before heading towards finding regressors related to tire forces.

3.3.1 Intelligent Tire Signal Analysis for Noise

This section covers some basic analysis of signals for Noise in frequency domain and the estimation of SNR for different excitations. The noise in sensor measurements can originate from various sources, most of the noises are white random noise, having uniform distribution. But there can be some colored noises as well for e.g. DC-AC power conversion noise (dominant around 60Hz). The noise analysis for two cases is shown below:

3.3.1.1 Noise analysis for Straight Constant speed

In this analysis, the vehicle is running at 10mph which is the minimum speed of interest. The

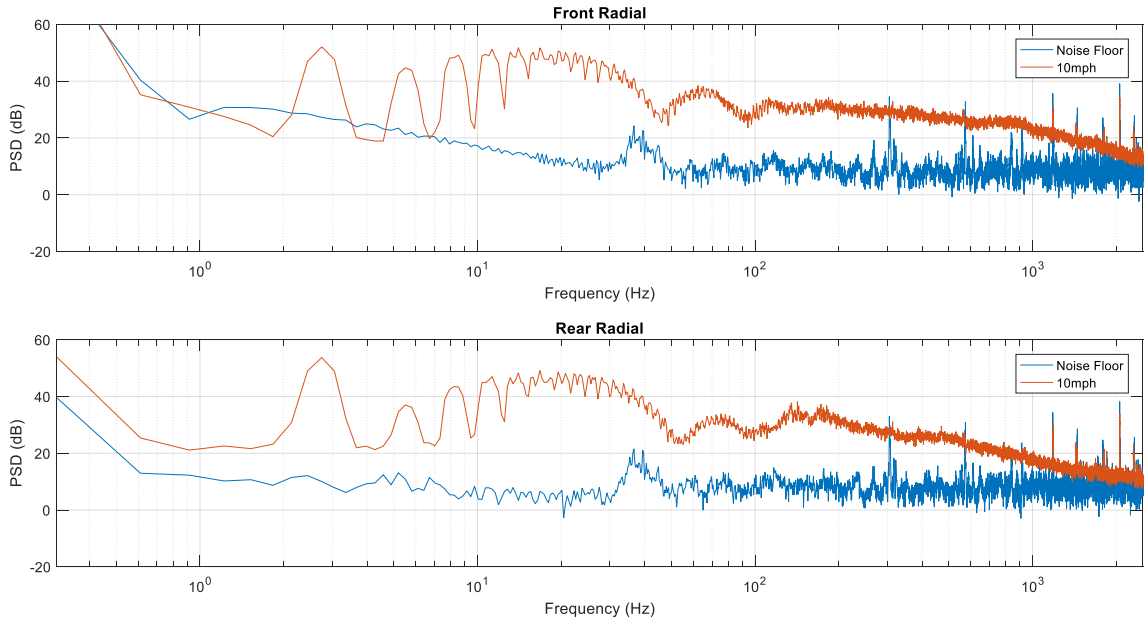

Figure 24-Noise Analysis for Straight Running Radial Direction

noise signal was collected by acquisition of data without any excitation to the sensors. The vehicle is then run at 10mph and the signal of the three accelerometers is plotted on the noise signal for each front and rear accelerometer. The SNR (signal to noise ratio was then calculated for each signal)

From the observations as described in later sections, it was observed that the main frequency of interest for the speed/steering range lies within 2-200Hz. Hence the SNR was calculated in this range.

SNR Front: 25.40 dB

SNR Rear: 24.88 dB

As can be seen from **Error! Reference source not found.** the signal lies above the noise floor a nd the SNR value is high hence meaningful information can be extracted from the radial sensor signal.

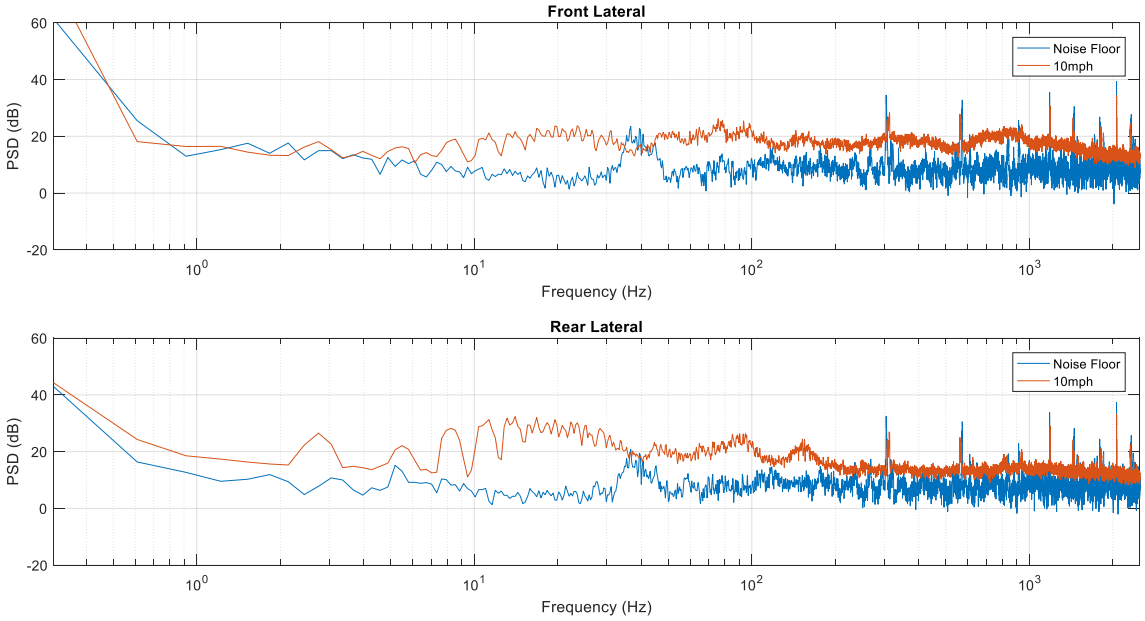

Figure 25-Noise Analysis of Lateral Signal for Straight Running 10mph

SNR Front: 8.58 dB

SNR Rear: 12.77 dB

The signal is close to the noise floor and the SNR is also low which is expected since the vehicle is running straight there is no excitation in the lateral direction. However, there is some excitation observed which might be because of the alignment geometry of the vehicle (toe, camber).

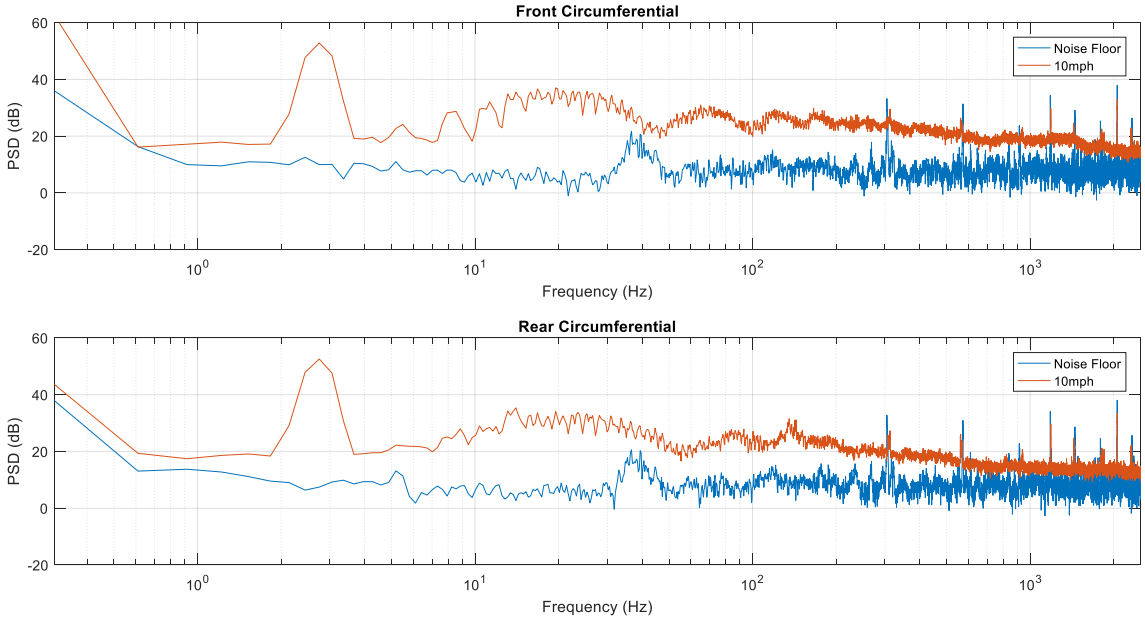

Figure 26-Noise Analysis for Circumferential Signal Straight Running 10mph

SNR Front: 19.68 dB

SNR Rear: 18.85 dB

The circumferential signal has a good SNR and the frequency plot is above the noise floor, hence some meaningful parameters can be extracted from this data at 10mph straight running.

3.3.1.2 Noise Analysis for Steering of 0.2g sweep

Since for straight running the lateral acceleration signal is not excited, the lateral acceleration signal is checked for a Steering sweep signal of 0.2g. As can be seen from Figure 27 the signal is above the noise floor and the SNR values are higher, hence the signal can be used to extract meaningful information.

SNR Front: 14.08 dB
SNR Rear: 16.09 dB

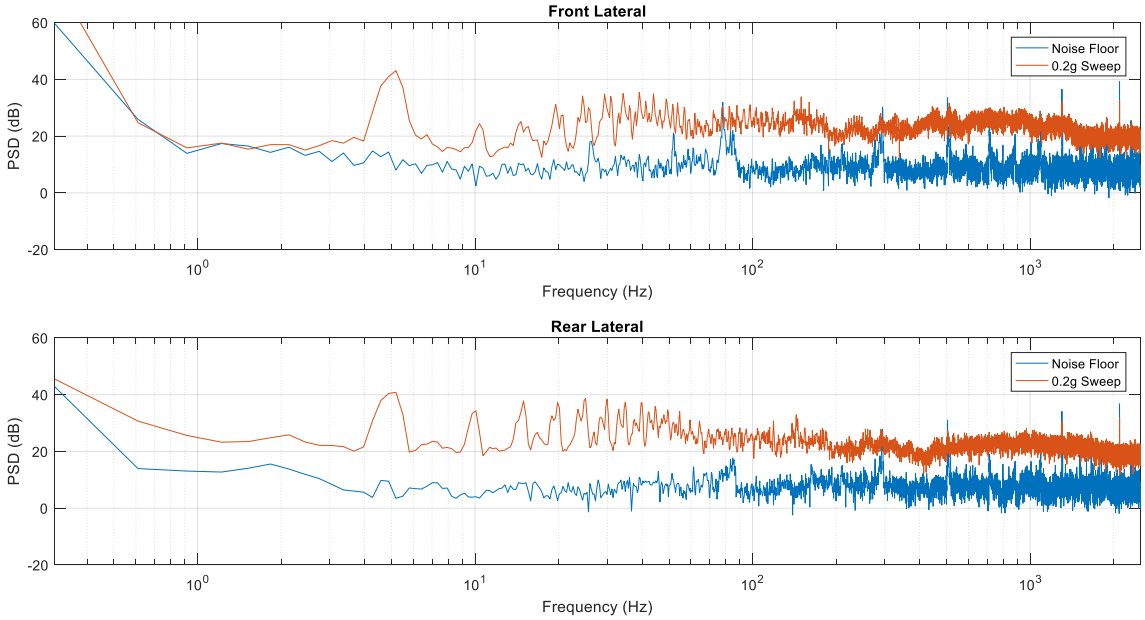

Figure 27- Noise Analysis Lateral Signal for 0.2g sweep

3.3.2 Analysis of Intelligent Tire signal for Speed and Steering

This section focuses on the analysis of the intelligent tire signal in the frequency domain to extract frequencies of interest for changes in steering, speed. Before getting into the discussion of results it's worth looking at some of the analysis done on tire vibrations using an accelerometer.

3.3.2.1 Literature on Tire Vibration analysis

The study done in [39] analyzed the motion of the point on the tread in radial direction as it goes through the revolution. The accelerometer placed inside the tire was single axes with radial direction measurement. The paper also states that the radial acceleration vibration can be formulated using the Equation 8

$$\tau(t)_{rm} = u_r(t) - \omega^2(\ddot{a}_0 + u_r(t))$$

Equation 8[39]

The first part of the equation is termed as "relative" and the second as "driving"
It then classifies the vibration into two categories:

- Stationary rolling motion: This vibration is characterized by the "driving" term of the equation and is periodic with period of $T = {}^{2\pi}/_{\omega}$. These vibrations are of low frequencies.
- Bending waves motion: These vibrations are characterized by the "relative" term of the equation above and are induced by the interaction of the road and tire.

The paper goes ahead with analyzing the effect of rolling speed on tread vibration and states that the magnitude of each spectrum is shifted up when the rolling speed is increased.

Another study done in[40] analyzes the lateral vibration of the vibration caused due to wheel alignment settings(toe, camber). This paper formulates the lateral force acting on the tire tread as a forced spring damper system as show in Equation 9.

$$m\ddot{s} + c\dot{s} + Ks + F_y(V_r) = 0$$

Equation 9

Where $F_y(V_r)$ is the lateral force caused due to tire friction. The paper also states that load, tire pressure and speed have significant effect on the lateral tread vibrations.

3.3.2.2 Effect of Tire rolling speed on the Intelligent Tire signal

The study done in [40][39] concludes that rolling speed has an effect on the radial and lateral signal of the tire. This section compares the straight running at constant speed for three different rolling speeds(12mph,20mph,30mph). The result is shown in Figure 28. The following observations were made from this analysis:

- The first peak in the Radial and Circumferential signal corresponds to the angular speed of the wheel. Also, it is noticed that the peak's shifts to the right with increase in rolling speed. These peaks are caused due to the accelerometer experiencing jerk caused because when the tire hits the ground.
- The other peaks, after the first one which are the harmonics can be described in terms of the first peak. E.g. the nth peak will have frequency of:

$$freq(nth\ peak) \approx n * f(\ f = freq\ of\ first\ peak)$$

Equation 10

- The magnitude shifts up with increase in rolling speed for all the three axis, however the peak are almost the same magnitude at lower frequencies but increase with increase in frequency.
- The magnitude doesn't go down much at higher frequencies which indicates some useful information even at those frequencies.
- The tire resonance modes can be seen dominating in the region of 10-100 Hz and it can also be seen in 100-600Hz but with lower power.

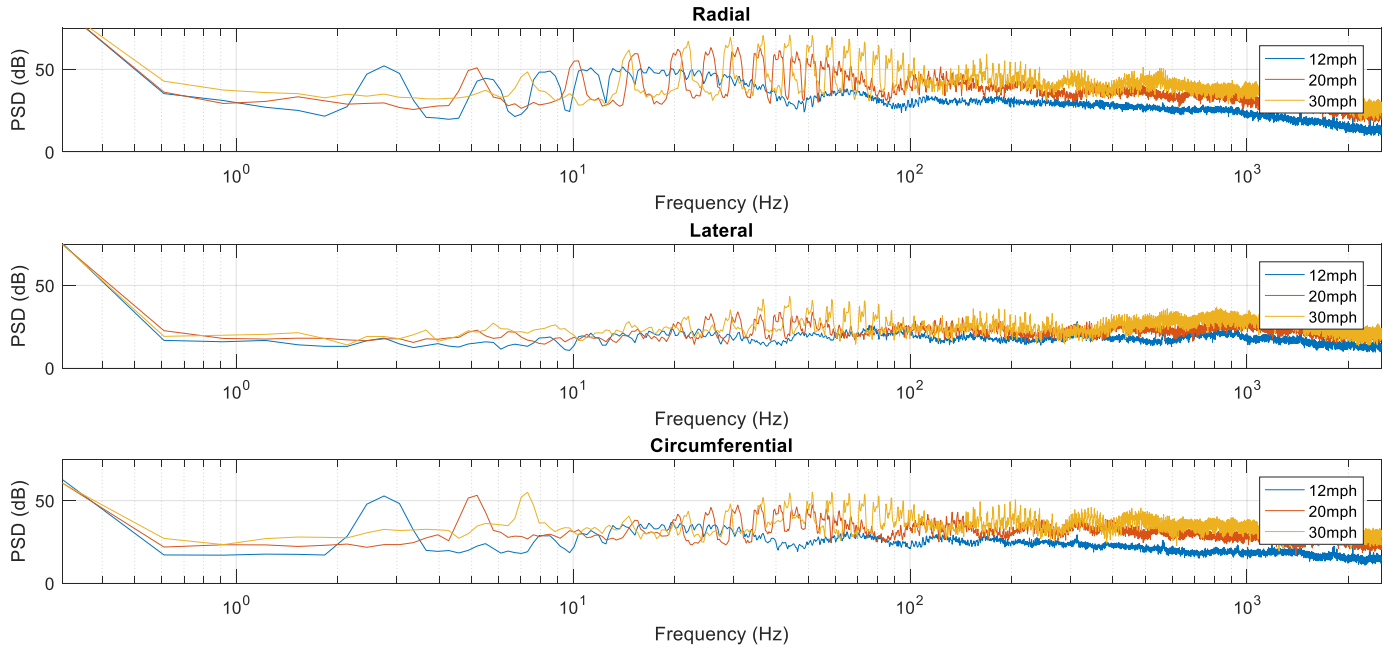

Figure 28-Effect of Rolling speed on Intelligent Tire signal

3.3.2.3 Effect of Steering Maneuver on Intelligent Tire signal

In this section, the effect of steering maneuver on the intelligent tire signal is analyzed in the frequency domain. The two cases compared are:

- Vehicle running at 30mph with no steering input.
- Vehicle running at 30mph with a 0.3g Sine Steering input.

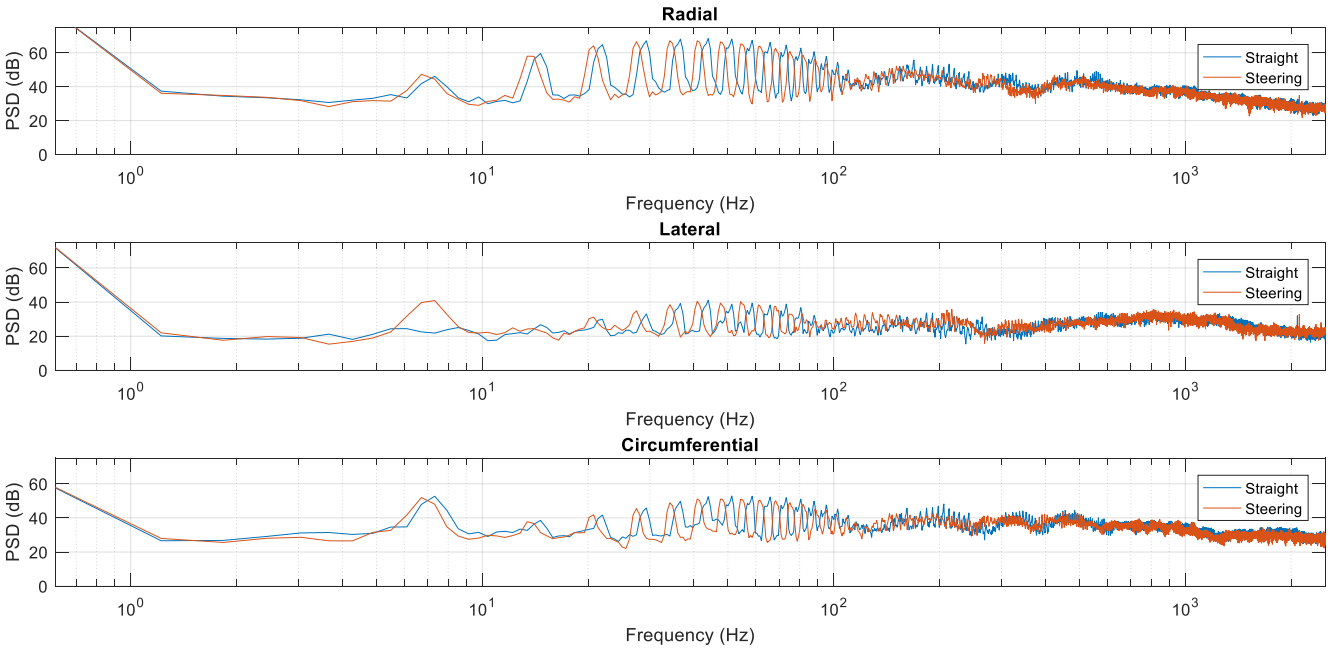

Figure 29-Effect of Steering on Intelligent Tire Signal at 30mph

As can be seen from Figure 29 the since the speed was kept constant in both the cases Steering maneuver had an effect only on the Lateral acceleration signal, also it was noticed that the first peak of the lateral acceleration signal had a major change because of the Steering maneuver.

3.3.3 Time domain analysis of Intelligent Tire Signal

The frequency domain analysis gives a good indication of the signal characteristics for the Intelligent Tire signal, however analyzing the signal in frequency domain requires some batch of data (revolutions in this case). The advantage of considering time domain is that the signal can be analyzed at every revolution and features can be extracted out of it. The unfiltered and filtered signals are shown in Figure 31 & Figure 30. The filter used here is a bandpass Butterworth filter of 2-200 Hz.

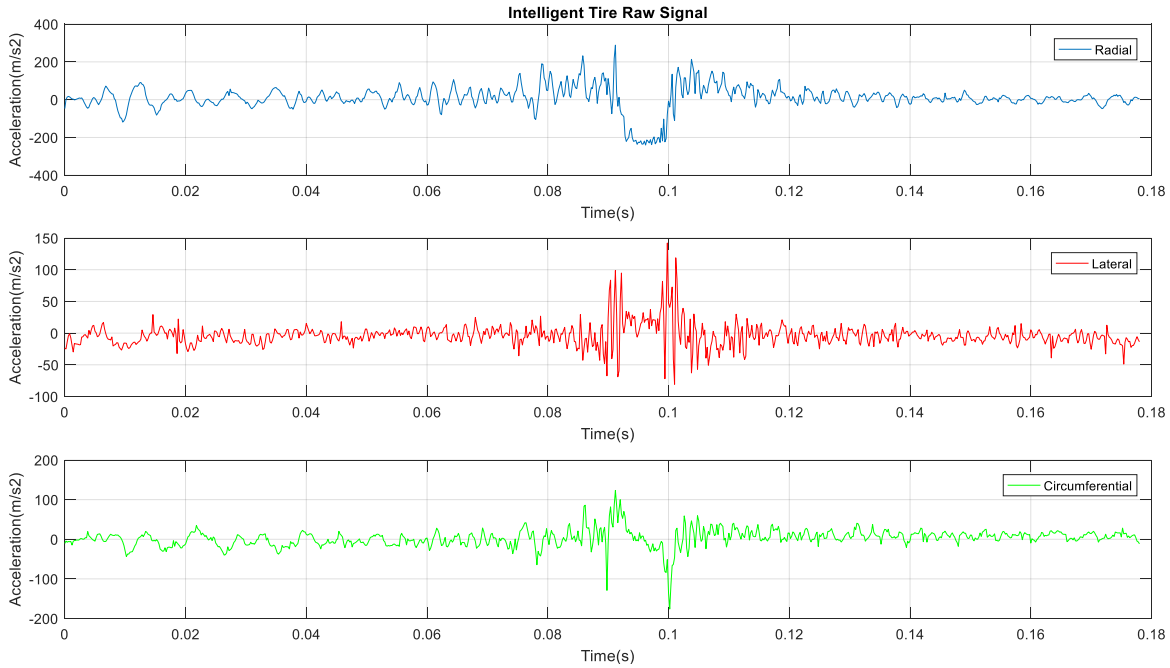

Figure 31-Unfiltered Intelligent Tire Signal One revolution

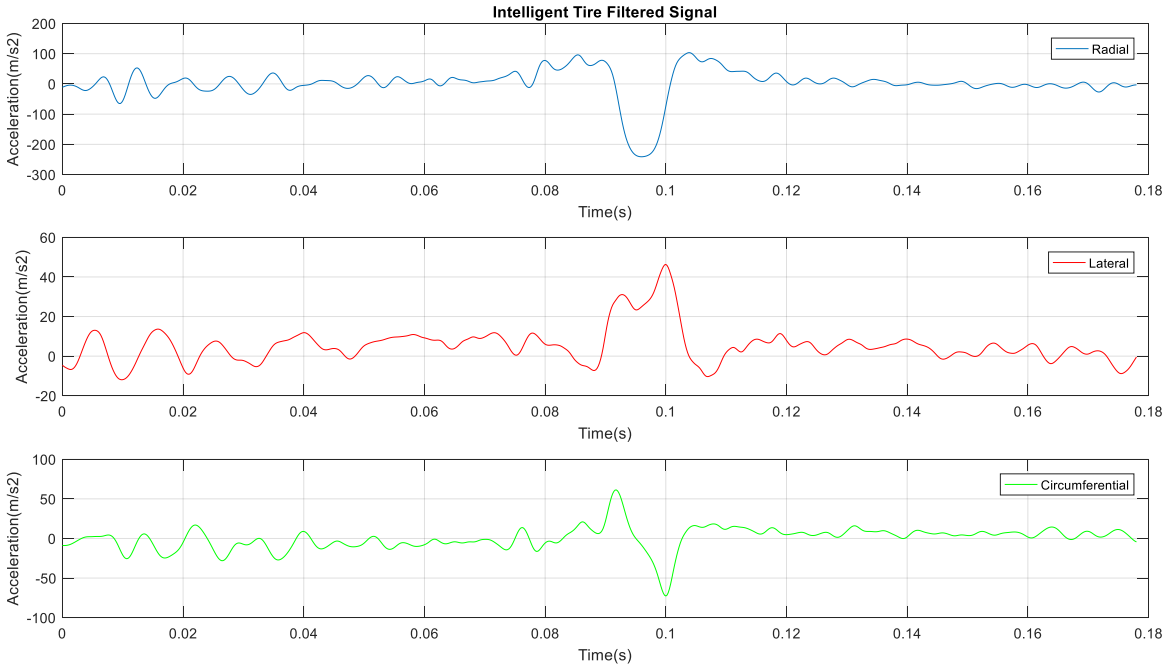

Figure 30-Filtered Time Domain Signal One revolution

- Each accelerometer has a rise/fall in magnitude once every revolution which can be related to its contact with the road surface.

- The radial and longitudinal accelerations can be used to extract the leading and trailing edge of the contact patch, this has been discussed in detail in the later sections.
- The magnitude of the radial signal is the highest compared with the other two signals, this can be related to the impact due to the load on tire in the Z direction.

3.4 Applications of Contact Patch Length estimation

The contact patch length of the tire has a strong correlation with the load acting on the tire. A lot of published literature can be found with regards to this relation. This section explores the possibility of using the load estimation algorithm developed in [41] to estimate the lateral and longitudinal load transfer due to steering & acceleration/ braking maneuvers. This load transfer algorithm can be used in conjunction with the roll estimation algorithms to predict the roll over limit for the vehicle. The advantage of having an accelerometer in the center of the tire is that it is insensitive to the effects of lateral force/camber/toe and can be used to estimate the contact length in all conditions.
Before going into the details of the algorithms. Some of the literature has been reviewed in the section below.

3.4.1 Literature for Contact Patch length estimation and its relation to load.

In the study conducted by [27] the contact patch has been denoted in terms of the angle subtended by the leading and trailing edge at the center of the wheel. It states that this angle which corresponds to the contact patch length changes when applied with a normal load. The patent[42] describes a second order polynomial relation between the contact patch length and the normal load.

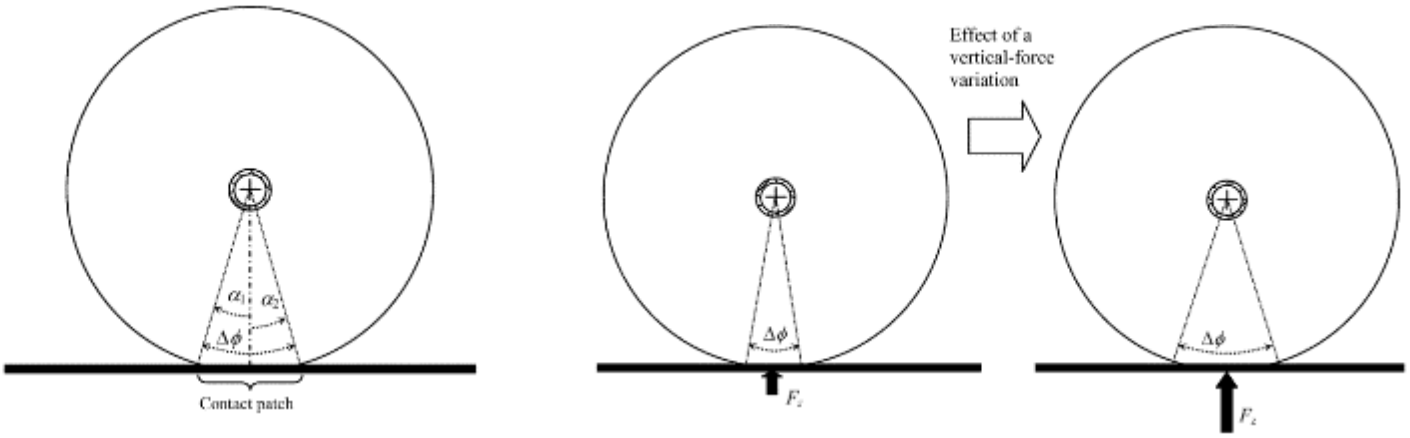

Figure 32-Change of Contact Patch angle with load[27]

The algorithm stated in this study to estimate the leading and trailing edge is to detect the zero crossing of the descending and ascending edge of the radial accelerometer signal.

In the studies conducted by [26][41] the leading and trailing edge of the contact patch length has been estimated using the circumferential acceleration signal. The peaks as can be seen in the circumferential signal in Figure 30 are stated as the leading and trailing edges of the contact patch

Another study [23] used the differential of the radial acceleration signal referred to as the jerk signal to estimate the leading and trailing edge of the contact patch.
The contact patch length can be estimated knowing the “Time” which the tire was in contact with the road the “Rotational speed” of the wheel and the “Radius” of the wheel.

3.4.2 Comparison of the different leading trailing edge techniques

This section compares the three techniques given in literature to detect the leading and trailing edge of the contact patch. In this study, it was found that zero detection technique is not robust for detecting the edges, the reason being that the exact zero crossing point is difficult to detect and needs some computations/interpolation. Hence the two techniques using the Circumferential signal and Jerk signal (derived from Radial signal) have been compared for two scenarios:

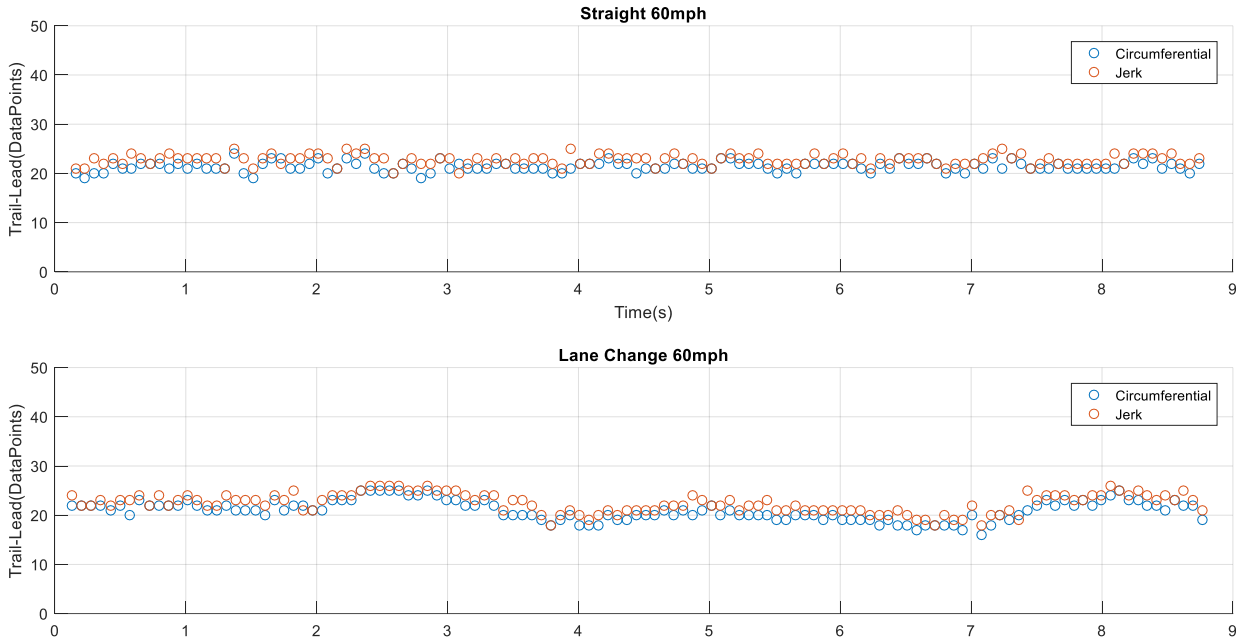

Figure 33-Comparison of Techniques for Contact patch edge detection

Straight Running at 60mph, Lane change maneuver at 60mph. Higher speed was chosen to compare the results, since the estimation is difficult at higher speeds.

The plot in Figure 33 shows the comparison of the (Trailing Edge-Leading Edge) data points for the Circumferential and the Jerk based method. The Figure 34 shows cross correlation of circumferential and jerk signal at different speeds, the peak is obtained at the same lag in both the cases, which means that it is insensitive to speed variation. Both the methods give similar results as can be seen from the plot above and can be used to estimate the Time tire was in contact. In this study, a fusion of both the methods has been used to overcome the short comings of one another in case of any corrupt signal from one of the axis.

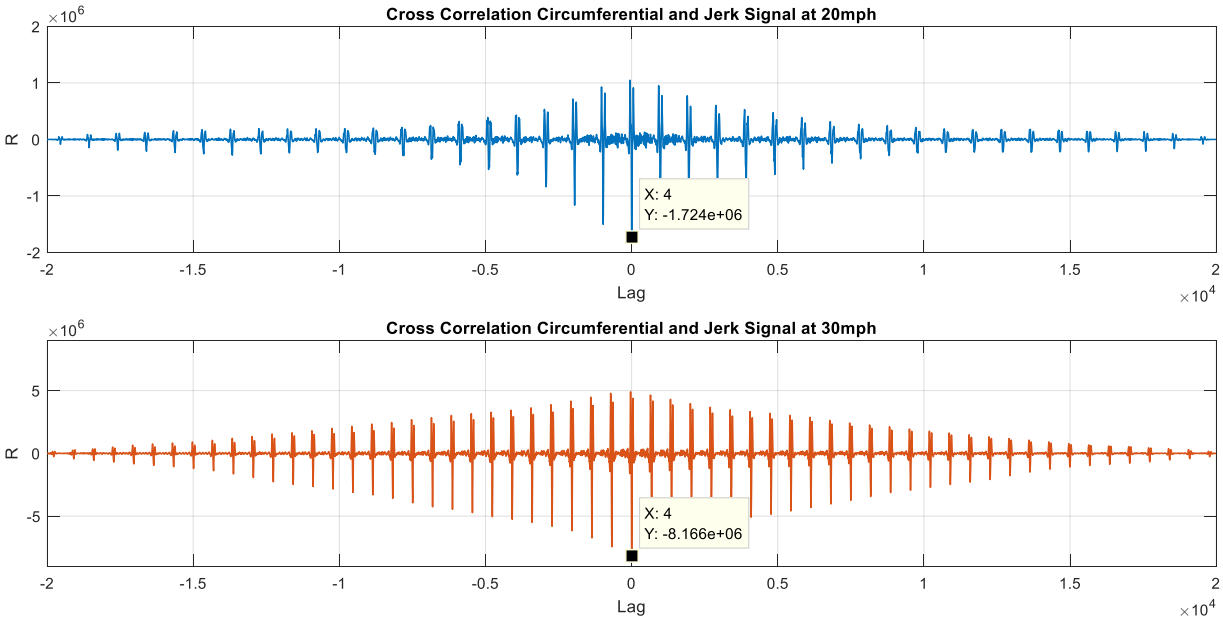

Figure 34-Cross Correlation of Circumferential and Jerk Signal

3.4.3 Derivation of Wheel Speed from the Encoder signal

The encoder was set in a mode to detect each wheel rotation as shown in Figure 35(1). This configuration of the encoder was chosen to separate each wheel rotation

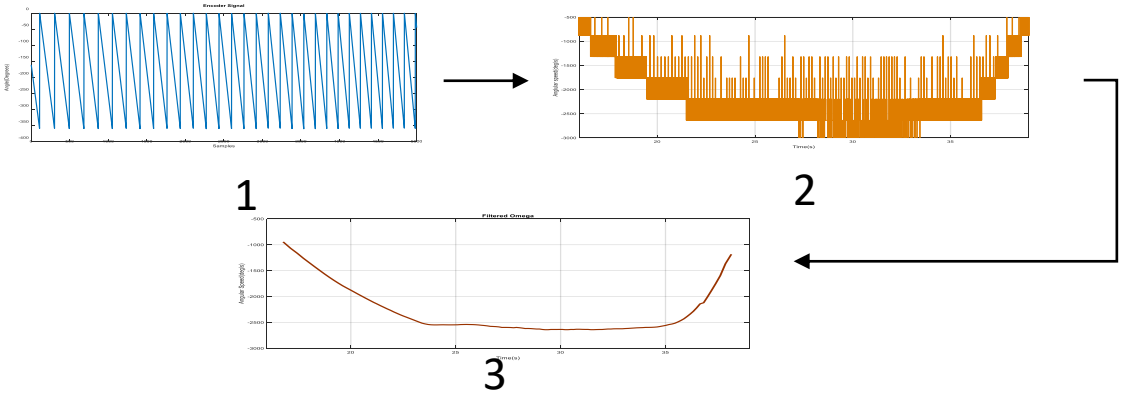

Figure 35-Encoder Angular Speed

1. The raw encoder signal (resets to 0 after one complete rotation)
2. Converted to angular displacement and derivative is taken to get angular speed(noisy)
3. Result after smoothing the noisy angular speed.

3.4.4 Load Transfer estimation and its applications

This section expands the applications of load estimation algorithms developed in[41] to dynamic maneuvers such as steering and braking/acceleration. In the study conducted in [41] the contact patch length is found to have effect on three factors

- Load
- Speed of the Wheel
- Tire pressure

The study also found that the tire pressure and wheel speed had a good correlation with the "Radial Peak Difference" as shown in Figure 36. It was also found that between tire pressure and speed, tire pressure has more influence on the length of the contact patch.

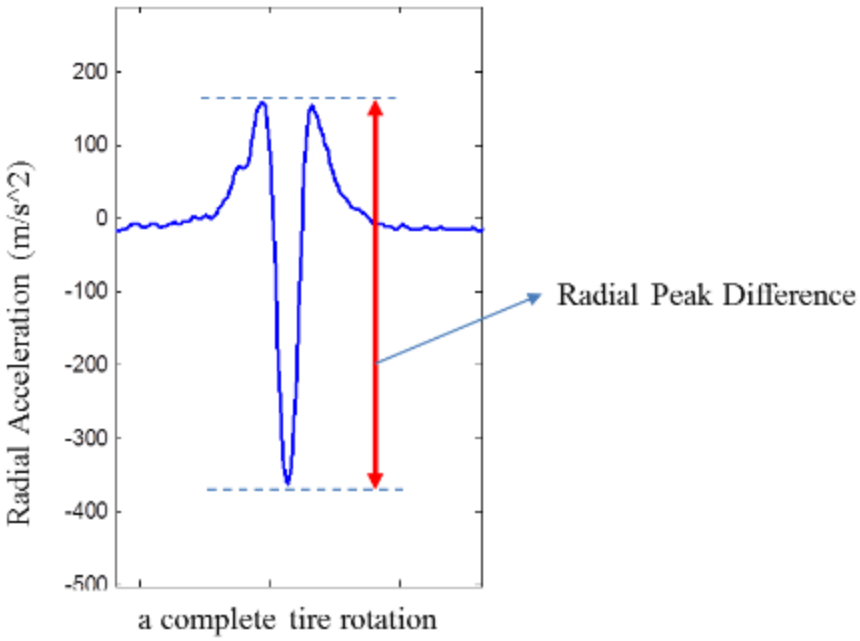

Figure 36-Radial Peak Difference

In this study, the objective is to find a correlation between the load transfer caused due to steering/acceleration/braking and the change of contact patch length. The factors of speed and tire pressure have been kept constant in the test conditions.

Two maneuvers were tested to check for change in contact patch length as shown in Figure 37 & Figure 38

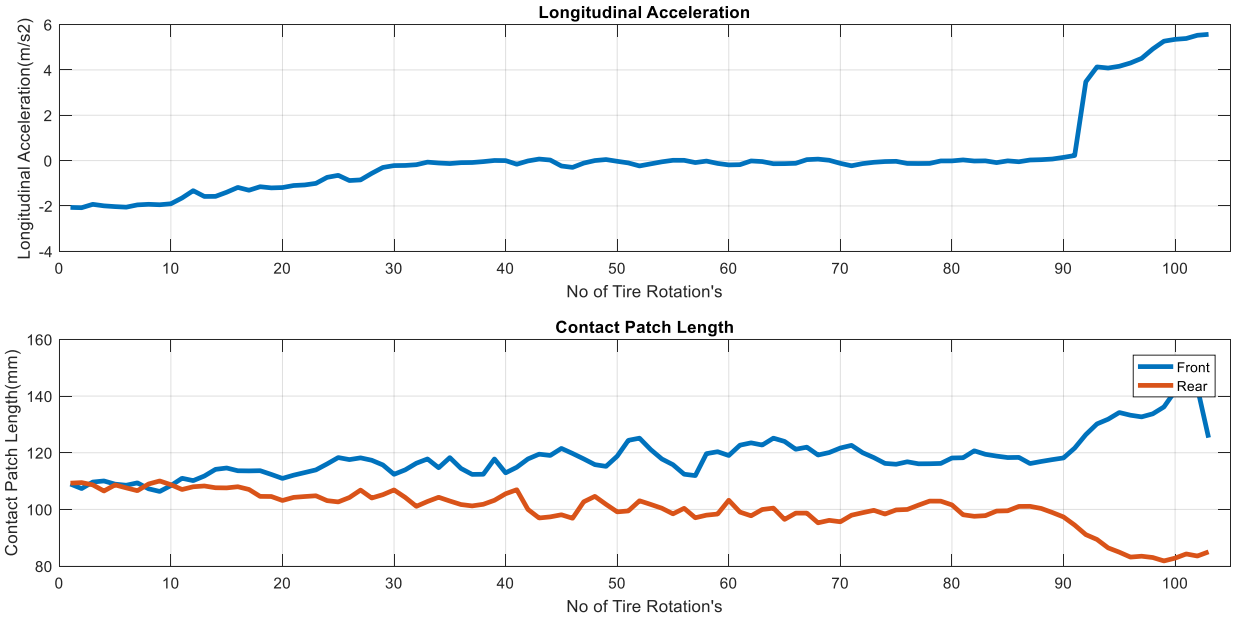

Figure 37-Contact Patch Length-Braking

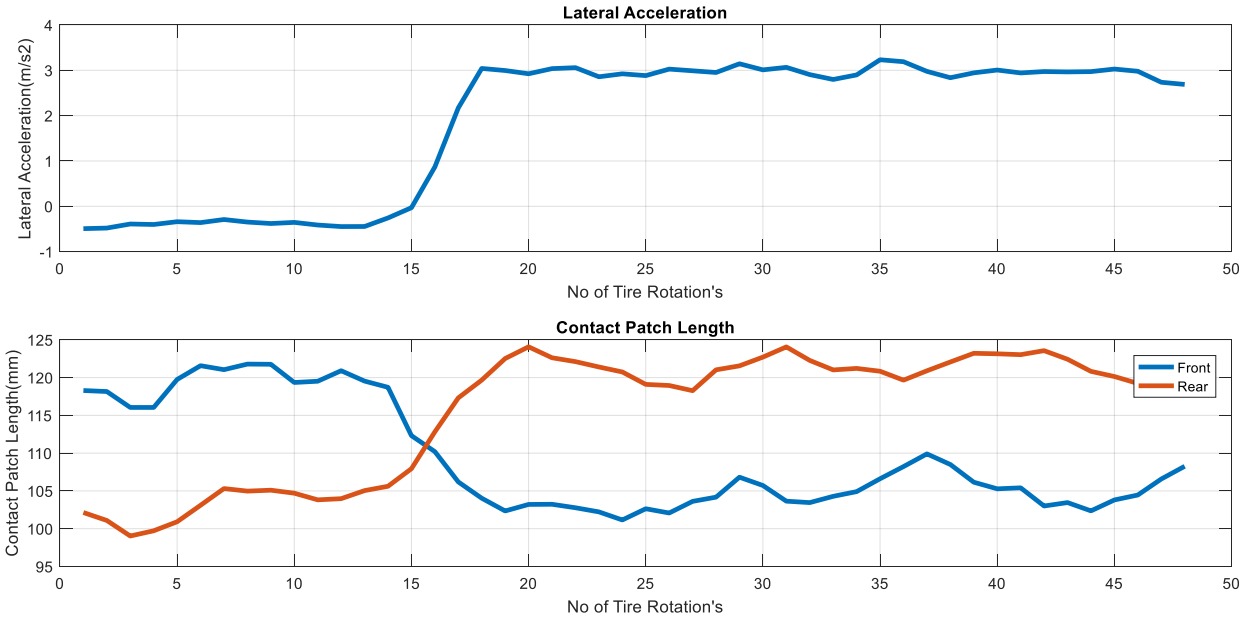

Figure 38-Contact Patch Length-Lateral Acceleration

- From Figure 37 when braking the front contact length increases and the rear contact length decreases. During braking the load transfer occurs from the rear to the front and we know that the contact patch length increases when normal load is applied to the tire. Hence it can be said that longitudinal load transfer can be detected using the contact patch length/Normal load estimation algorithm

- From Figure 38 when steering to the right (load transfer to the left side of the vehicle) the Rear left tire contact patch increases and the Front Right tire contact patch decreases. Hence contact patch length (at constant speed/tire pressure) can be used to estimate the load transfer.

3.4.4.1 Applications of Load Transfer estimation algorithm

Lateral load transfer is an important criterion when it comes to vehicle stability and performance. Excessive load transfer can result in losing the traction or rollover. One of the uses of contact patch length based load transfer estimation can be to estimate the Lateral Load Transfer Ratio.

Lateral Load Transfer Ratio(LTR)

Rollover prevention and detection have been studied by many researchers[43][44][45]. Most of the study conducted in this area has been through estimation of load transfer based on vehicle dynamics model using measurements from Inertial Sensors (Lateral Acceleration, Roll Rate, Yaw Rate).

In [46] a study on LTR based rollover detection is conducted. LTR is defined as shown in Equation 11

$$LTR = \frac{F_{zR} - F_{zL}}{F_{zR} + F_{zL}}$$

Equation 11

LTR varies between -1 to +1, extremes correspond to the rollover point and zero means that the normal forces on both the sides of the vehicle are equal.

In this study since only one sensor was used on each axle (Front Right and Rear Left). The LTR based algorithm cannot be implemented, however if the vehicle has all the four wheels equipped with intelligent tires. As stated in the earlier section the contact patch length depends on the tire pressure and the normal load acting on it. However, the accurate determination of tire pressure is difficult unless there is an additional sensor installed for it.
An algorithm is developed to be used in conjunction with the normal load estimation algorithm. This algorithm can be used along with the vehicle dynamics based load transfer to improve the accuracy of model based estimations.

The assumptions taken in this algorithm are:

- All the wheels have almost the same angular speed.
- All the tires are running on the same surface.
- Diagonal Load transfer is not considered.

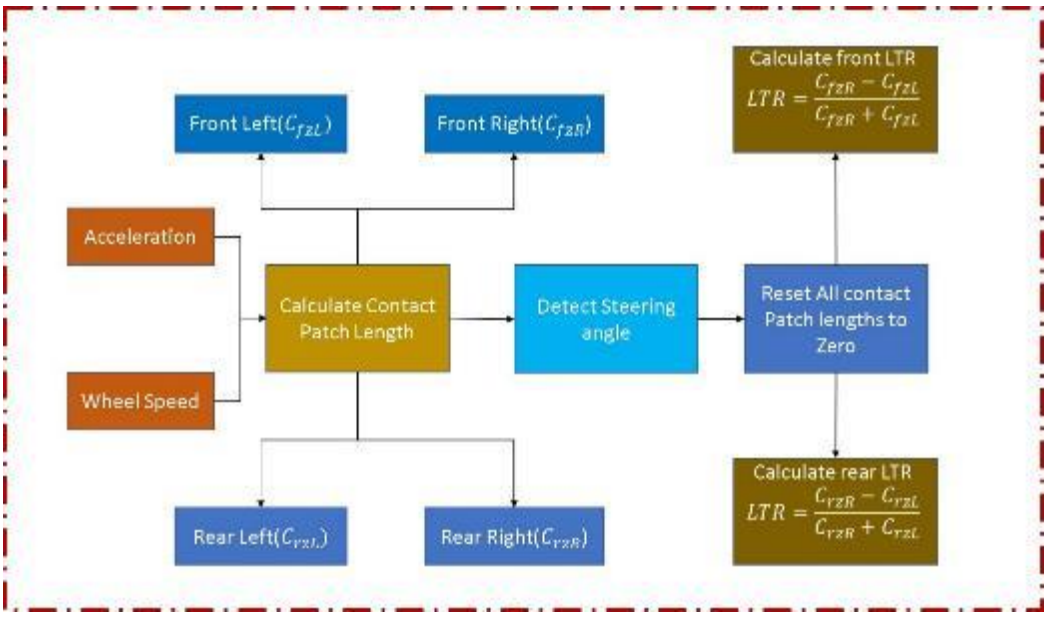

Figure 39-LTR calculation based on contact patch lengths

3.5 Development for Lateral Force/Slip angle Indicator

This section explores the Intelligent tire signal to find indicators for Lateral Force/Slip angle of the tire. The information can be used along with the friction potential available at the surface to limit the force/slip angle to a maximum threshold.

Studies have been conducted in the past to find potential indicators in accelerometer signal to estimate the force acting on the tire. Few of the techniques used are discussed in the section below.

3.5.1 Literature review

The study conducted by[25][47] uses three accelerometers inside the contact patch, one in center and two on each side of the center line as shown in Figure 41. Slip angle, camber is estimated through the shape of the contact patch, which in turn is estimated using the contact lengths of the three accelerometers as discussed in sections above.

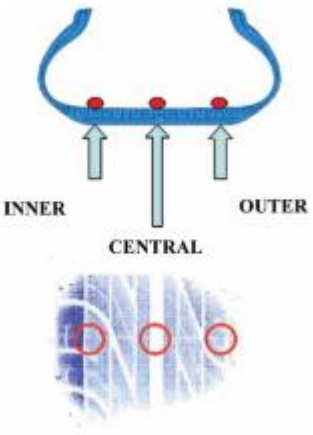

Figure 41-3 Accelerometer inside tire[25]

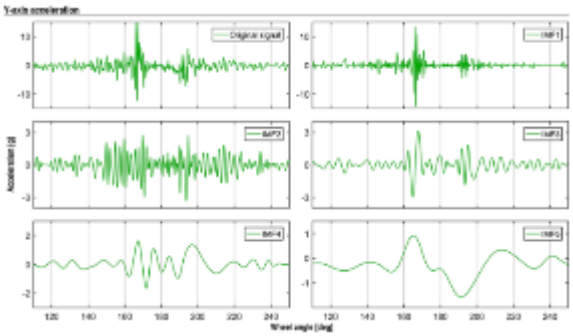

Figure 40-IMF Decomposition Lateral Signal

Another study in this area[23] uses single accelerometer at the center of the tire and integrates the lateral acceleration signal in the contact patch to get a lateral deflection profile and then curve fits the profile to get the coefficients using the Equation 12. The study also categorizes the deflection into two categories.

- Lateral Deflection with compressive force

- Lateral Deflection without compressive force

The compressive force refers to the stress developed due to the longitudinal force/rolling resistance on the tire when it hits the contact patch, this stress generates a force in the lateral direction of the tire, depending on the construction, material of the tire.

The study conducted in[48] uses Hilbert Huang Transform on the accelerometer signal to find the local sliding caused due to surface characteristics. The accelerometer signal is decomposed into subsections using the Intrinsic Mode Function as shown in Figure 40 and it states that some of the IMF's have correlation with the deflection of the tire which can be used to estimate the slip angle/force.
This study does not develop any algorithm but states that slip angle/force information can be extracted using lateral acceleration signal.

In the study,[49] states that the slip angle has a good correlation with the Root Mean square(per revolution) of the lateral acceleration signal from the intelligent tire. The study also states that the normal load has a big contribution to the lateral acceleration signal from the intelligent tire.

3.5.2 Frequency Domain analysis of Lateral Acceleration Signal

This section explores the lateral acceleration signal in the frequency domain to get the range of frequencies excited when a steering maneuver is conducted. Short Time Fourier transform is used to get the spectrogram of the lateral acceleration signal. The Lateral Acceleration of the Vehicle and the spectral content of the Intelligent tire lateral acceleration signal is shown in Figure 42 &Figure 43. The Vehicle speed was 30mph for the Sine Input and 60mph for the Double Lane Change. The following observations were made from the spectral analysis.

- Both the spectrogram plots show an increase in energy when there is an excitation in the lateral direction.
- The frequency range is different and has a relation with the speed of the vehicle. Although most of the primary energy is concentrated around the range of 0-250 Hz, the higher speed plot has some energy in the higher ranges till 400-500Hz.
- It can also be seen that the energy is concentrated in certain band of frequencies, this

phenomenon needs to be reviewed further.

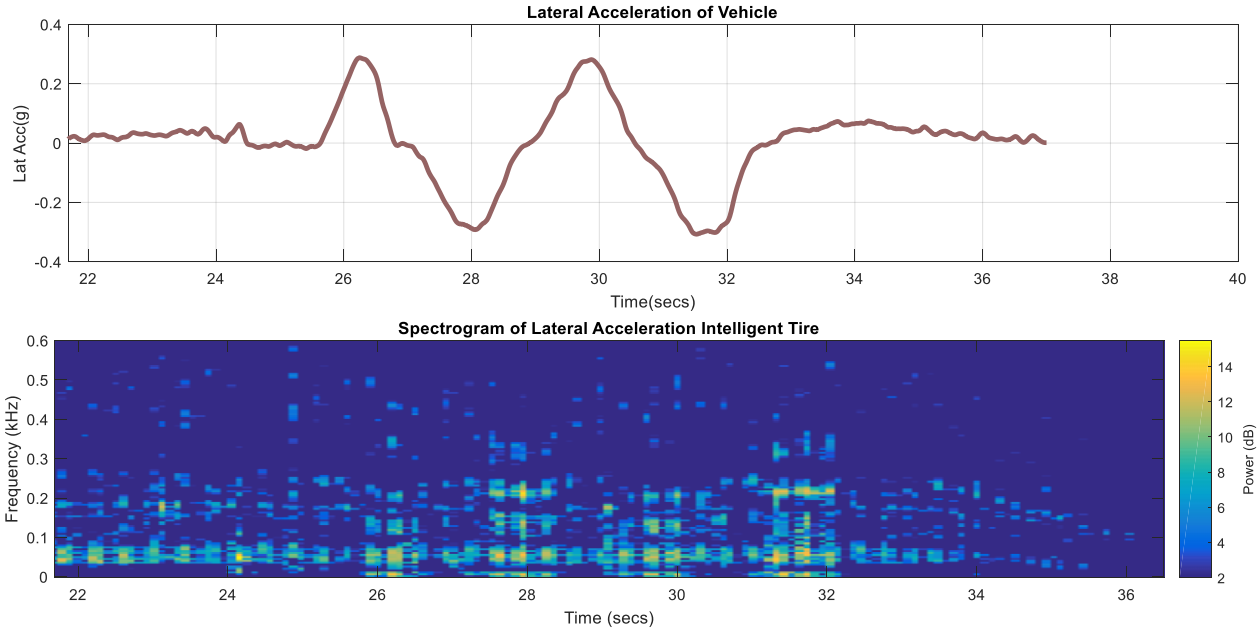

Figure 42-Spectrogram of Sine Input at 30mph

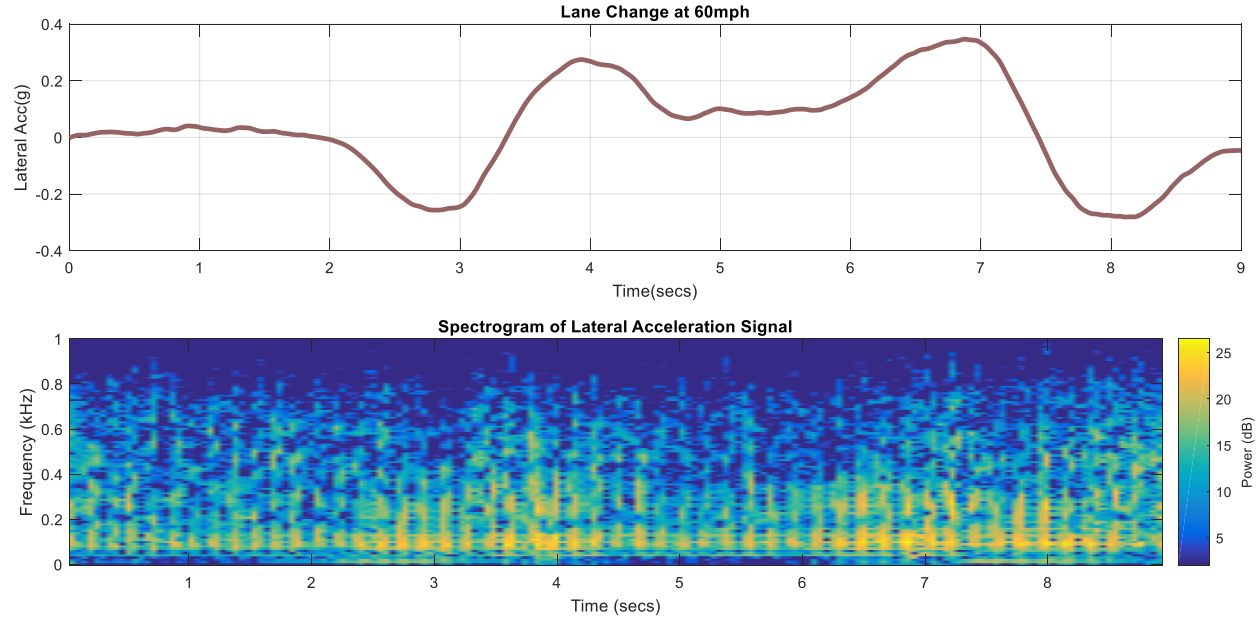

Figure 43-Spectrogram of Lane Change at 60mph

Hence based on the concentration of the spectral energy in the frequency range mentioned above,

it was decided to use a low pass filter with cutoff frequency of 200Hz.

3.5.3 Intelligent Tire Lateral Acceleration Signal Characteristics in Time domain

In this section, the lateral component of the Intelligent Tire signal is analyzed for its shape and potential features relating to force/slip angle.

Figure 44-Intelligent Tire Lateral Acceleration Signal one revolution

As can be seen from Figure 44, the lateral acceleration signal is sensitive to the direction of the force acting on it. The following observations can be made from the signal shape:

- The accelerometer registers a signal even when the vehicle is running straight, however the signal has around equal magnitude peaks in the positive and negative direction.
- For the left turn, from the leading edge the acceleration increases in the positive direction and had a small peak, followed by a high magnitude peak.
- For the right turn, at the leading edge the signal has a high magnitude peak and then registers a small peak. The nature of the peaks is different for the left and right turn, this needs to be explored further, however this can be caused due to the tire asymmetries.

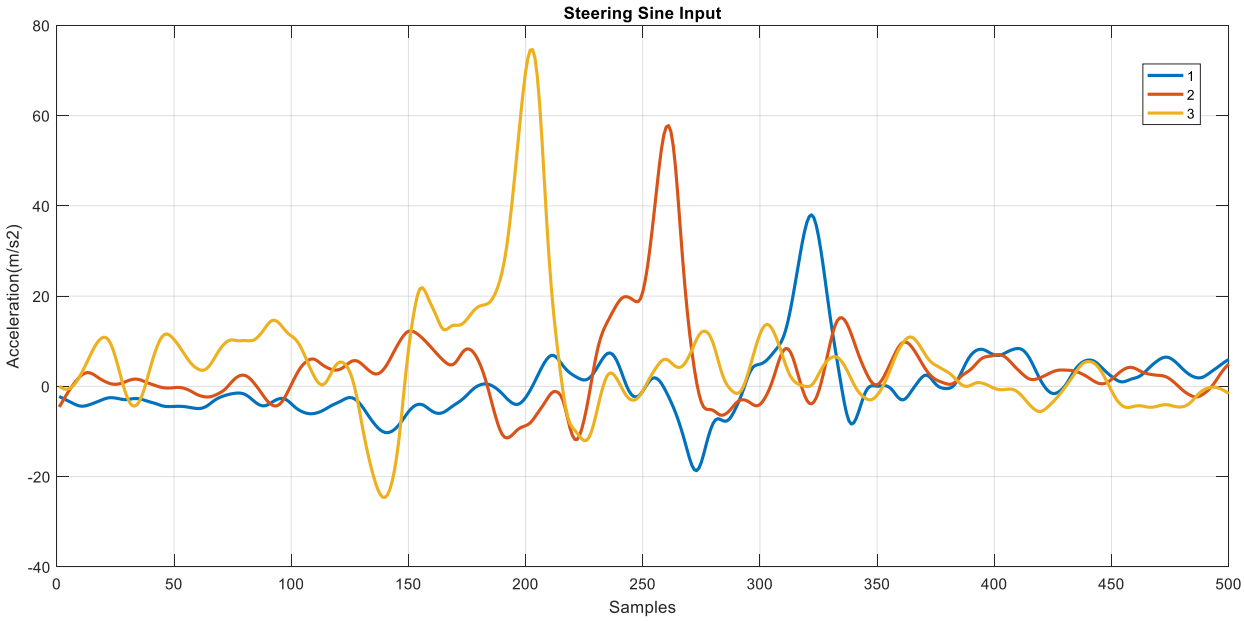

Figure 45-Intelligent Tire Lateral Signal (3 revolution) for Sine Steer Input

Test Condition: Speed-30mph, Maneuver: Sine Input (+/- 0.3g)

From the plot in Figure 45 it is seen that the lateral acceleration signal is sensitive to the magnitude change in the slip angle of the tire.

3.5.4 Identification of Features in the Lateral Acceleration Signal

In this section, various aspects of the Intelligent Tire Lateral acceleration signal are analyzed to find correlation with the Lateral Dynamics of the vehicle. The features which were analyzed are as below:

- RMS of each revolution
- Mean of each revolution
- RMS of each revolution in the Contact Patch
- Mean of each revolution in the Contact Patch

Before going through the results of this analysis. A brief description of the algorithm used to extract each revolution and contact patch edges is shown below.

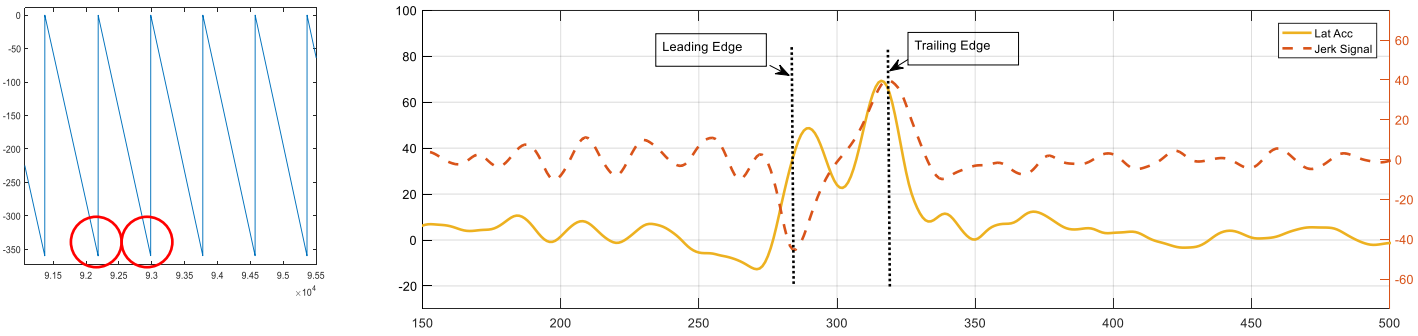

Figure 46-(Left)Encoder Signal (Right)Contact Patch Edge Detection

The figure on the (left)Figure 46 is the encoder signal set in the revolution mode. The edges of the encoder are detected when it goes to the peak and is used to separate each revolution of the tire. In the (Right) figure the contact patch leading and trailing edges are shown. The edges are found using the maximum and minimum peaks in each revolution. Since the jerk signal has good amplitude when it hits the contact patch, the contact patch edges can be extracted even in very low angular speed cases as well. It is worth mentioning here that before analyzing the features,

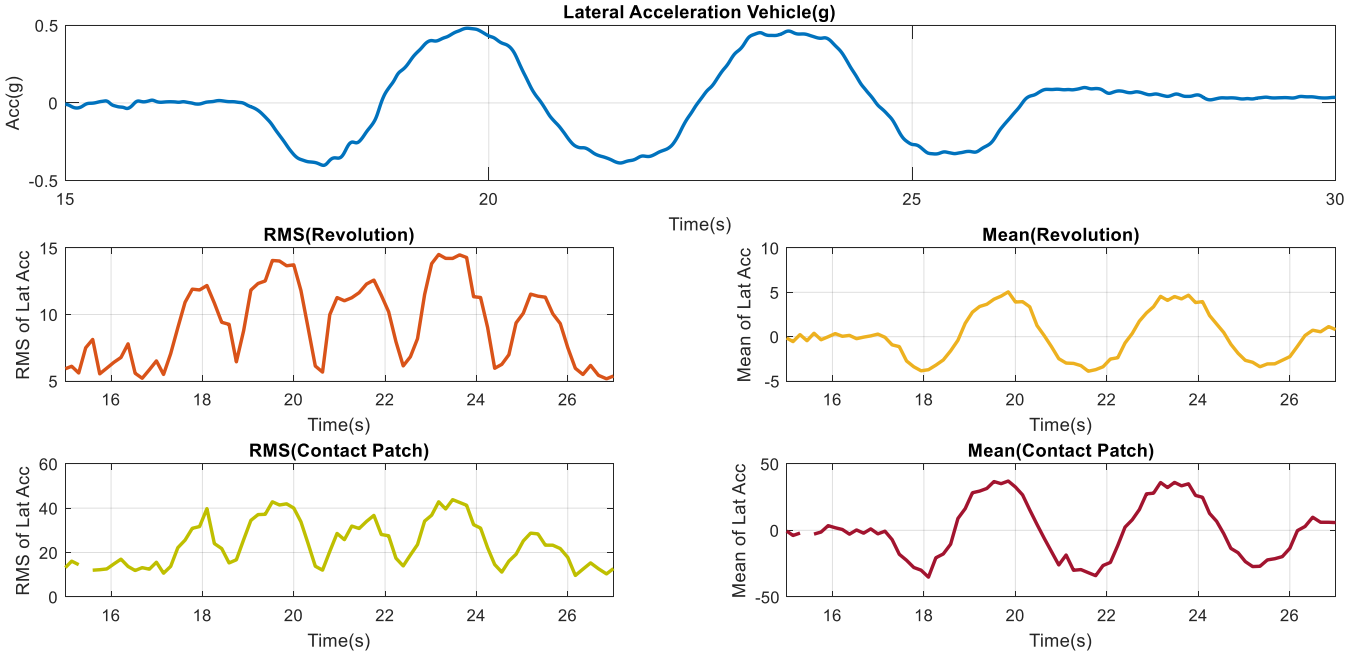

Figure 47-Comparison of different Indicators in Tire Lateral Acceleration Signal.

the data is passed through a low pass filter of 200Hz.

All the indicators show some correlation with the Lateral acceleration of the vehicle. The following observation can be made from the indicators.

- The RMS of the revolution and contact patch signal, show a good trend with the excitation, however since RMS gives a measure of the energy it cannot be used to determine the direction of the Force acting on the tire.
- The Mean on the other hand is sensitive to the direction of the force acting on the tire as can be seen from both the mean(revolution) and mean (contact patch).
- It is also seen that the mean/RMS over the revolution has less magnitude compared to the mean/RMS over the contact patch. This makes sense since the excitation is being provided mainly during the contact with the road.
- The RMS/mean over the whole revolution are sensitive to accelerations acting in the vehicle frame of reference. This can corrupt the measurements in cases when a very high lateral acceleration is acting on the vehicle. The signal needs to be detrended for such variations.

It is worth noting that the direction of the Intelligent Tire indicators have been changed to show the trend of correlation.

3.5.5 Feature extraction using Tire Tread Lateral deflection model

It is well known that the tire tread deforms in lateral direction when a lateral force is applied to it. The lateral deflection of the tire inside the tire contact patch can be modelled as a parabolic equation shown in Equation 12.

$$y = \alpha x^2 + \beta x + \gamma \; (\alpha := -\frac{F_y}{2C_{bend}} \quad \beta := \frac{M_z}{c_{yaw}} \quad \gamma := \frac{F_y}{c_{lat}})$$

Equation 12

Since the accelerometer is placed in the inner liner of the tread, the deflection of the surface in contact with the road is different from the deflection of the inner liner. Hence the coefficients (c_{bemd}, c_{yaw}, c_{lat}) will differ from the modelled/measured values.

The methodology followed here is to double integrate the Tire Lateral Acceleration signal in the contact patch to get deflection and curve fit the deflection shape to get the desired coefficients. Integration can be tricky specially in cases when the measured signal is prone to noise. Hence it

becomes necessary to filter the noise and drift before proceeding towards integration techniques. The main source of error during integration was the DC gain component present in the signal as can be seen in Figure 48. This can be removed in two ways:

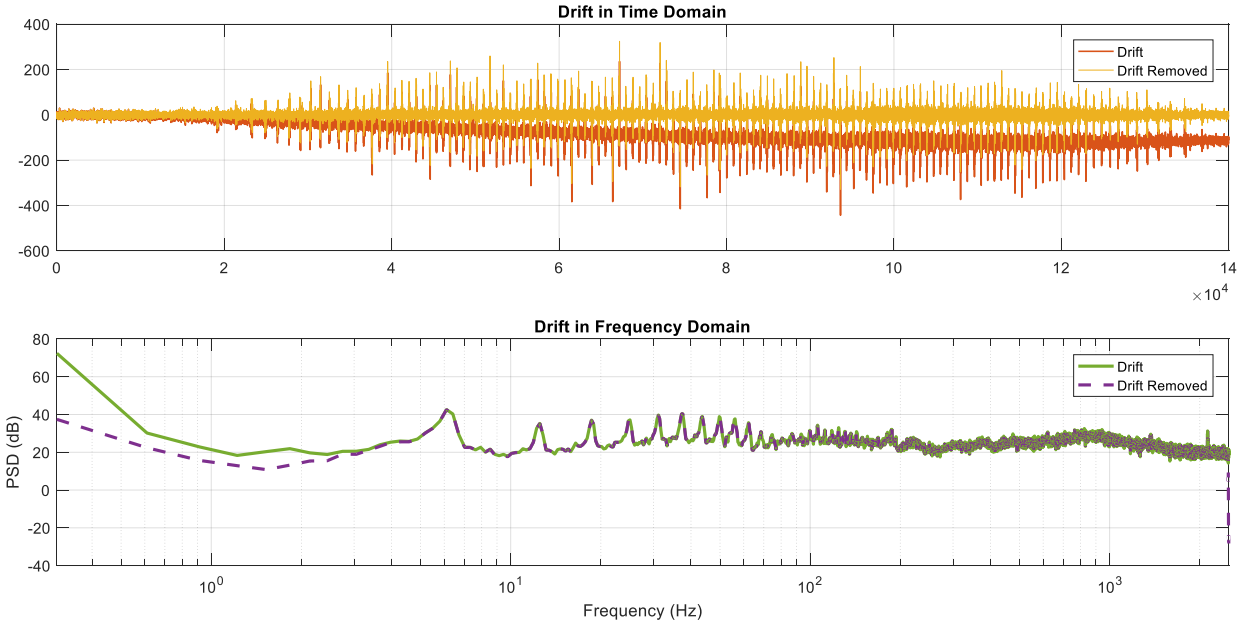

Figure 48-Drift in Acceleration

- Using a High pass filter of required break frequency.
- Detrending the signal.

The noise was similarly removed using a lowpass filter. Hence it was decided to use a bandpass filter with low and high frequencies of interest.

Once the drift and noise was cleared, the next step was to integrate the signal. Integration can be done using different techniques[50][51]. In this case, the Cumulative Trapezoidal Integration Technique was used for integration. The trapezoidal rule works by approximating the region under the curve as a trapezoid and calculating its area.

Figure 49-Integration Algorithm to get Displacement

After the integration is done and displacement is obtained, a second curve fitting is done between

the displacement and longitudinal displacement to get coefficients shown in the equation above.

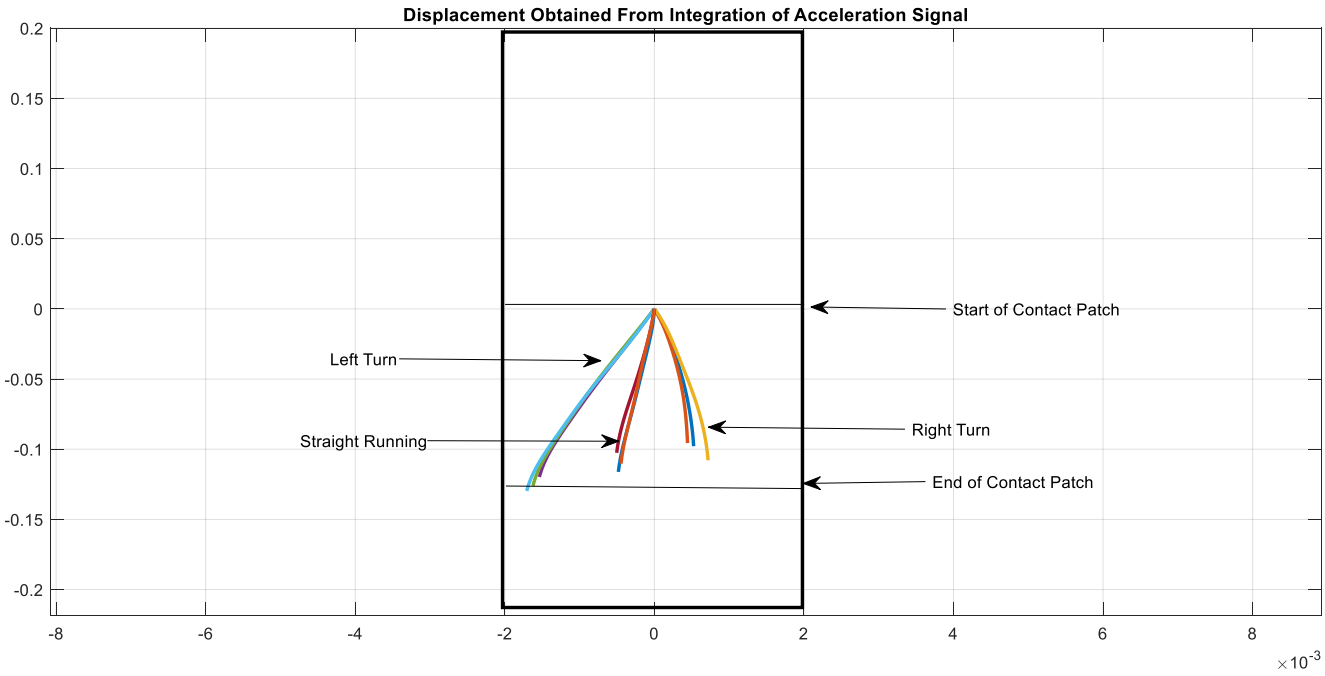

Figure 50-Displacement for 3 different Maneuvers

The longitudinal displacement is calculated using the Leading and trailing edge of the contact patch and the angular speed of the wheel.

As can be seen from Figure 50 the deflection obtained using double integration is in different directions for different maneuvers.

Interesting thing to be observed here is that even when the vehicle is running straight there is some deflection which can be seen. Two reasons can be possible for this observation:

- Even when the tire is rolling straight, there are stresses developed in the lateral direction due to the alignment of the tire (camber, toe) or tire construction. One way to validate this claim is if there is another sensor installed in the other side of the same axle and it shows a trend in the opposite direction.
- The other reason can be integration error which has accumulated. However, there is less possibility of this being the case since the noise and drift have been removed from the signal.

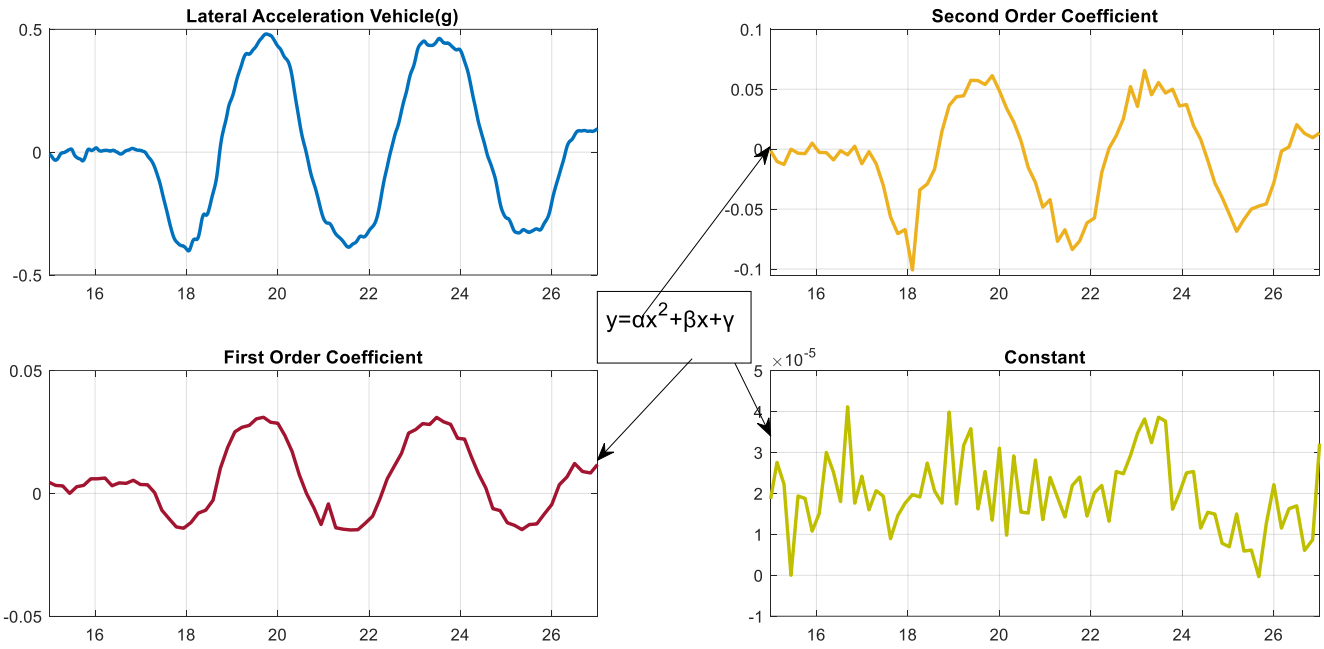

Figure 51-Intelligent Tire signal analysis using Lateral Deflection Model

As can be seen from Figure 51 the results of Integrating to get the displacement and second order polynomial curve fitting has some correlation with the force acting on the tire.

The observations which can be made are:

- The second order and the linear term have a correlation in the trend of the excitation (force, slip angle). If we refer to the lateral deflection equation, the polynomial term can be used to calculate the Force and linear term to calculate the moment acting on the tire. The validation of which can be seen in the next chapter.
- The constant term does not seem to have any correlation with the force acting on the tire.

It is worth noting that the direction of the regressors from Intelligent Tire has been changed to show the trend of correlation.

3.5.6 Applications of Lateral Force Estimation

The lateral force estimation algorithm has a lot of applications in the stability controller and for

tire related aspects.

- This algorithm can be used to predict alignment issues in the vehicle. When the vehicle is running straight and if one of the tire is having a force in the lateral direction over a period. This can trigger off a misalignment warning.
- The lateral force estimation algorithm can be used in conjunction with the existing model based stability control estimation algorithm to improve the accuracy of estimation in conditions all the conditions.
- The lateral force estimation algorithm can be used during the tire development for benchmarking activities and as an input to the tire wear model.

3.6 Longitudinal Force estimation algorithm

This section explores the indicators of Longitudinal force in the Intelligent Tire signal. The longitudinal force estimation from Intelligent Tire signal can be used in conjunction with the vehicle dynamics based estimation algorithms to improve the accuracy. Studies have been conducted in the past to estimate the longitudinal force using Intelligent tires, a summary of which is shown in the section below.

3.6.1 Literature Review for Longitudinal Force estimation

In the study conducted in[27] the Longitudinal force has been estimated using the phase shift of the signal wave, the study says that the effect of longitudinal force moves the center of the contact patch forward or backwards (Figure 52) based on the direction of the force and monitoring the center of the contact patch gives a good indicator of the longitudinal force acting .

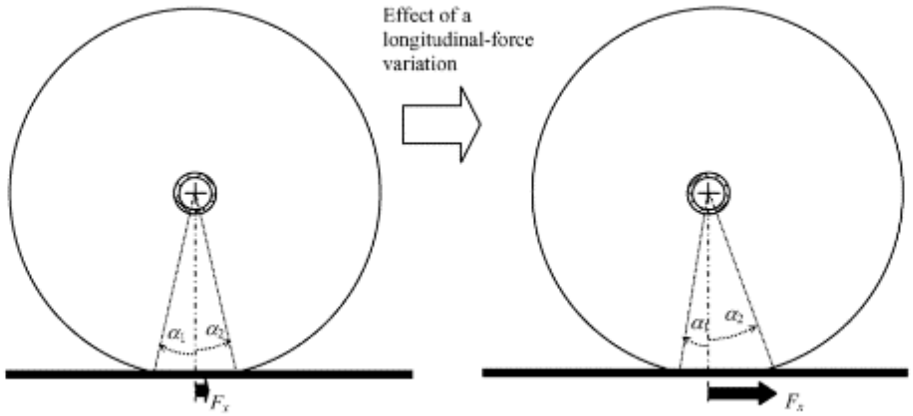

Figure 52-Effect of Longitudinal Force on the Center of contact patch

Another study [52] uses strain gauges along with PCA based model to estimate the longitudinal force.

3.6.2 Regressor for Longitudinal Force measurement

In this study, a new feature was studied which gave a good correlation with the Longitudinal force acting on the tire. The reason behind studying this regressor stems from the contact mechanics in the longitudinal direction.

When the tire experiences longitudinal forces during acceleration and braking there is a deformation which occurs at the contact patch in the longitudinal plane. The idea used here was to consider the radial/circumferential signal near the contact patch to see features relating to Longitudinal force. The study conducted in [53] analyses the in plane deformation of the tire and compares it with flexible ring tire model , the deformation analysis is done for longitudinal force and wheel load.

The feature in radial acceleration signal which showed a good correlation with the longitudinal force is shown below in Figure 53.

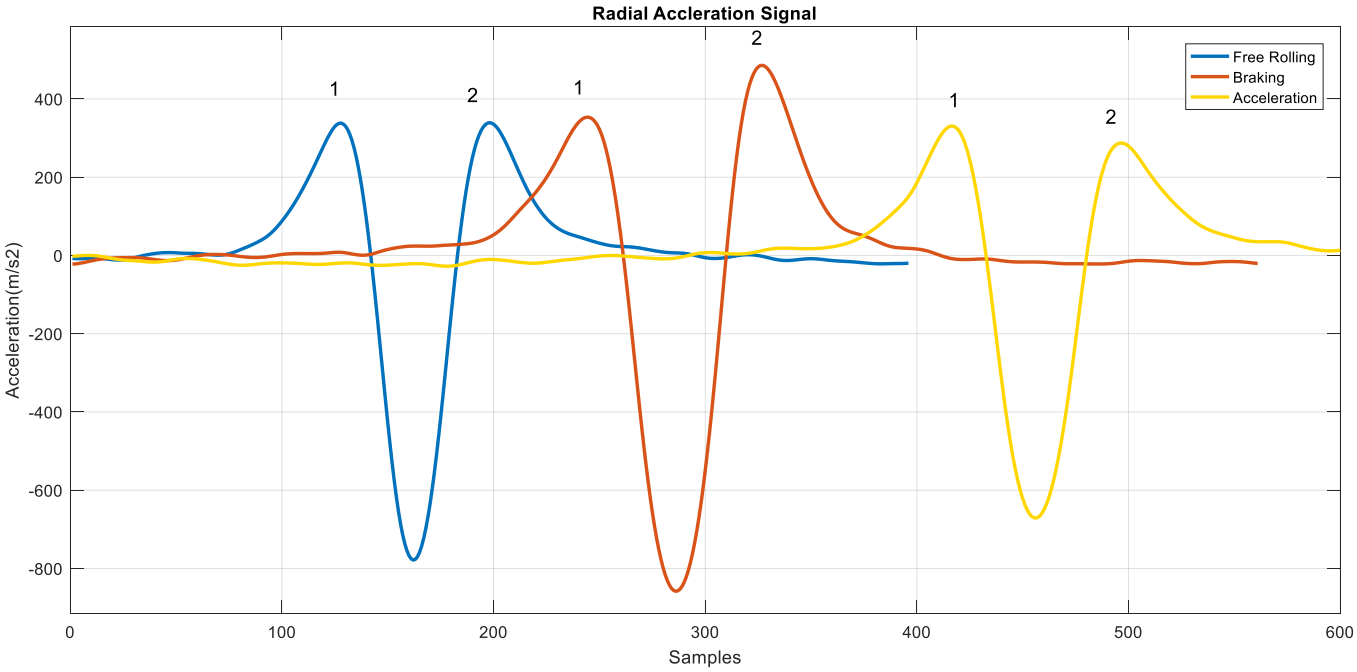

Figure 53-Longitudinal Force Feature Radial Signal

As can be seen from the figure above:

Free Rolling: Magnitude of Peak1 = Magnitude of Peak2

Braking: Magnitude of Peak2 > Magnitude of Peak1

Acceleration: Magnitude of Peak1 > Magnitude of Peak2

Hence the difference of the peaks was used as a regressor to find correlation with the longitudinal force on the tire. The results of this regressor and its correlation with longitudinal force is shown in the next chapter.

3.7 Tire pressure detection using Intelligent Tire

Tire pressure is one of the critical parameter when it comes to vehicle safety and tire performance. Tire pressure also has a significant impact on the contact patch length and the force generation. Developing an algorithm for tire pressure detection enables better accuracy with load estimation and tire force algorithms. Lot of studies have been conducted in the past for tire pressure monitoring. The two major ways in which this can be classified is:

- Direct TPMS: Measurement done using pressure measuring sensors inside the tire.

- Indirect TPMS(i-TPMS): Signals such as acceleration/ wheel speed are used to detect the pressure inside the tire.

3.7.1 Literature review

Conventional Direct TPMS have been in the automotive industry for a long time but prove to be costly hence they are being replaced with i-TPMS using the wheel speed sensors[54] and other mediums. In the study conducted by[55] vertical stiffness is used as a regressor to detect tire pressure. The study conducted by[56] gives a detailed account of the different methods used for tire pressure monitoring.

3.7.2 Indicators for Tire Pressure in Intelligent Tire Signal

With the change in tire pressure many characteristics change, the vertical stiffness of the tire changes resulting in change of rolling radius. However, rolling radius is also sensitive to the load acting on the tire which is difficult to determine independently.
The other aspect which changes is the resonant frequencies in the tire, this has been studied in detail by[57] and other researchers. In the study conducted in[1], the author states that tire pressure has a profound influence on the natural frequencies of the tire.

It was found that the circumferential signal can be used to extract the features relating to the tire pressure. Figure 54 shows the frequency plot of the circumferential signal for different speeds at same tire pressure.

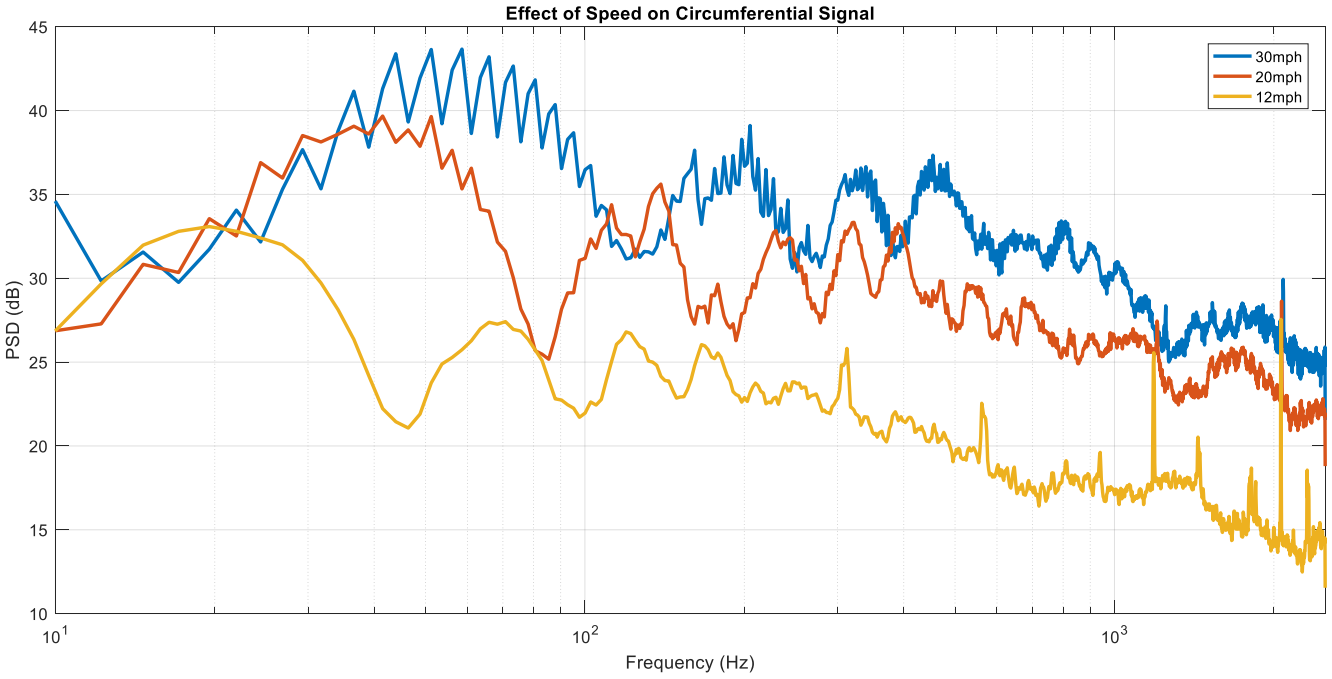

Figure 54 FFT of Circumferential Signal for different speeds

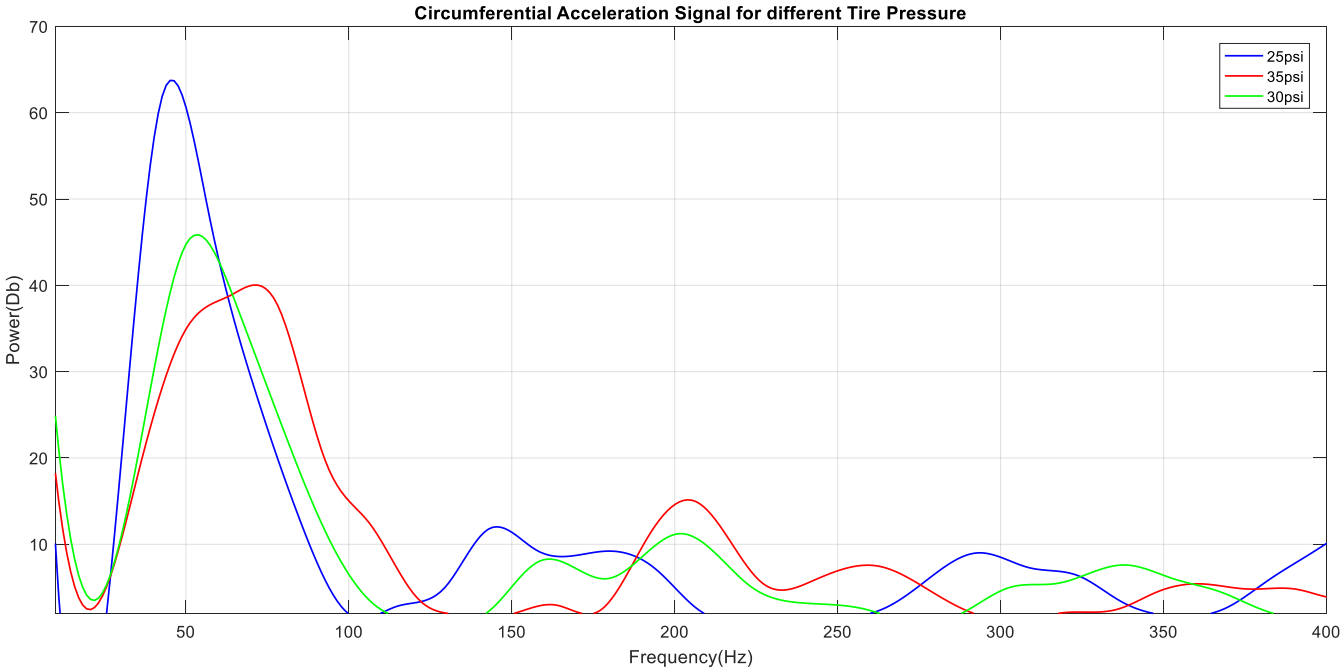

Figure 55-Effect of Tire pressure on Circumferential signal at 30mph

From the figures above it can be clearly seen that the tire pressure influences the resonance peaks in the circumferential signal.

The following observations can be made from the plots above:

- Vehicle speed causes a shift in all the modes to a higher frequency and the power of the signal increases across all frequencies.
- From Figure 55 it can be clearly seen that due to change in tire pressure there is a significant change in the frequency and power seen in the first resonance mode.
- Load also has a significant effect on the resonance mode and power of the signal , however in this study the load was considered constant.

The algorithm which was developed to sense the tire pressure is shown below:

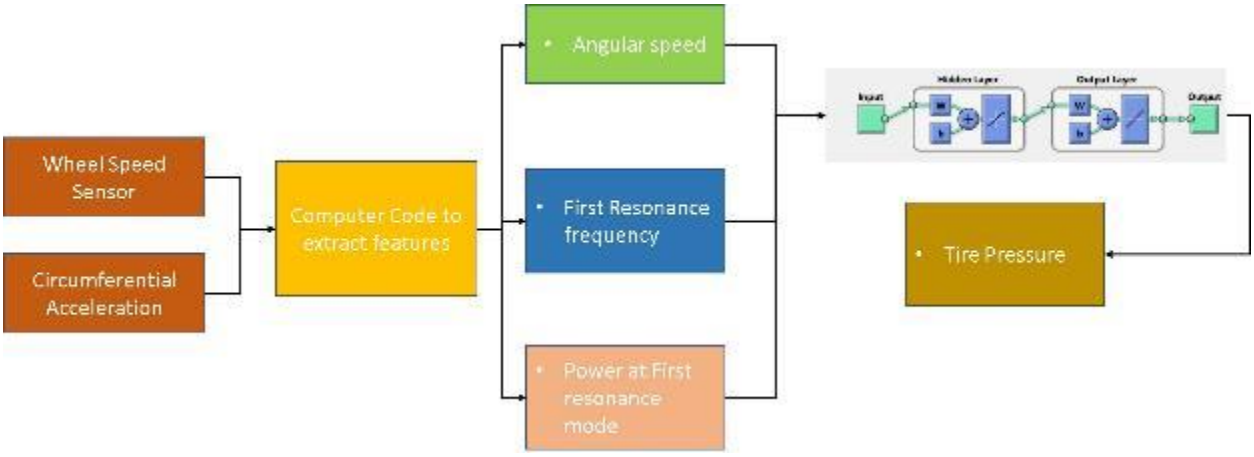

Figure 56-Algorithm for Tire Pressure monitoring

The method to extract the desired resonance frequencies from the signal is shown below in

- Spectrogram function in Matlab was used to extract the frequency domain information

for a set of rotations, which were decided based on conditions: speed being constant, no steering input.

- Envelope function was used to get a smooth curve joining the peaks of the frequency plot.
- The frequencies and power of the First mode and its magnitude was saved, however this algorithm can be extended to include the frequency and power of the subsequent modes, if the extraction of those modes can be done robustly.

3.8 Conclusions

The main contents discussed in this chapter were:

- Different Signal analysis techniques in Frequency and Time domain were discussed.
- The tire contact patch mechanics was discussed using the tire brush model.
- Intelligent tire signal was analyzed for noise in frequency domain and SNR was calculated.
- Frequency domain analysis was done to study the effect of speed, steering input on the signal.
- Load transfer estimation based on contact patch length was checked for robustness and an algorithm for LTR based on contact length was developed.
- The lateral acceleration signal was studied for features relating the lateral force.
- Regressors relating to longitudinal force were studied from the radial acceleration signal.
- Features for tire pressure monitoring were studied in frequency domain.

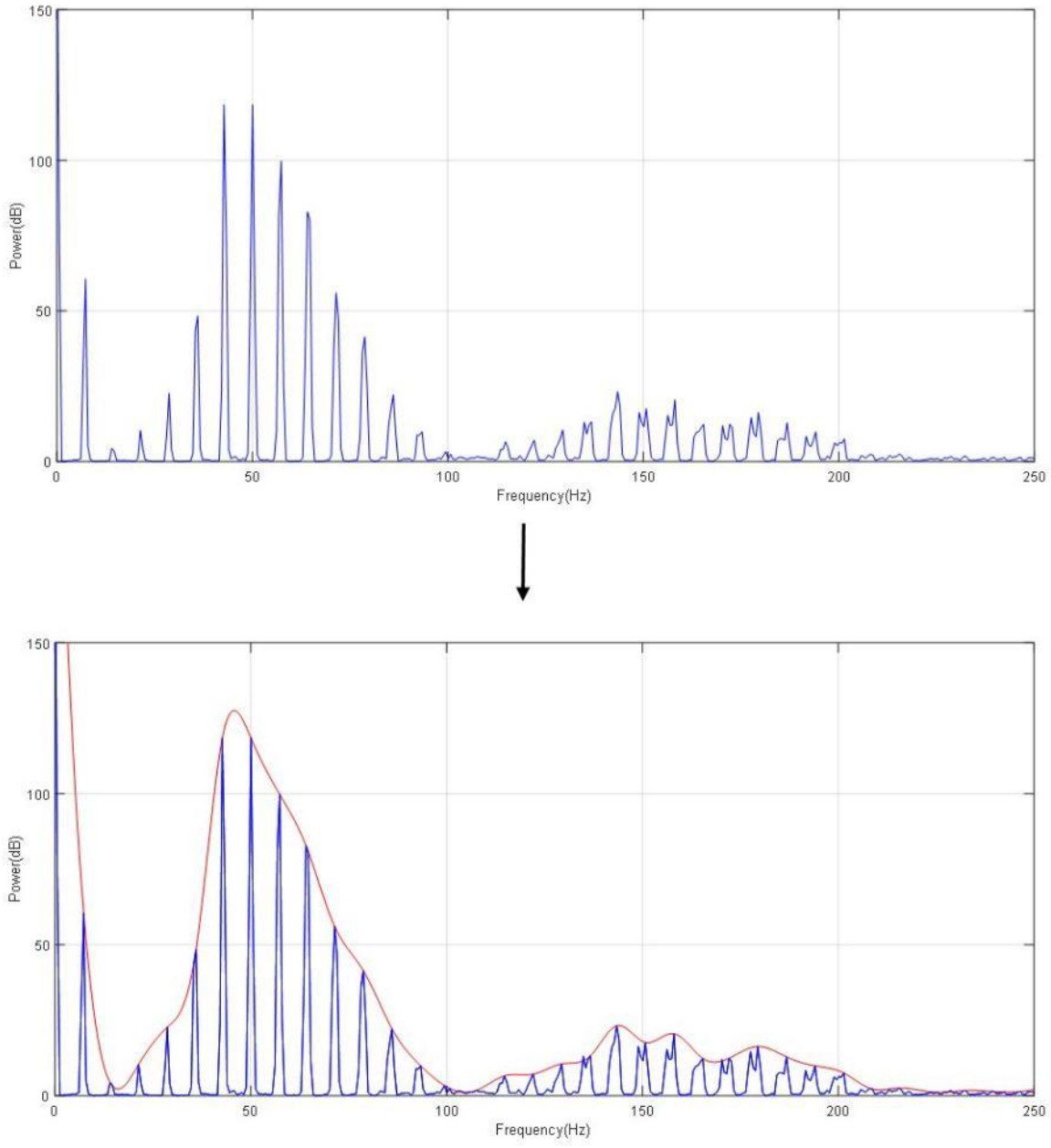

Figure 57-Extraction of first mode

Figure 58-CarSim OverviewFigure 59-Extraction of first mode

4 Simulation Model using CarSim and Results

The primary objectives of this chapter are:

- Develop and validate simulation model of VW Jetta
- Validate the robustness of Load transfer estimation from Contact Patch length using CarSim model.
- Validate the regressor for Lateral Force using CarSim model
- Show correlation of regressors for Longitudinal force for braking and acceleration maneuvers.
- Result of Tire pressure monitoring algorithm.

The regressors/features extracted in the previous chapters cannot be validated unless they are compared with known force value and a regression or empirical relation is established between the output of the algorithm and the measured/estimated force values. Since the vehicle did not have any force measurement mechanism installed on it. It was decided to develop a simulation model in CarSim with the available parameters of VW Jetta and validate it. This simulation model was then used as a reference for the output of the algorithms developed and a regression model was setup.

4.1 Simulation Model and Validation

CarSim is a lookup table based Vehicle Dynamics simulation software. The Kinematics and compliance parameters for the VW Jetta 2002 model was available from a previous benchmarking report and was used to build the simulation model. An overview of the different subsystems and Test parameters is shown below in Figure 60-CarSim Overview

Figure 61-Simulink/CarSim ModelFigure 62.

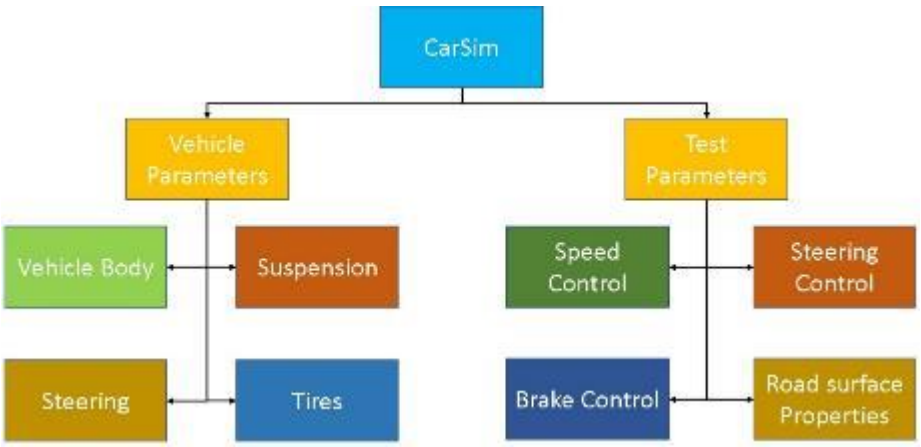

Figure 60-CarSim Overview

Figure 61-Simulink/CarSim ModelFigure 62-CarSim Overview

4.1.1 Vehicle Parameters

The vehicle parameters mainly consist of the subsystems shown above, it also includes engine, aerodynamics related parameters but default values were used for them as it did not have a major effect on the model for our tests.
The modelling of each subsystem is described below

- **Vehicle Body**: The vehicle body parameters include vehicle sprung/unsprung mass, inertia in all the three axes, Center of Gravity location, Track width, Wheel base. The inertia parameters were estimated using the relation given in CarSim help file. The curb weight of the vehicle was available, two pax weight was added and distributed according to seating position.

- **Steering:** Steering parameters include gear ratio, steering kinematics, kingpin geometry. In this model only the gear ratio was available and was sufficient for our use as steering moment was not required to be mapped.

- **Suspension:** The suspension parameters are modelled in two parts: Kinematic, Compliance. Kinematic parameters include change of properties (camber, toe, dive) in relation to the movement of suspension. Spring stiffness, damper curve, information

related to bushes fall under compliance. The main parameters which were sensitive to correlation with actual data were Spring stiffness and Roll Stiffness.

- **Tires**: Tires have significant effect on the accuracy of the model. The tires can be modelled in two ways in CarSim, using the tire test data (Lateral/Longitudinal force vs slip angle/ratio, aligning moment) or using an empirical model like Pacejka or MF Swift. In this case tire test data was not available, however a MF Swift model was available from the previous research**.** The tire was modelled using Pacejka model, the coefficients were extracted from the. tir MF Swift file. Some changes were made to the scaling factor of load transfer coefficient to get a good correlation with actual test data. The limitation of the Pacejka model was its accuracy only in the slip range of +/- 1.5, hence all the tests were conducted in the linear region within the give value.

4.1.2 Test Parameters

The test parameters include the speed control, steering input and surface related parameters. Since the main objective of the model was to have a reference of the force values at the tire, the exact test conditions had to be simulated. Accurate information of the road surface was not available hence they were modelled as default values in CarSim with friction coefficient of 0.85. The Steering and Speed information available from the sensors in VW Jetta was directly fed to the CarSim model to simulate the exact conditions.

4.1.3 Validation of Simulation Model

To validate the simulation model, the parameters measured by the IMU from the vehicle: Lateral Acceleration and Yaw Rate were compared with the values obtained from simulation. A model was developed in Simulink using the vehicle model 'S' block from CarSim. This model was developed to integrate the output of the CarSim model (Lateral, Normal force) with the output of the algorithms developed for intelligent tire. The Simulink model is shown in Figure 63- Simulink/CarSim Model

Figure 64-Steady State InputFigure 65.

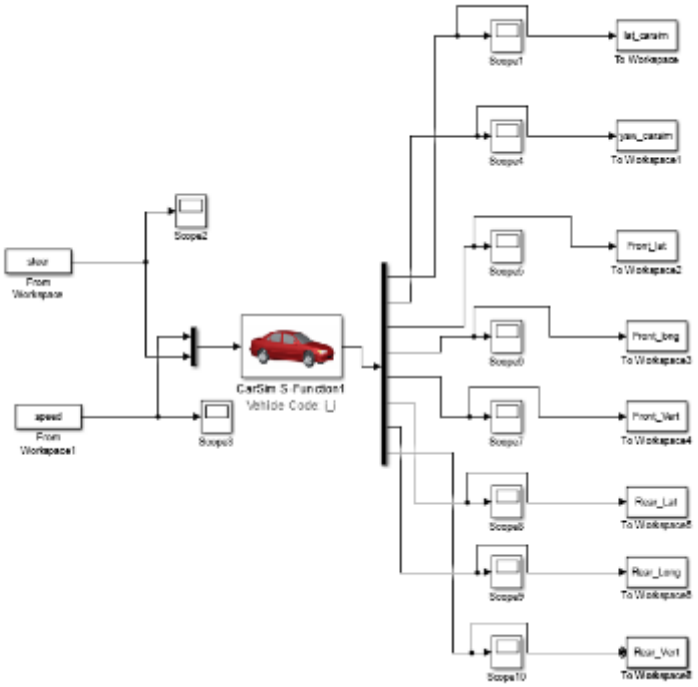

Figure 63-Simulink/CarSim Model

To validate the Simulink model, the following maneuvers were tested.

Figure 64-Steady State InputFigure 65-Simulink/CarSim Model

- Steady state steering input 0.4g
- Transient Low Frequency Sine Input
- Transient Medium Frequency Sine Input
- Double Lane Change at 45mph.

The steady state input validates the properties related to the vehicle mass, inertia and all the compliance. Transient inputs are used to validate the tire characteristics, the transient inputs have been chosen at two different frequencies to check the robustness of the model. It's worth mentioning here that due to test track unavailability the tests had to be done at parking lot with a speed limit of 35mph and the lane change was done at highway ensuring all the safety measures.

4.1.3.1 Steady State Steering Input

Test conditions:

Speed: 25mph

Tire Pressure: 30psi (All Tires)

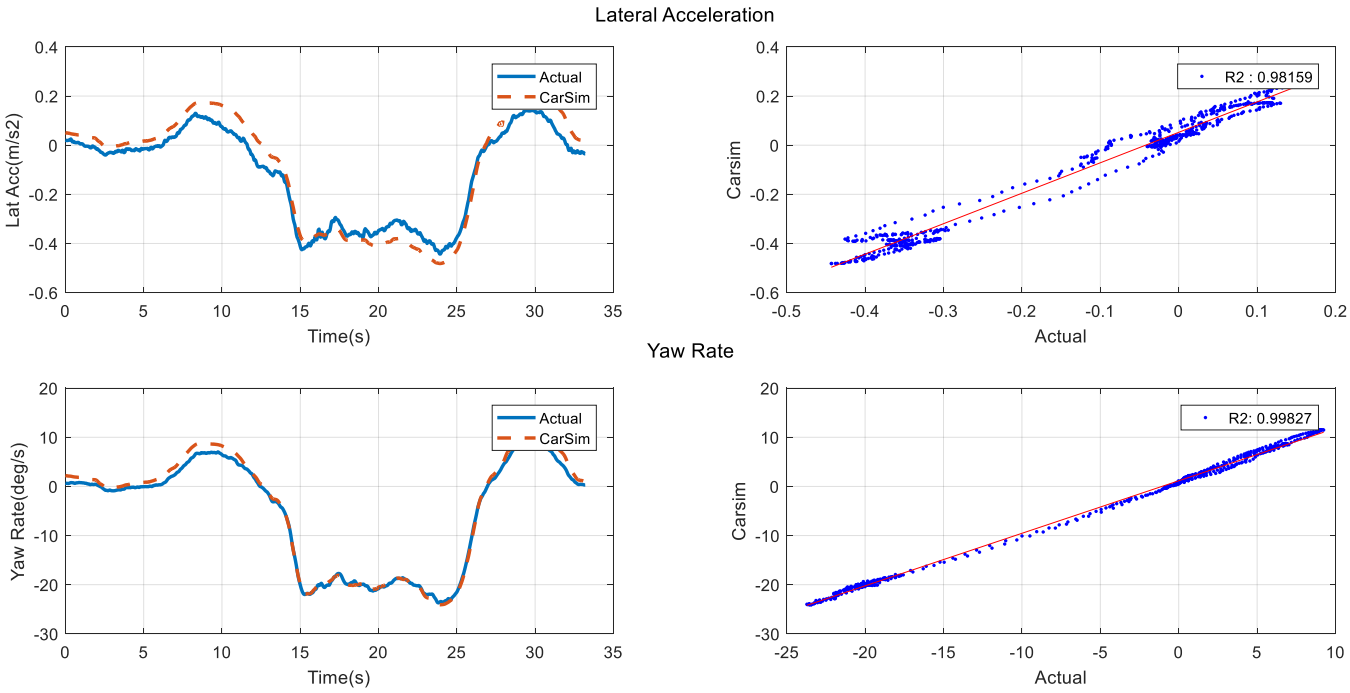

Figure 66-Steady State Input

Figure 67-Transient Low Frequency InputFigure 68-Steady State Input

4.1.3.2 Transient Low Frequency Sine Input

Test Conditions: Test Speed: 25mph

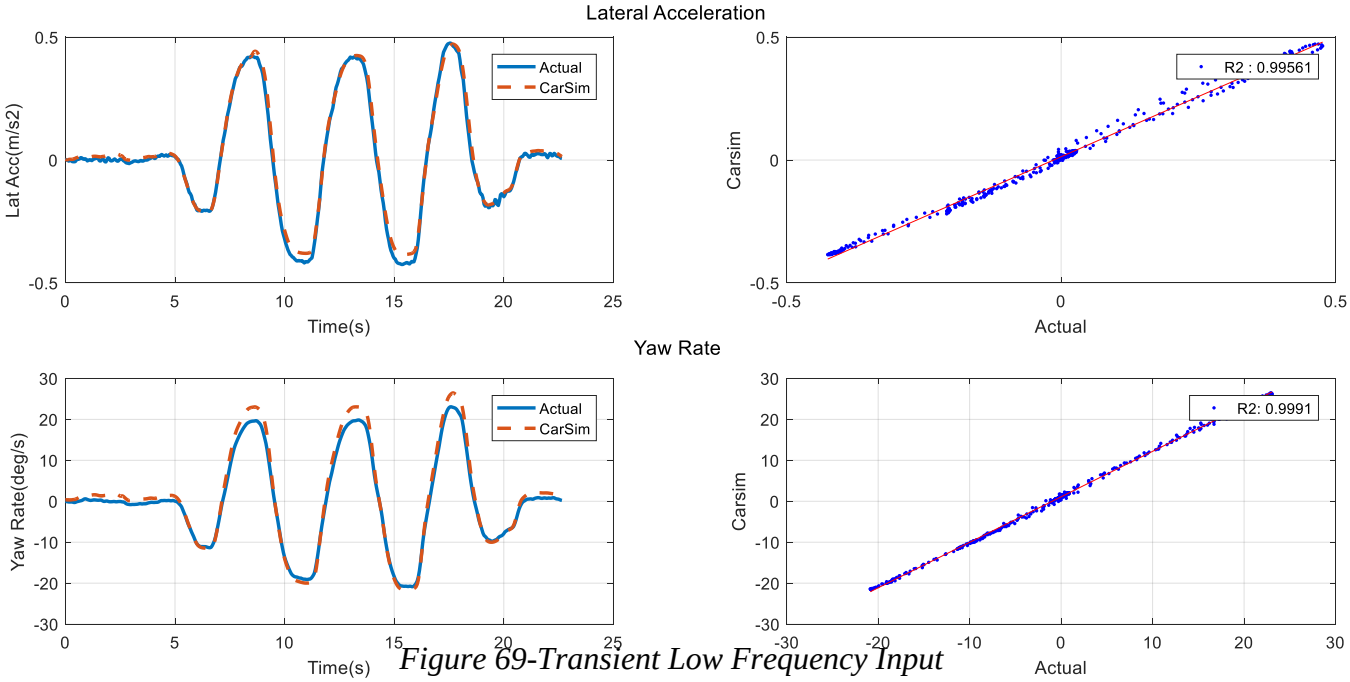

Figure 69-Transient Low Frequency Input

Figure 70-Transient Medium Frequency InputFigure 71-Transient Low Frequency Input

Tire Pressure: 30psi (All tires)
Steering Input Frequency: 0.2 Hz

4.1.3.3 Transient Medium Frequency Input

Figure 72-Transient Medium Frequency Input

Figure 73-Double Lane ChangeFigure 74-Transient Medium Frequency Input

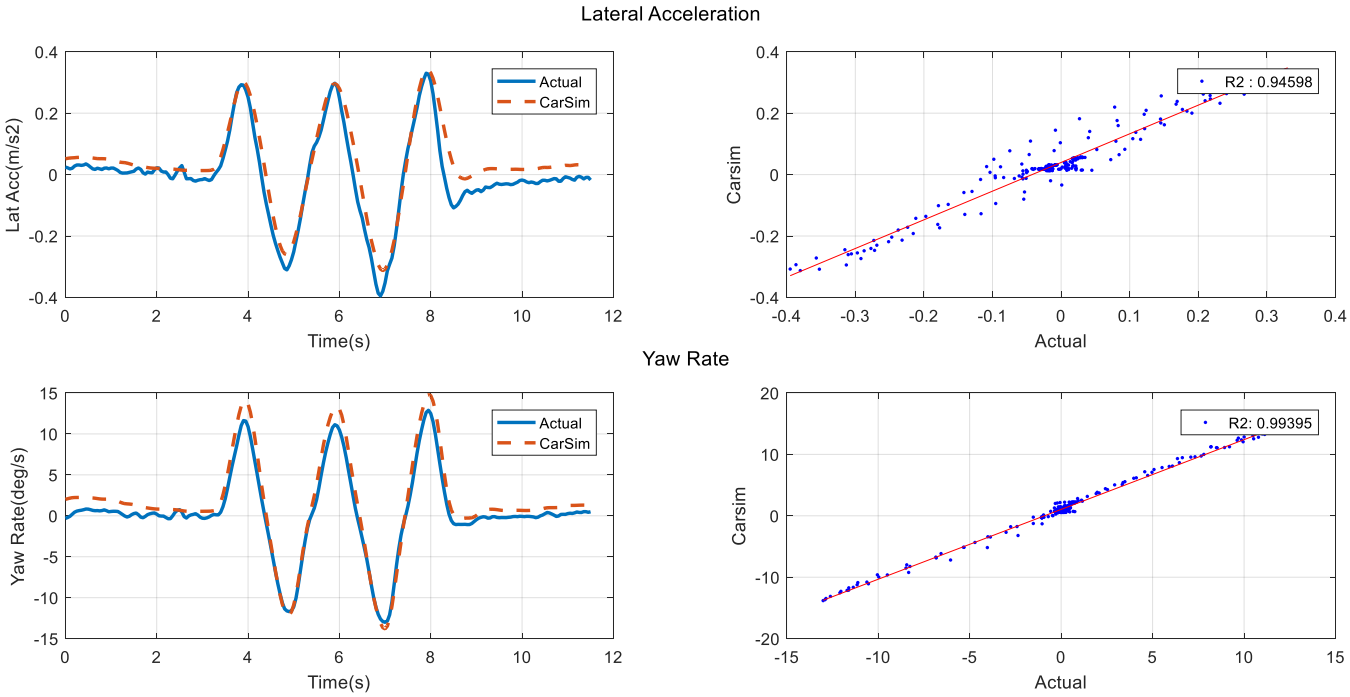

Test Conditions
Speed: 25mph
Tire Pressure: 30psi (All tires)
Input Frequency: 0.5 Hz

4.1.3.4 Double Lane Change

Test Conditions:
Test Speed: 45mph
Tire Pressure: 30psi (All Tires)

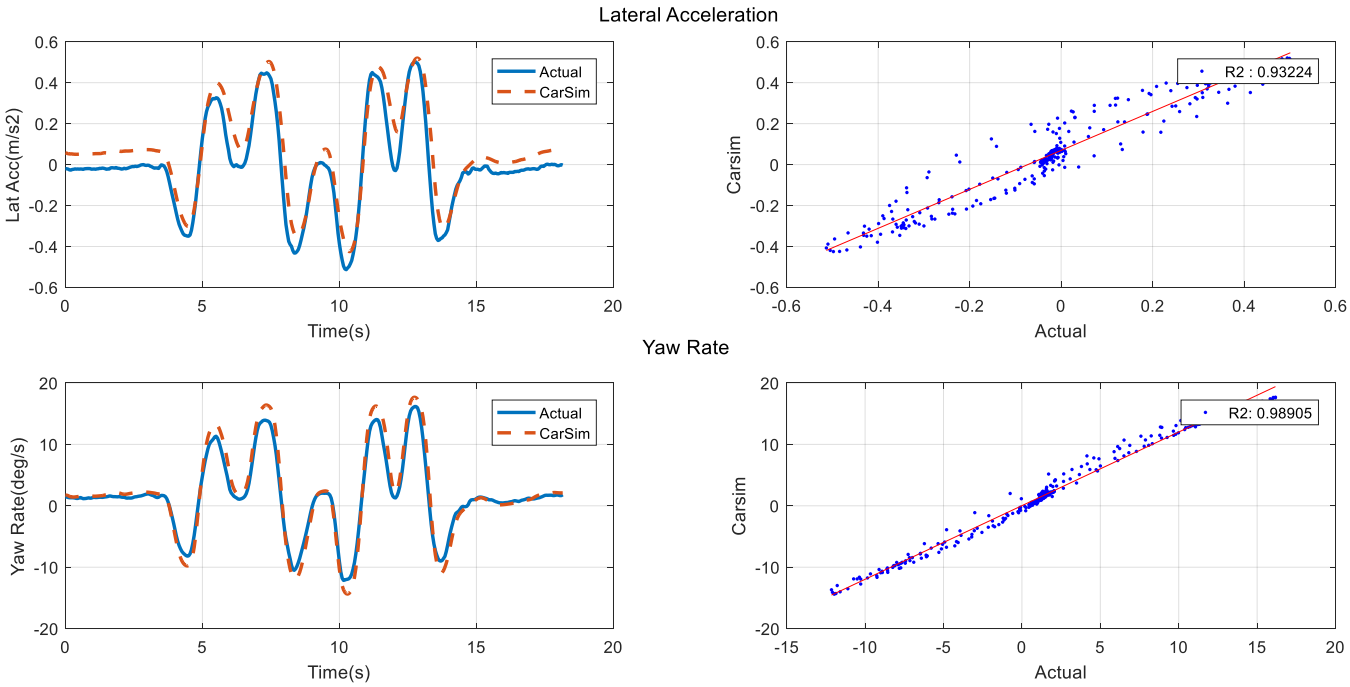

Figure 75-Double Lane Change

Figure 76-Lane Change at 45mphFigure 77-Double Lane Change

4.2 Sampling Rate Selection

Before proceeding with validation of the regressors extracted in previous chapters, it is essential to stress on the effect of sampling rate for data acquisition. A small calculation is shown on how to decide on the sample rate required.

Through simple approximation, a relation can be established between the resolution required (degree/sample: Res), vehicle speed(V,m/s) and sampling rate(Fs).

$$Fs = 57.3\frac{V}{R * Res}$$

Equation 13

Speed(mph)/Res	1^0	2^0	5^0
30	2356.261682	1178.130841	471.2523364
50	3927.102804	1963.551402	785.4205607
70	5497.943925	2748.971963	1099.588785
100	7854.205607	3927.102804	1570.841121

Table 7-Sampling Frequency (speed /resolution)

The contact patch angle varies from 20^0-25^0 for speeds from 30-60mph. Hence with a sampling rate of 1000Hz we can get only 5 samples in the contact patch. The recommended sampling rate for speeds of 70mph is approximately around 2500Hz to get a resolution of 2^0. The result is shown for 1000Hz and 5000Hz for lane change at 45mph in Figure 78-Lane Change at 45mph

Figure 79-Comparison of Sample Rate at 35mphFigure 80

The data acquisition was done at two sampling rates for this study. At 1000Hz and 5000Hz. The validation of regressors with CarSim was done with 1000Hz sampling rate due to some hardware limitations. The figure below is to demonstrate that sampling at 5000Hz would result in a better result.

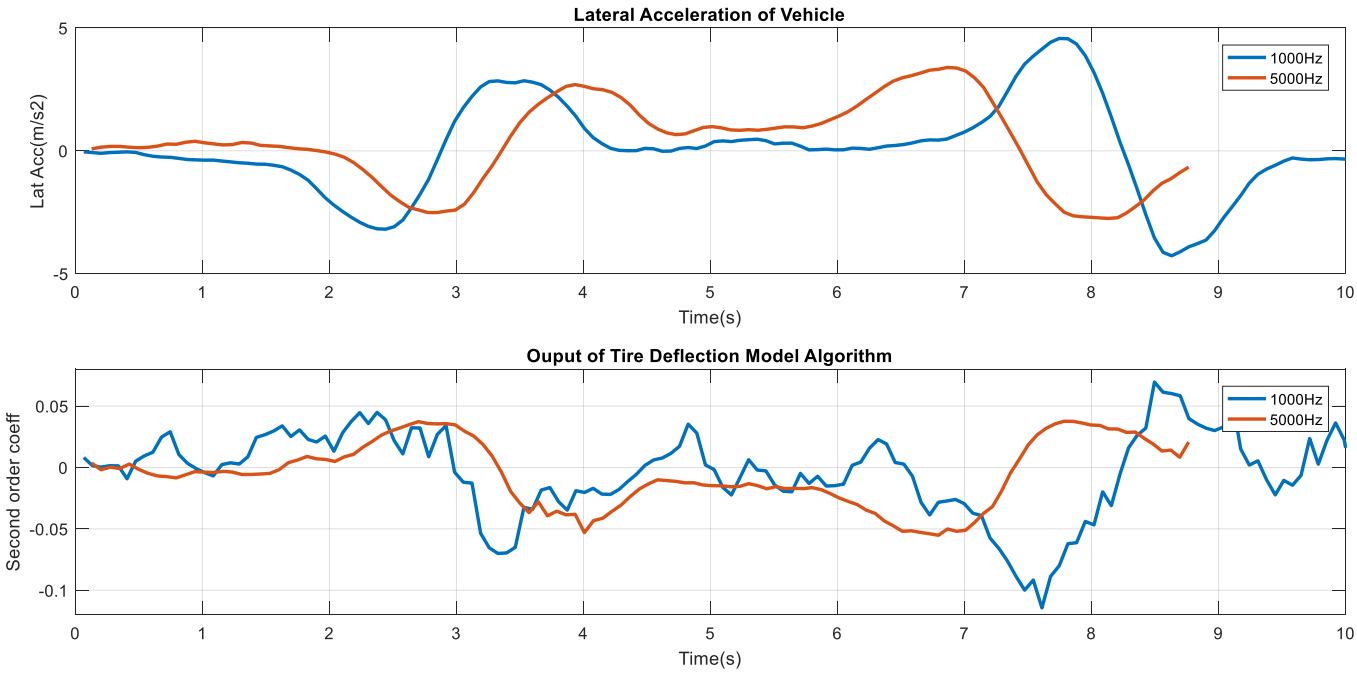

Figure 78-Lane Change at 45mph

Figure 79-Comparison of Sample Rate at 35mphFigure 80-Lane Change at 45mph

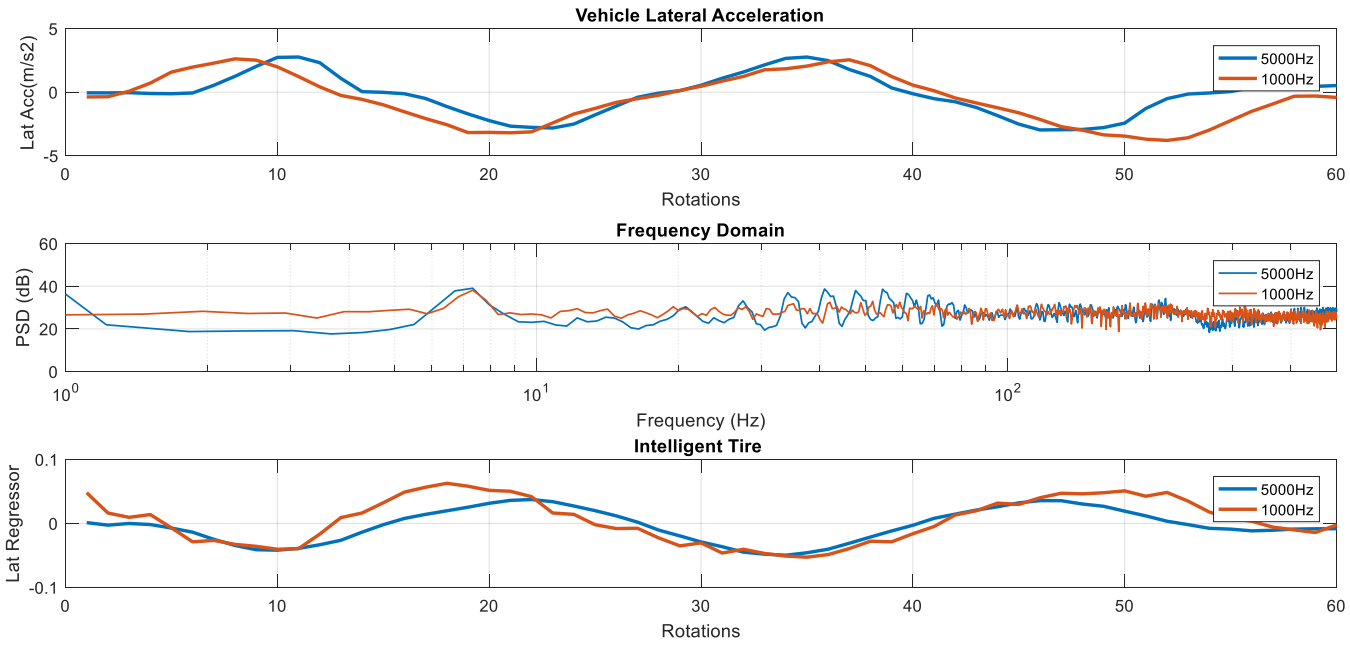

Figure 81-Comparison of Sample Rate at 35mph

Figure 82-Steady State Load TransferFigure 83-Comparison of Sample Rate at 35mph

As can be seen from Figure 81-Comparison of Sample Rate at 35mph

Figure 82-Steady State Load TransferFigure 83 sampling at 1000Hz and 5000Hz yield the same results, this comparison is done to show the validity of results at speeds up to 35mph.

4.3 Results of Contact Patch Length based Load Transfer Estimation

The objective of this section is to compare the change in contact patch length to the load transfer in the CarSim model and develop an empirical relation between the change in contact patch length and the Load transferred to/from the tire.

The methodology followed is as follows:

1. Detect Steering Angle Input
2. Reset the Contact Patch Length to zero.
3. Reset the Normal Load from CarSim to zero.
4. Compare the regression coefficients for different maneuvers.

The reason for resetting the contact patch length to zero is to eliminate the effects of tire pressure, speed etc. on the contact patch length. However more study needs to be conducted on the change of contact patch length with different tire pressures since the stiffness of the tire changes with change in tire pressure.

4.3.1 Steady State Input Lateral Load Transfer

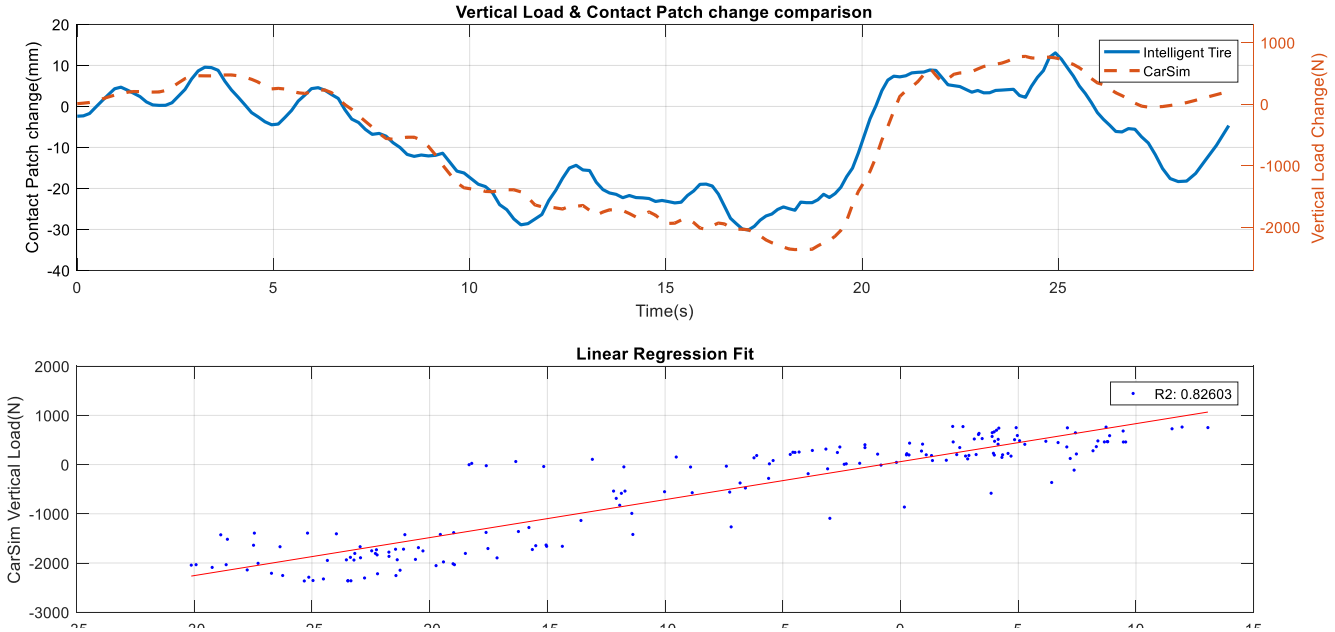

Figure 84-Steady State Load Transfer

Figure 85-Transient Low Frequency Steering Input Load TransferFigure 86-Steady State Load Transfer

y = 77.207 *x + 59.9584

RMSE: 438.73

R^2: 0.82

Test Conditions:

Test Speed: ~ 23mph

Tire Pressure: 30psi (All tires)

4.3.2 Transient Low Frequency Sine Input

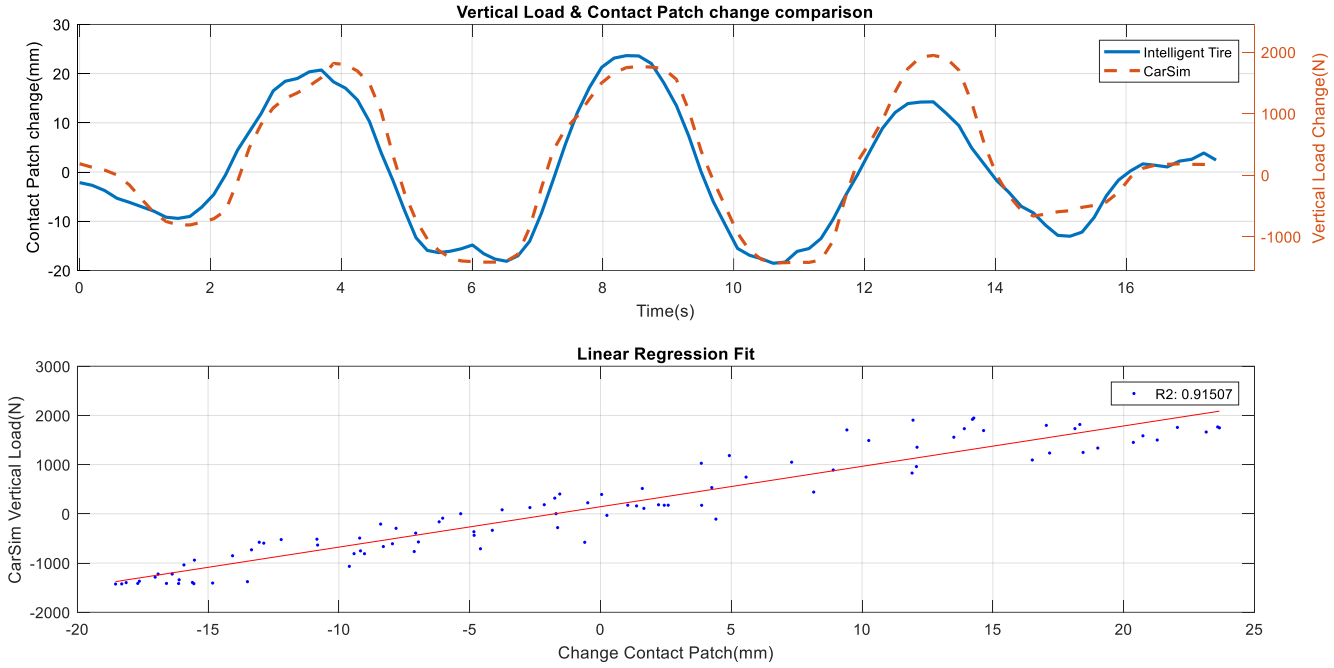

Figure 87-Transient Low Frequency Steering Input Load Transfer

Figure 88-Double Lane Change Load TransferFigure 89-Transient Low Frequency Steering Input Load Transfer

y = 82.0852 *x + 146.6666

RMSE: 313.05

R^2: 0.91

Test Conditions:

Test Speed: ~25mph

Tire Pressure: 30psi (All tires)

Frequency of Input: ~ 0.20-0.23 Hz

4.3.3 Double Lane Change

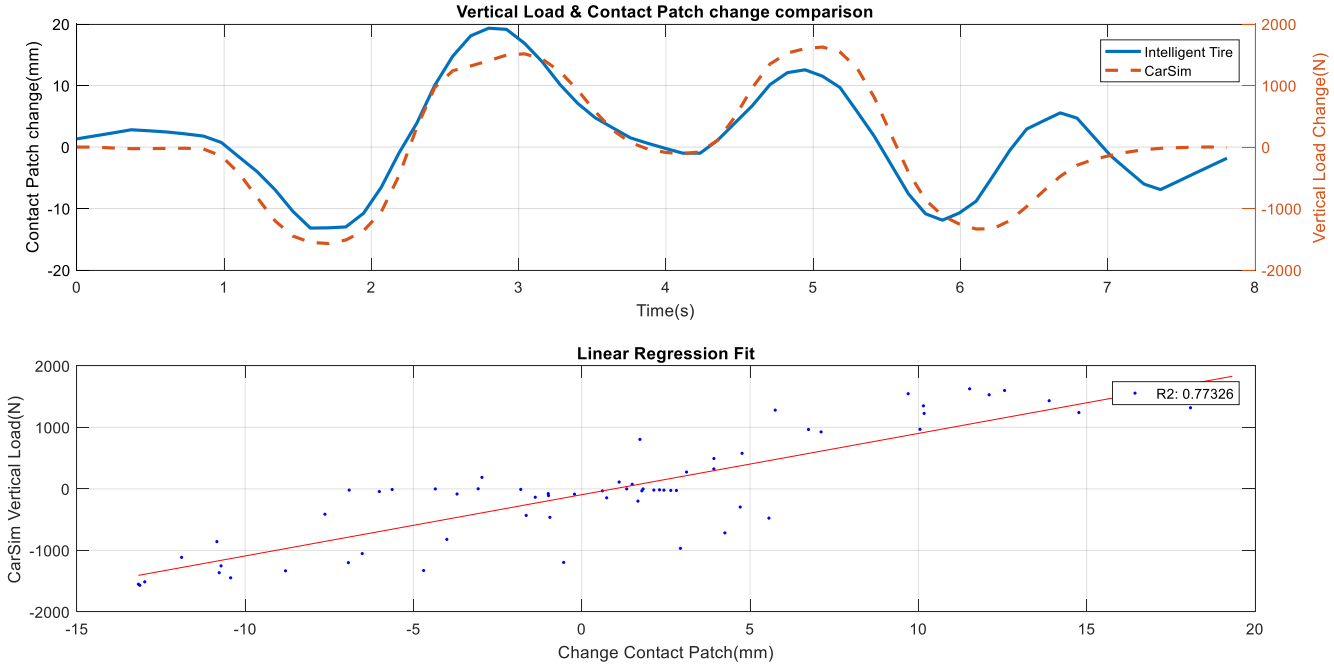

Figure 90-Double Lane Change Load Transfer

Figure 91-Transient Medium Frequency InputFigure 92-Double Lane Change Load Transfer

y = 99.5908 *x + -94.4945
RMSE: 442.51
R^2: 0.77

Test Conditions
Test Speed: ~35mph
Tire Pressure: 30 psi (All Tires)

4.3.4 Transient Medium Frequency Sine Input

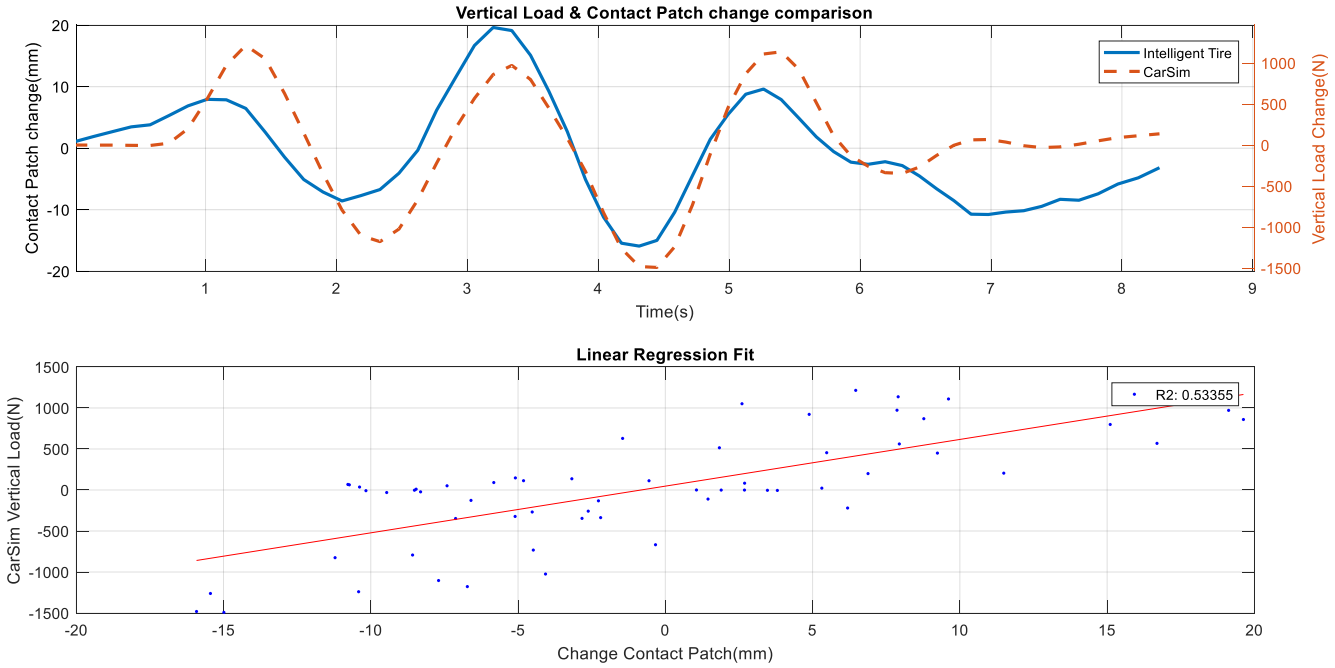

Figure 93-Transient Medium Frequency Input

Figure 94 Test1-Sine Sweep InputFigure 95-Transient Medium Frequency Input

y = 78.94 *x + 46.9118

RMSE: 457.71

R^2: 0.53

Test Conditions:

Test Speed: ~30mph

Tire Pressure: 30 psi (All Tires)

Frequency of Input: 0.5 Hz

4.3.5 Discussions

From the results, the change of contact patch length has a correlation with the Change of vertical load on the tire. The following observations were made based on the results:

- The steady state and transient low frequency inputs show a good correlation factor. Both the test has similar slopes for the curve fit line, however the constant is different for these tests, this can be corrected by modifying the algorithm for resetting the contact patch and vertical load when steering input is detected.

- The slope of the Double lane change maneuver was different compared to the other two. One reason for this could be the difference in speeds between both the tests. More study needs to be done to study the effects of speed on contact patch length change.

- With the higher frequency input, the correlation is less compared to the other inputs. At high frequency inputs damper plays an important role and since the model does not have measured damper values, this could be one of the reasons for less correlation.

4.4 Validation of Regressor for Lateral Force measurement

The objective of this section is to compare the regressors obtained through the two methods in section 3.5 with the Lateral Force obtained from the CarSim simulation model. This comparison is for the proof of concept of regressors extracted from the signal. The tests have been done at constant tire pressure and since there was a limitation of speed in the parking lot, the max speed tested was 35mph.

All the tests were done with the sampling rate of 1000Hz, the results with a higher sampling rate will have a better resolution and accuracy.

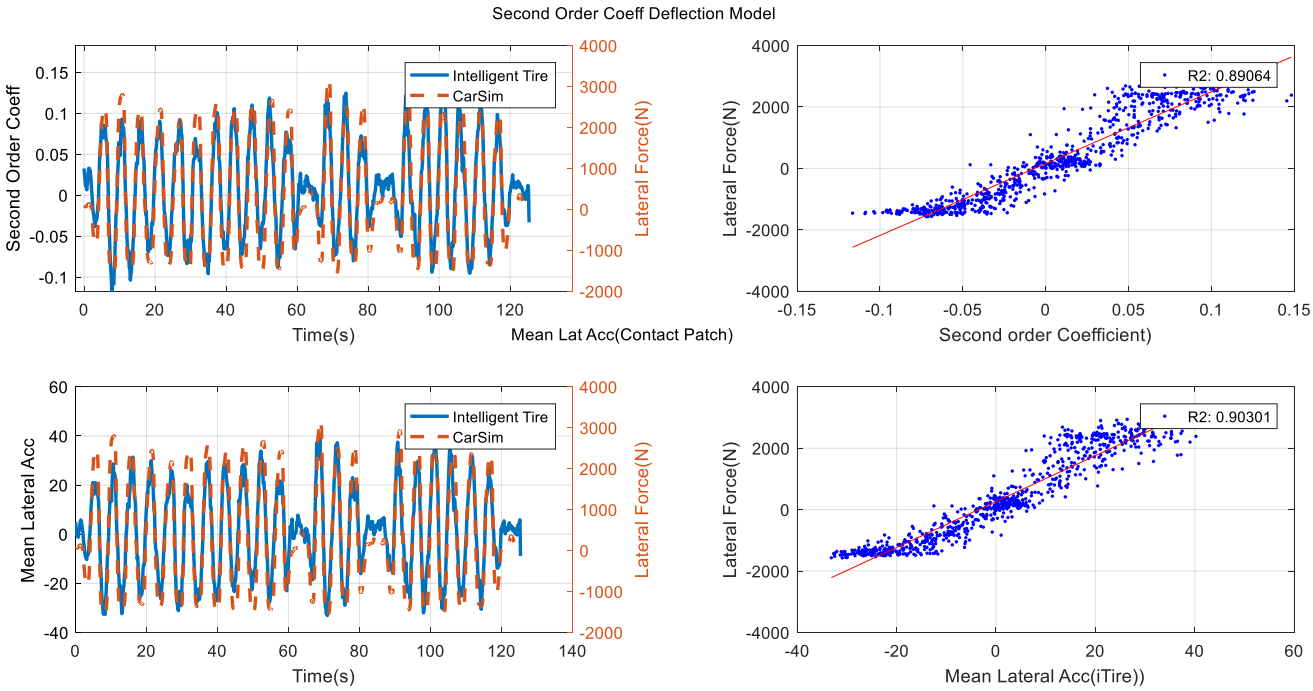

Figure 96 Test1-Sine Sweep Input

Figure 97 Test2- Double Lane ChangeFigure 98 Test1-Sine Sweep Input

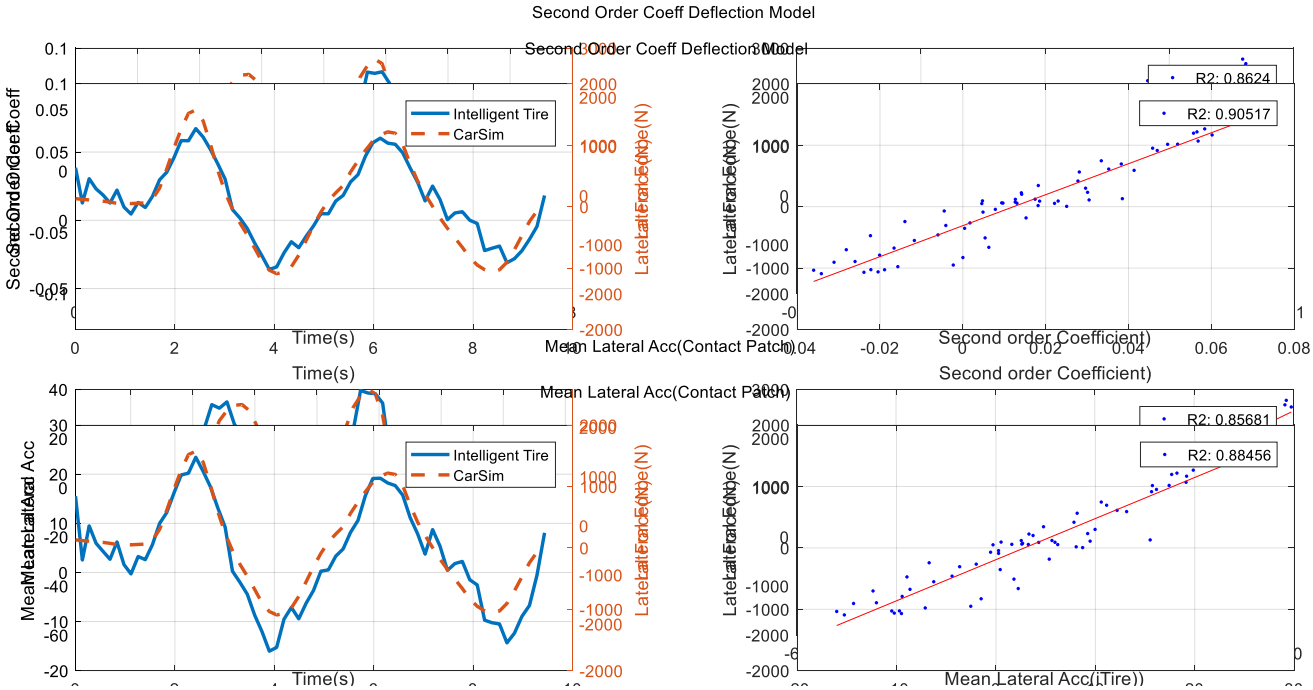

Figure 102 Test3- Sine Input

Figure 103 Test4-Medium Frequency InputFigure 104 Test3- Sine Input

Figure 100 Test3- Sine InputFigure 101 Test2- Double Lane Change

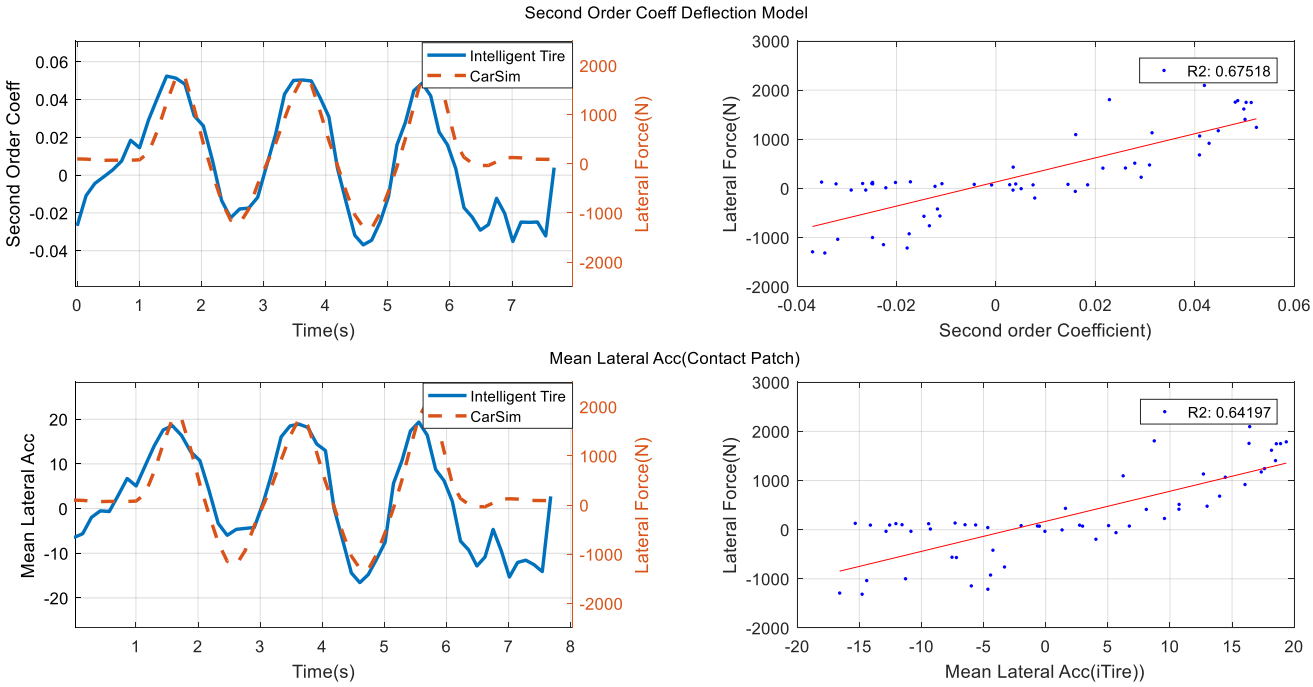

Figure 105 Test4-Medium Frequency Input

Figure 106-Correlation of Longitudinal Force RegressorFigure 107 Test4-Medium Frequency Input

Test No	Speed(mph)	Slope(Deflection)	Constant (Deflection)	Slope(Mean)	Constant(Mean)
1	26	23394.55	155.70	74.78	261.56
2	32	25579.89	509.05	48.92	605.39
3	30	25217.52	-309.80	66.93	-191.64
4	30	24545.35	131.17	61.17	169.64

Table 8 Summary of Regression coefficient for the lateral force features

4.4.1 Discussion & Conclusion

The results show a good trend of correlation between the two different methods of Lateral force measurement and the estimated force from CarSim. Some observations are discussed below”

- Since all the tests have been done at similar speeds, the effect of vehicle speed on the intelligent tire output cannot be inferred. The effect needs to be studied further in

controlled conditions on a proving ground.

- At higher speeds as discussed before the sampling rate needs to be increased to get a good resolution of the accelerometer signal.

- Some deflection/lateral force is observed in the intelligent tire signal even when the vehicle is running straight. This is observed to be caused due to the circumferential and radial stress and the alignment of the tire.

- The linear term of the Deflection model corresponds to the aligning moment of the tire. The Pacejka tire model used here is not properly validated for the aligning moment, hence it cannot be used for correlating the estimated aligning moment from the tire. This can be studied in detail further for detection of tire pressure, since aligning moment is sensitive to tire pressure.

4.5 Results of Longitudinal Force Regressor

The results of the output obtained from the algorithm for longitudinal regressor cannot be

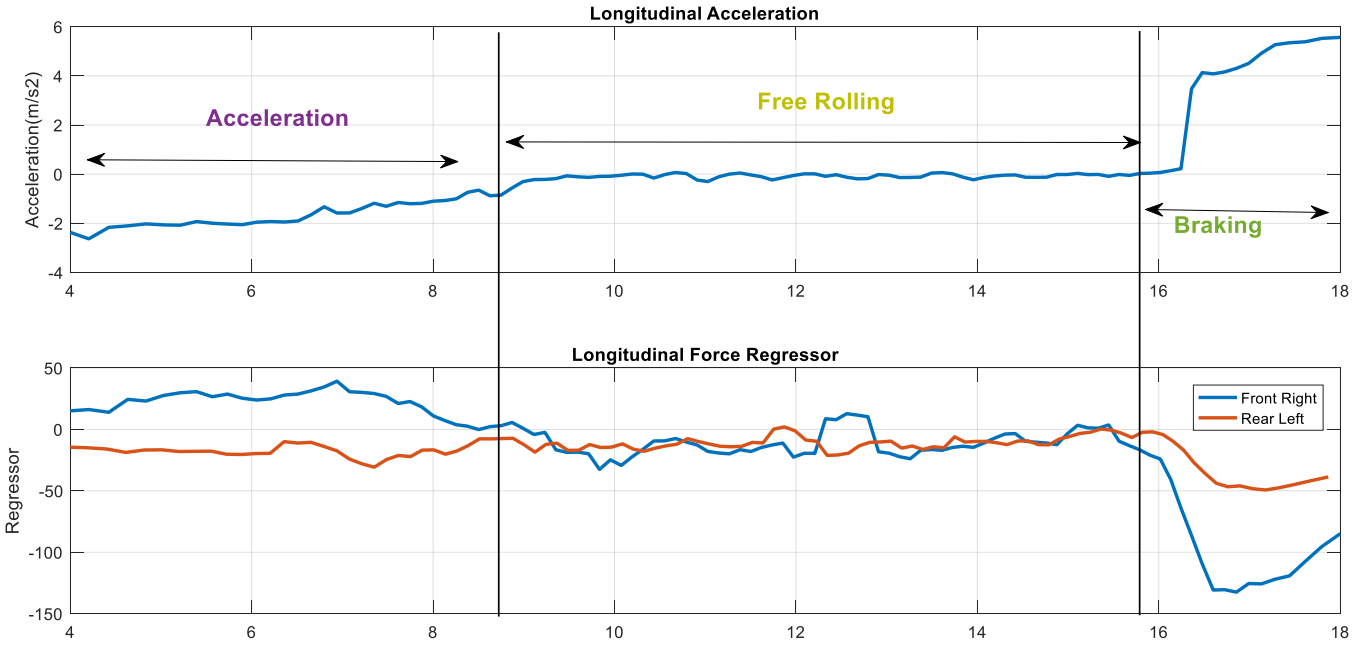

Figure 108-Correlation of Longitudinal Force Regressor

Figure 109-Result for 3 different TestsFigure 110-Correlation of Longitudinal Force Regressor

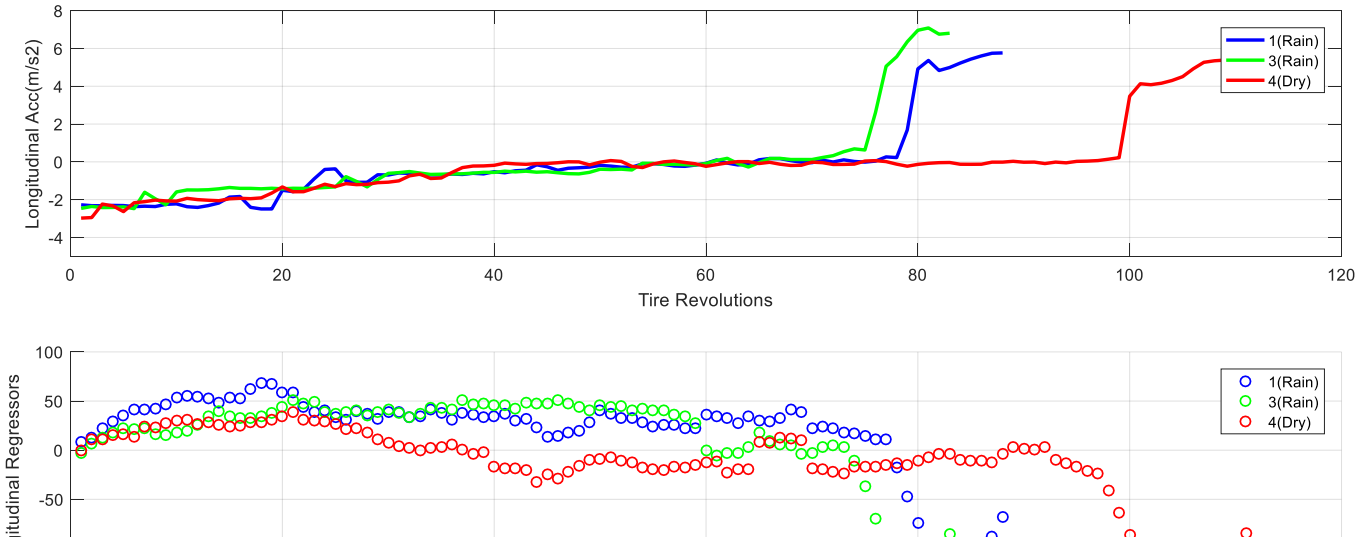

Figure 111-Result for 3 different Tests

Figure 112-35psi Tire pressureFigure 113-Result for 3 different Tests

compared with CarSim since acceleration and braking require the engine and brake system to be modelled which has not been done due to insufficient data. However, the results between the front right and the rear left tires are compared and shown in Figure 108-Correlation of Longitudinal Force Regressor

Figure 109-Result for 3 different TestsFigure 110

The following observations were made from the Longitudinal Force Regressor

In the acceleration region, the front tire has a positive value which is logical since the drive torque is applied to the front wheels.

- In the free rolling region both the front and the rear have similar values.
- The Braking region has higher values for the Front tire compared to the rear tire which is logical from the standpoint of load transfer.
- Free rolling in dry and wet shows different results and this observation needs to be reviewed further.

4.6 Results of Tire Pressure estimation algorithm

This section shows the results of the Tire pressure estimation algorithm. Due to lack of controlled tire pressure data an algorithm for tire estimation could be developed but two different tire pressures at two different speeds was compared to show the validity of the method.

Assumptions of this test are

- The load on the tires is considered constant in this algorithm for the results shown in this algorithm.
- The vehicle was running straight with no input to the steering.
- The surface is uniform throughout the run of the test.

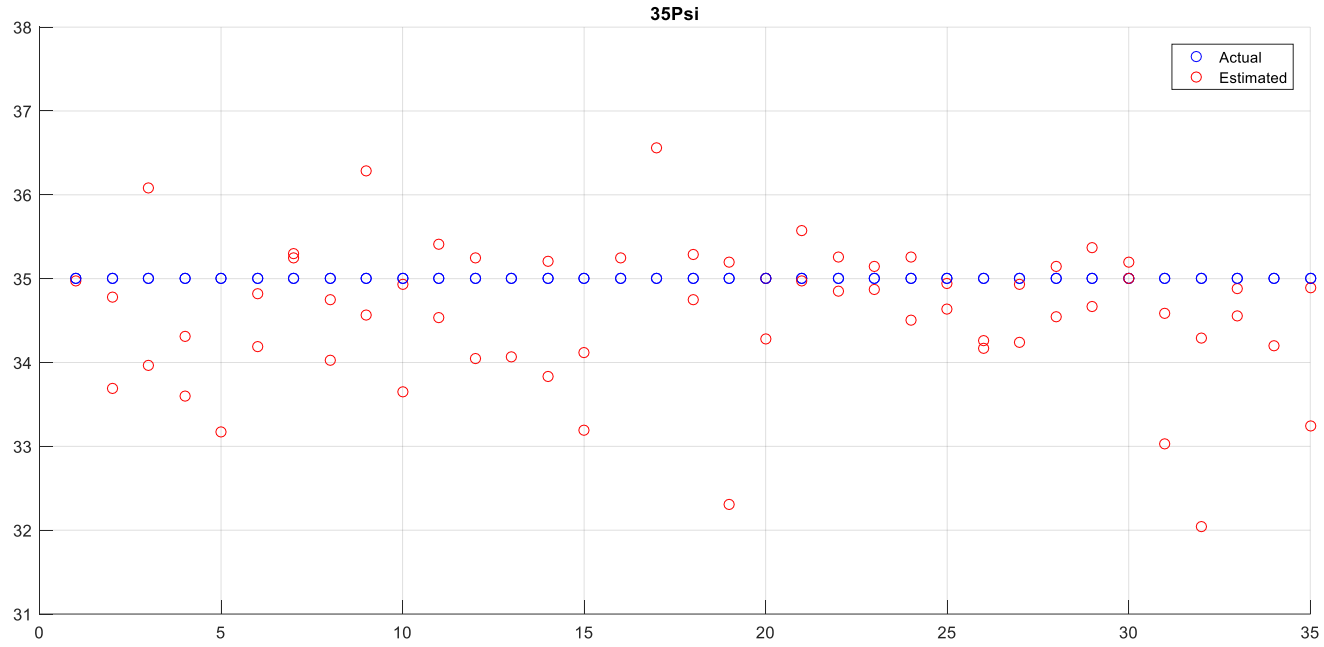

Figure 114-35psi Tire pressure

Figure 115-25psi Tire PressureFigure 116-35psi Tire pressure

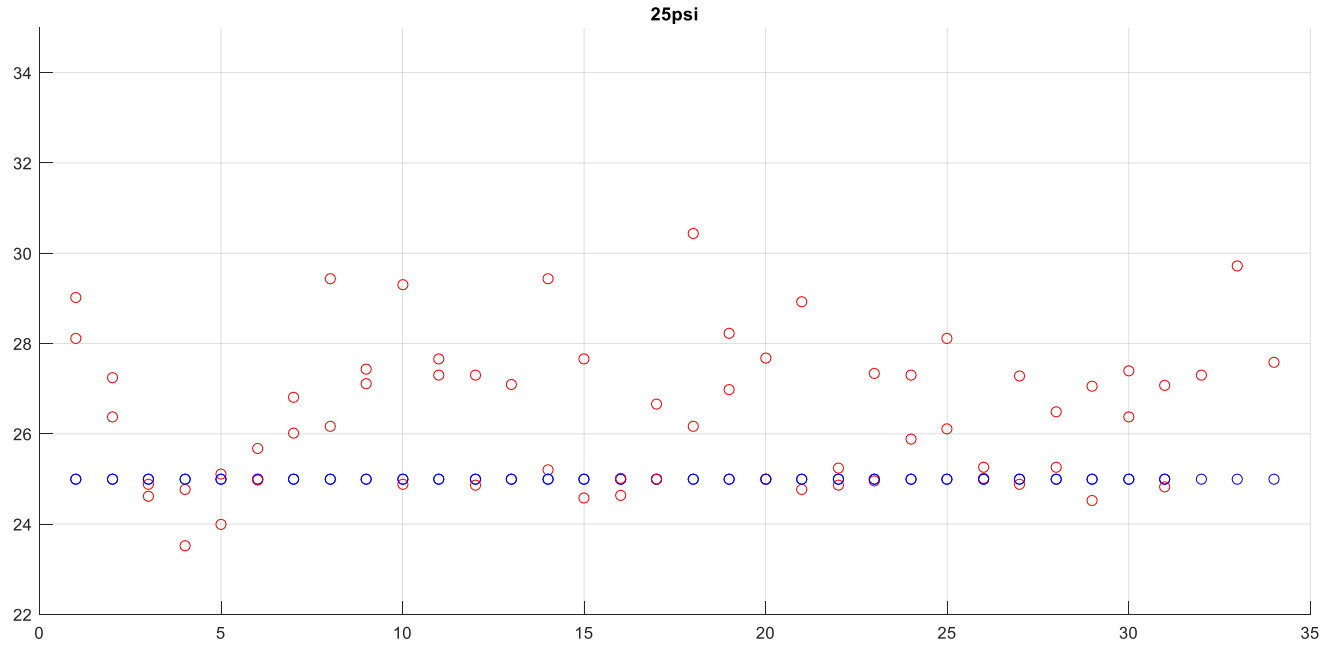

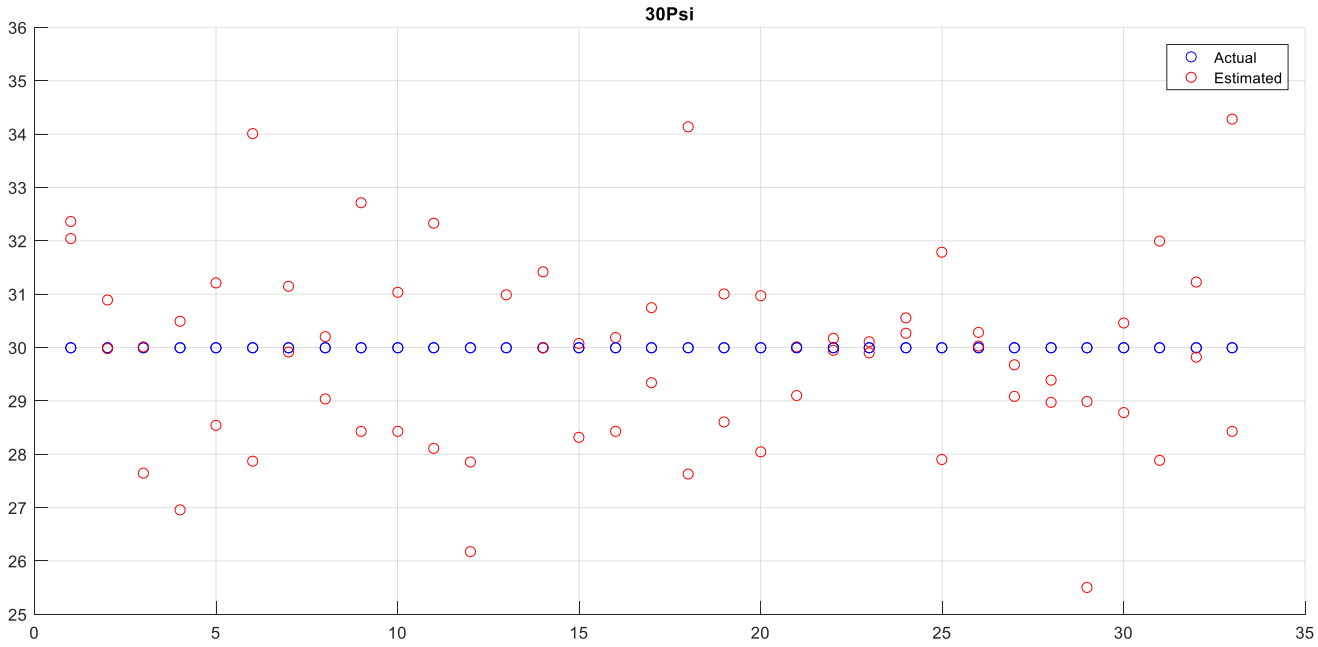

Figure 120-30psi Tire Pressure

Figure 121-Test for wheel alignmentFigure 122-30psi Tire Pressure

Observations

The results of the algorithm show a good trend but are not perfect, the reasons could be

- Not having enough data for training.
- Inaccurate measurement of tire pressure, changes with temperature and the vehicle runs.
- Vehicle speed and load was not used as an input.

This algorithm can be made more robust by including regressor for load as an input to the neural network training algorithm.

Figure 117-25psi Tire Pressure

Figure 118-30psi Tire PressureFigure 119-25psi Tire Pressure

4.7 Applications of the Regressors extracted

This section goes through the results of some applications of the regressors extracted.

4.7.1 Result of Wheel Alignment Test

Another application of the tire force measurement can be to find any issues with the alignment such as toe, camber etc. The plot below shows the difference in forces generated by front and rear tire when the vehicle is running straight caused because of toe in the rear tire.

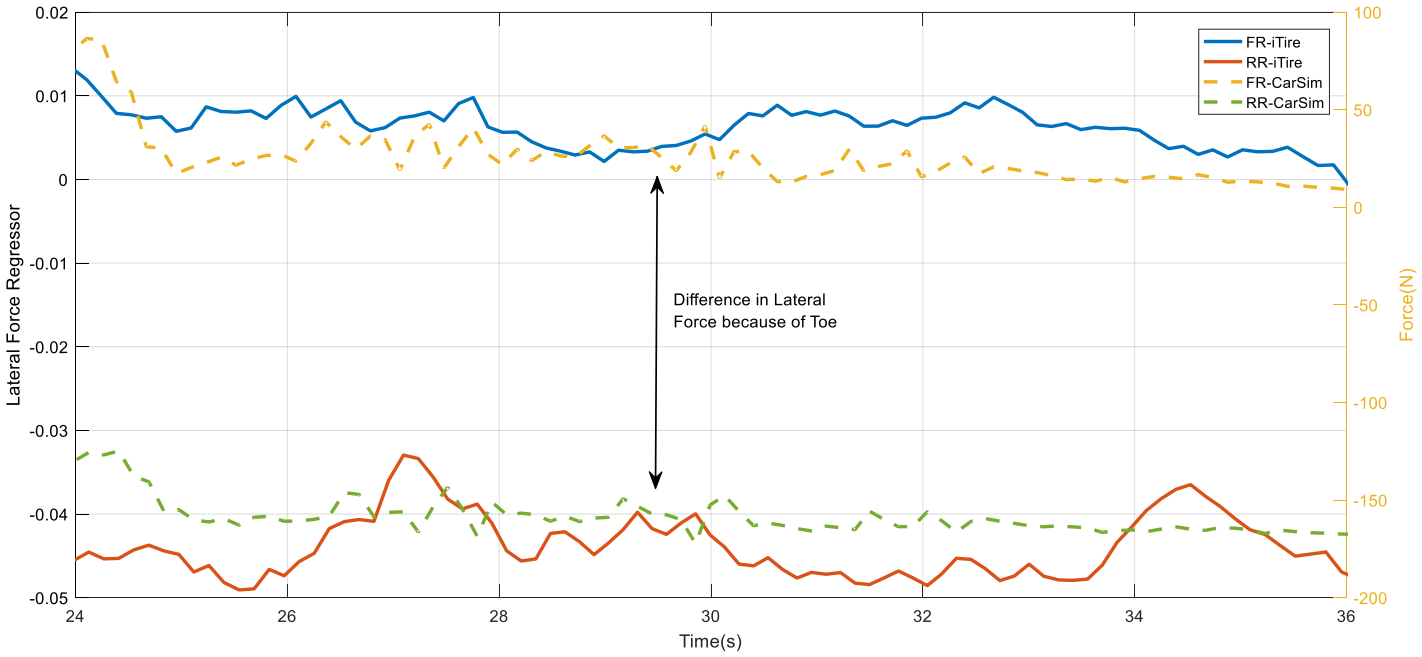

Figure 123-Test for wheel alignment

Figure 124-Tire state plotFigure 125-Test for wheel alignment

4.7.2 Application of Intelligent Tire in benchmarking and Development

The result of the running state of tire is shown below. This information can be particularly useful for tire benchmarking and tire design. Instead of using WFT which requires special fixtures and is expensive, a wireless accelerometer can be placed inside the tire and benchmarking can be done across different tires for the same test condition. An example of the tire state plot consisting

of the lateral, longitudinal and normal load regressors plotted together.

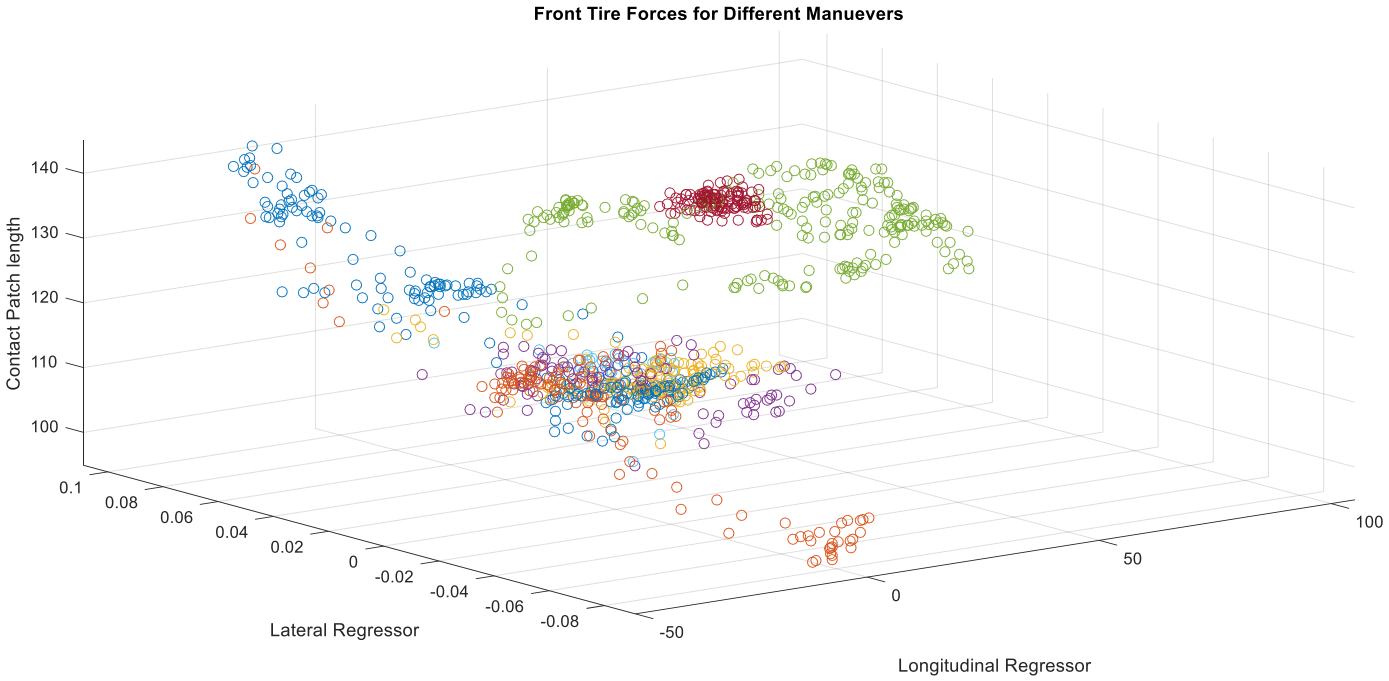

Figure 126-Tire state plot

Figure 127-Low Cost accelerometer and protection capFigure 128-Tire state plot

4.8 Conclusions

This chapter considered the results of the different features and their correlation with the CarSim model. The main points from this chapter are:

- CarSim model for VW Jetta was developed and validated with actual test results.
- Load transfer estimation with intelligent tires was compared with the results of CarSim and good correlation was found.
- Lateral force regressor using the intelligent tire was compared with the results of CarSim for different maneuvers and a good correlation was observed in the results.
- Longitudinal force regressors from the intelligent tire were compared with the longitudinal acceleration of the vehicle as the Carsim model was not validated for engine and brake system. Good correlation in trend was observed when compared with the Longitudinal Acceleration.
- The results of preliminary tire pressure estimation algorithm were shown and there is a

good scope to develop this algorithm for further analysis.

- Applications of force generation have been demonstrated through some results.

5 Summary and Future Work

With the advent of autonomous vehicles, it becomes critical to know the tire-road interaction in real time, different estimation algorithms are currently used to estimate the state of the vehicle and the tire forces however there is a need to make those models more robust in conditions such as side wind, banking etc. This study analyses the Intelligent tire signal to extract features relating to the Tire forces & pressure. The summary of different chapters is shown below.

5.1 Summary of the Chapters

Chapter 1 discussed the motivation of doing this study and explored the different techniques used currently for getting the tire force information. It then examines the different model based and measurement based estimation techniques. Different sensors used for measuring tire forces are discussed with the advantages and disadvantages of each. The selection of accelerometer for this purpose is justified and different applications of the tire force estimation are discussed.

Chapter 2 talked about the setup developed for the intelligent tire testing. The instrumentation of VW Jetta was discussed along with the specifications of the different sensors used. The chapter also discusses the way the sensor is installed inside the tire and the mechanism to bring the signal out using a slip ring. The data acquisition setup is explained along with the LabView interface to collect the data.

Chapter 3 examines all the different techniques used to extract the features out of the Intelligent tire signal. It studies the different frequency and time domain techniques used in signal analysis and the intelligent tire signal is analyzed for noise and sensitivity to speed and steering inputs. The regressors correlating with load transfer estimation, lateral force, longitudinal force and tire pressure are identified through different signal analysis methods.

Chapter 4 In this chapter a CarSim model was developed and validated for different test results. The lateral load transfer based on contact patch length was validated from the CarSim results and

found to be having a good correlation. The lateral force generation was correlated for two regressors and both showed good correlation to the CarSim results. The longitudinal force and tire pressure regressors could not be validated since the CarSim model was not setup for tire pressure/engine/brake hence the trend was compared with the vehicle acceleration to validate the longitudinal force measurement. Different applications of the force estimation were then mentioned.

5.2 Future Work

This study did a preliminary analysis of tire force extraction using Intelligent tire signal. However due to the limited resources with regards to controlled test facility all parameters could not be evaluated. Following studies are proposed to make the algorithms more robust and to include the effect of parameters such as load, camber etc.:

- The effect of contact patch length change with different camber/tire pressure/speed settings needs to be studied. During some of the analysis it was observed that the contact patch length change differs slightly with speed.
- Tests need to be conducted which include high rate of load transfer to check if the load transfer algorithm can be used to estimate the roll over limit.
- The lateral tire force regressor needs to be analyzed at higher speeds and in nonlinear regions to check the robustness of the regressor. The effect of speed, tire pressure, load needs to be studied in detail.
- The longitudinal force regressor needs to be compared with measured force values to validate the regressor and develop a longitudinal force estimation algorithm.
- The coupling between load and tire pressure needs to be studied further in the frequency domain to have a more accurate estimation of tire pressure monitoring.

A plan to use a low-cost accelerometer is underway, the objective is to check the performance of the low-cost sensor and to make this technology commercially feasible. This sensor along with the cap designed is shown in Figure 129-Low Cost accelerometer and protection cap

- Figure 130.
- A strain gauge/ accelerometer fusion sensor can be explored to compensate for the

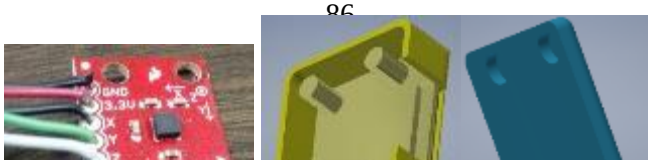

weakness of each type of sensor and get a robust estimate.

6 References

[1] S. Khaleghian, A. Emami, and S. Taheri, "A technical survey on tire-road friction estimation," *Friction*, pp. 1–24, 2017.

[2] VTT, "In *Figure 129-Low Cost accelerometer and protection cap* ıologies," *Traffic*, pp. 1–12[illegible]

[3] Y. Fukad . 3114, no. June, 2017. *Figure 130-Low Cost accelerometer and protection cap*

[4] G. Baffet, A. Charara, and D. Lechner, "Estimation of vehicle sideslip, tire force and wheel cornering stiffness," *Control Eng. Pract.*, vol. 17, no. 11, pp. 1255–1264, 2009.

[5] H. Zhang, X. Huang, J. Wang, and H. R. Karimi, "Robust energy-to-peak sideslip angle estimation with applications to ground vehicles," *Mechatronics*, vol. 30, pp. 338–347, 2015.

[6] C. R. Carlson, J. C. Gerdes, and J. D. Powell, "Practical Position and Yaw Rate Estimation with GPS and Differential Wheelspeeds," *Proc. 2002 AVEC*, 2002.

[7] R. Daily and D. M. Bevly, "The use of GPS for vehicle stability control systems," *IEEE Trans. Ind. Electron.*, vol. 51, no. 2, pp. 270–277, 2004.

[8] W. Cho, J. Yoon, S. Yim, B. Koo, and K. Yi, "Vehicle Stability Control," vol. 59, no. 2, pp. 638–649, 2010.

[9] W. Klier, A. Reim, and D. Stapel, "Robust Estimation of Vehicle Sideslip Angle -- An Approach w/o Vehicle and Tire Models," *Proc. SAE World Congr.*, vol. 2008, no. 724, 2008.

[10] A. Rezaeian, A. Khajepour, W. Melek, S. K. Chen, and N. Moshchuk, "Simultaneous Vehicle Real-Time Longitudinal and Lateral Velocity Estimation," *IEEE Trans. Veh. Technol.*, vol. 66, no. 3, pp. 1950–1962, 2017.

[11] H. Lee and S. Taheri, "Intelligent Tires?A Review of Tire Characterization Literature," *IEEE Intelligent Transportation Systems Magazine*, vol. 9, no. 2. pp. 114–135, 2017.

[12] O. Yilmazoglu, M. Brandt, J. Sigmund, E. Genc, and H. L. Hartnagel, "Integrated InAs/GaSb 3D magnetic field sensors for 'the intelligent tire,'" *Sensors Actuators, A Phys.*, vol. 94, no. 1–2, pp. 59–63, 2001.

[13] V. Magori, V. R. Magori, and N. Seitz, "On-line determination of tyre deformation, a novel sensor principle," *1998 IEEE Ultrason. Symp. Proc. (Cat. No. 98CH36102)*, vol. 1, pp. 485–488, 1998.

[14] A. Pohl, R. Steindl, and L. Reindl, "The 'intelligent tire' utilizing passive SAW sensors measurement of tire friction ," *IEEE Transactions on Instrumentation and Measurement* , vol. 48, no. 6. IEEE , pp. 1041–1046, 1999.

[15] A. J. Tuononen, "Optical position detection to measure tyre carcass deflections," *Veh. Syst. Dyn.*, vol. 46, no. 6, pp. 471–481, 2008.

[16] J. Y. J. Yi, "A Piezo-Sensor-Based “Smart Tire” System for Mobile Robots and Vehicles," *IEEE/ASME Trans. Mechatronics*, vol. 13, no. 1, pp. 95–103, 2008.

[17] G. Erdogan, L. Alexander, and R. Rajamani, "Estimation of tire-road friction coefficient

using a novel wireless piezoelectric tire sensor," *IEEE Sens. J.*, vol. 11, no. 2, pp. 267–279, 2011.
[18] D. Garcia-Pozuelo, O. Olatunbosun, J. Yunta, X. Yang, and V. Diaz, "A novel strain-based method to estimate tire conditions using fuzzy logic for intelligent tires," *Sensors (Switzerland)*, vol. 17, no. 2, 2017.
[19] A. Nepote and P. D. La Pierre, "The Intelligent Tire : Acceleration Sensors Data Acquisition," *Engineering*, no. Ivi, 2005.
[20] A. J. Niskanen, X. Yi, and A. J. Tuononen, "Towards the friction potential estimation: A model-based approach to utilizing in-tyre accelerometer measurements," *IEEE Intell. Veh. Symp. Proc.*, vol. 2016–Augus, no. June, pp. 625–629, 2016.
[21] G. Erdogan, S. Hong, F. Borrelli, and K. Hedrick, "Tire Sensors for the Measurement of Slip Angle and Friction Coefficient and Their Use in Stability Control Systems," *SAE Int. J. Passeng. Cars - Mech. Syst.*, vol. 4, no. 1, pp. 2011-01–0095, 2011.
[22] V. D'Alessandro, S. Melzi, M. Sbrosi, and M. Brusarosco, "Phenomenological Analysis of Hydroplaning Through Intelligent Tyres," *Veh. Syst. Dyn.*, vol. 50, no. sup1, pp. 3–18, 2012.
[23] S. Hong, G. Erdogan, K. Hedrick, and F. Borrelli, "Tyre–road friction coefficient estimation based on tyre sensors and lateral tyre deflection: modelling, simulations and experiments," *Veh. Syst. Dyn.*, vol. 51, no. 5, pp. 627–647, 2013.
[24] R. Matsuzaki, K. Kamai, and R. Seki, "Intelligent tires for identifying coefficient of friction of tire/road contact surfaces using three-axis accelerometer," *Smart Mater. Struct.*, vol. 24, no. 2, p. 25010, 2015.
[25] F. Braghin, M. Brusarosco, F. Cheli, A. Cigada, S. Manzoni, and F. Mancosu, "Measurement of contact forces and patch features by means of accelerometers fixed inside the tire to improve future car active control," *Veh. Syst. Dyn.*, vol. 44, no. sup1, pp. 3–13, 2006.
[26] M. Matilainen and A. Tuononen, "Tyre contact length on dry and wet road surfaces measured by three-axial accelerometer," *Mech. Syst. Signal Process.*, vol. 52–53, no. 1, pp. 548–558, 2015.
[27] S. M. Savaresi, M. Tanelli, P. Langthaler, and L. del Re, "New regressors for the direct identification of tire deformation in road vehicles via 'In-tire' accelerometers," *IEEE Trans. Control Syst. Technol.*, vol. 16, no. 4, pp. 769–780, 2008.
[28] A. J. Tuononen, "Vehicle lateral state estimation based on measured tyre forces," *Sensors*, vol. 9, no. 11, pp. 8761–8775, 2009.
[29] E. Sabbioni, D. Ivone, F. Braghin, F. Cheli, and P. Milano, "In-Tyre Sensors Induced Benefits on Sideslip Angle and Friction Coefficient Estimation," 2017.
[30] S. Khaleghian and S. Taheri, "Terrain classification using intelligent tire," *J. Terramechanics*, vol. 71, pp. 15–24, 2017.
[31] F. Cheli, G. Audisio, M. Brusarosco, F. Mancosu, D. Cavaglieri PhD, and S. Melzi, "Cyber Tyre: A Novel Sensor to Improve Vehicle's Safety," 2011.
[32] M. Bäcker, A. Gallrein, and M. Roller, "Noise, vibration, harshness model of a rotating tyre," *Veh. Syst. Dyn.*, vol. 54, no. 4, pp. 474–491, 2016.
[33] A. J. C. Schmeitz and M. Alirezaei, "Analysis of wheel speed vibrations for road friction classification," *Veh. Syst. Dyn.*, vol. 54, no. 4, pp. 492–509, 2016.
[34] A. R. P. D and S. Venkatesh, "Time-Frequency Analysis methods : A Comparative study," pp. 2016–2021, 2016.

[35] L. Xiang and A. Hu, “Comparison of methods for different timefrequency analysis of vibration signal,” *J. Softw.*, vol. 7, no. 1, pp. 68–74, 2012.
[36] E. W. Hansen and E. W. Hansen, *Fourier Transforms*. Somerset, UNITED STATES: John Wiley & Sons, Incorporated, 2014.
[37] R. A. Wehage, *Vehicle dynamics*, vol. 24, no. 4. 1987.
[38] H. B. Pacejka, I. Besselink, and I. ebrary, “Tire and vehicle dynamics .” Elsevier/BH , Amsterdam;Boston; , 2012.
[39] J. PÉRISSE, “a Study of Radial Vibrations of a Rolling Tyre for Tyre–Road Noise Characterisation,” *Mech. Syst. Signal Process.*, vol. 16, no. 6, pp. 1043–1058, 2002.
[40] Y. Li, S. Zuo, L. Lei, X. Yang, and X. Wu, “Characteristics’ analysis of lateral vibration of tire tread,” *J. Vib. Control*, vol. 17, no. 14, pp. 2095–2102, 2011.
[41] S. Khaleghian, O. Ghasemalizadeh, and S. Taheri, “Estimation of the Tire Contact Patch Length and Normal Load Using Intelligent Tires and Its Application in Small Ground Robot to Estimate the Tire-Road Friction,” *Tire Sci. Technol.*, vol. 44, no. 4, pp. 248–261, 2016.
[42] “Patent Issued for Method and System for Determining a Tyre Load during the Running of a Motor Vehicle ,” *Journal of Engineering* . p. 7171, 2014.
[43] A. Hac, “Rollover stability index including effects of suspension design,” *Sae Tech. Pap. 2002-01-0965*, vol. SP–1656, no. 724, pp. 68–78, 2002.
[44] S. Cong, L. Zan, and S. Shangbin, “Vehicle Roll Stability Analysis Considering Lateral-load Transfer Rate,” pp. 398–402, 2015.
[45] L. Xu and H. E. Tseng, “Robust model-based fault detection for a roll stability control system,” *IEEE Trans. Control Syst. Technol.*, vol. 15, no. 3, pp. 519–528, 2007.
[46] V. Tsourapas, D. Piyabongkarn, A. C. Williams, and R. Rajamani, “New method of identifying real-time predictive lateral load transfer ratio for rollover prevention systems,” *Proc. Am. Control Conf.*, pp. 439–444, 2009.
[47] “Method and system for determining a cornering angle of a tyre during the running of a vehicle .” 2003.
[48] A. J. Niskanen and A. J. Tuononen, “Detection of the local sliding in the tyre-road contact by measuring vibrations on the inner liner of the tyre,” *Meas. Sci. Technol.*, vol. 28, no. 5, 2017.
[49] K. B. Singh and J. B. Ferris, “Development of an Intelligent Tire Based Tire - Vehicle State Estimator for Application to Global Chassis Control Development of an Intelligent Tire Based Tire - Vehicle State,” 2012.
[50] Y. K. Thong, M. S. Woolfson, J. A. Crowe, and D. A. Jones, “Numerical double integration of acceleration measurements in noise,” vol. 36, pp. 73–92, 2004.
[51] S. Han, “Measuring displacement signal with an accelerometer †,” vol. 24, no. 6, 2010.
[52] D. Krier, G. S. Zanardo, and L. Del Re, “A PCA-based modeling approach for estimation of road-tire forces by in-tire accelerometers,” *IFAC Proc. Vol.*, vol. 19, pp. 12029–12034, 2014.
[53] Y. Xiong and A. Tuononen, “Case Studies in Mechanical Systems and Signal Processing The in-plane deformation of a tire carcass : Analysis and measurement,” *Case Stud. Mech. Syst. Signal Process.*, vol. 2, pp. 12–18, 2015.
[54] N. Persson, F. Gustafsson, and M. Drevo, “Indirect tire pressure monitoring using sensor fusion,” *SAE Tech. Pap.*, no. 724, 2002.
[55] Z. Fuqiang, W. Shaohong, W. Yintao, and X. Zhichao, “Indirect tire pressure monitoring

system based on tire vertical stiffness," pp. 100–104, 2015.
[56] A. E. Kubba and K. Jiang, "A comprehensive study on technologies of tyre monitoring systems and possible energy solutions," *Sensors (Switzerland)*, vol. 14, no. 6, pp. 10306–10345, 2014.
[57] Q. Zhang, B. Liu, and G. Liu, "Design of tire pressure monitoring system based on resonance frequency method," *2009 IEEE/ASME International Conference on Advanced Intelligent Mechatronics*. pp. 781–785, 2009.
[58] M. Doumiati, A. Charara, A. C. Victorino, and D. Lechner, "Vehicle dynamics estimation using Kalman filter : practical applications ." Wiley-ISTE , p. 304, 2012.